WSRC-TR-2002-00580

SRT-RPP-2002-00266

Laboratory-Scale SuperLig® 639 Column Tests with Hanford Waste Simulants (U)

Westinghouse Savannah River Company
Savannah River Site
Aiken, SC 29808

SAFETY • RESPONSIBILITY • SECURITY
SRS
SAVANNAH RIVER SITE

Prepared for the U.S. Department of Energy under Contract No. DE-AC09-96SR18500

WSRC-TR-2002-00580
SRT-RPP-2002-00266

KEYWORDS:
River Protection Project
Waste Treatment Plant
Ion Exchange
Rhenium
Perrhenate
Technetium
Pertechnetate
Temperature
241-AN-105
241-AZ-102
241-AN-102
On-line analysis
ICP-ES

RETENTION – Permanent

Laboratory-Scale SuperLig® 639 Column Tests with Hanford Waste Simulants (U)

SAVANNAH RIVER TECHNOLOGY CENTER

William D. King, 773-42A
William A. Spencer, 773-42A
Myra P. Bussey, 735-11A

Publication Date: May 2003

Westinghouse Savannah River Company
Savannah River Site
Aiken, SC 29808

Prepared for the U.S. Department of Energy under Contract No. DE-AC09-96SR18500

DOCUMENT: **WSRC-TR-2002-00580 (SRT-RPP-2002-00266)**
TITLE: **Laboratory-Scale SuperLig® 639 Column Tests with Hanford Waste Simulants (U)**

APPROVALS

_____

William D. King/SRTC/Waste Processing Technology Date

_____

William A. Spencer/SRTC/Sensor and Analyzer Technology Date

_____

Myra P. Bussey/SRTC/Waste Processing Technology Date

_____

L. Larry Hamm/SRTC/Technical Reviewer Date

_____

James C. Marra/SRTC/Level 4 Manager/Waste Processing Technology Date

_____

Reid Peterson/Bechtel/R&T Pretreatment Manager/River Protection Project Date

_____

Walt Tamosaitis/Bechtel/ R&T Manager/River Protection Project Date

TABLE OF CONTENTS

LIST OF TABLES

LIST OF FIGURES

TABLE OF NOTATION

ADS	Analytical Development Section
BV	Bed volume
C	Concentration
C_a	Average concentration
C_i	Initial concentration
C_o	Original concentration
ICP-ES	Inductively Coupled Plasma – Emission Spectroscopy
ICP-MS	Inductively Coupled Plasma – Mass Spectroscopy
IC Anion	Ion Chromotography – Anion Analysis
K_d	Distribution coefficient, mL/g
$\tilde{K}_{ji}$	Selectivity coefficient between species j and i
NA	Not available
NM	Not measured
RCRA	Resource Conservation and Recovery Act
RPP	River Protection Program
SED	Spherical Equivalent Diameter
SRTC	Savannah River Technology Center
TIC	Total inorganic carbon
TOC	Total organic carbon
WSRC	Westinghouse Savannah River Company
WTP	Waste Treatment Plant

Symbols

<	Analyte concentrations below the instrumental detection limit
>	Indicates bounding selectivity coefficient values for columns not loaded to saturation

(This Page Intentionally Left Blank)

1.0 Executive Summary

This report describes the results of SuperLig® 639 column tests conducted at the Savannah River Technology Center (SRTC) in support of the Hanford River Protection Project - Waste Treatment Plant (RPP-WTP). The RPP-WTP contract was awarded to Bechtel National Inc. (BNI) for the design, construction, and initial operation of a plant for the treatment and vitrification of millions of gallons of radioactive waste currently stored in tanks at Hanford, WA. Part of the current treatment process involves the removal of technetium from tank supernate solutions using columns containing SuperLig® 639 resin. This report is part of a body of work intended to quantify and optimize the operation of the technetium removal columns with regard to various parameters (such as liquid flow rate, column aspect ratio, resin particle size, loading and elution temperature, etc.). The tests were conducted using nonradioactive simulants of the actual tank waste samples containing rhenium as a surrogate for the technetium in the actual waste. A previous report focused on the impacts of liquid flow rate and column aspect ratio upon performance (King, et al., 2000). More recent studies have focused on the impacts of resin particle size, solution composition, and temperature. This report describes column loading experiments conducted varying temperature and solution composition. Each loading experiment was followed by high temperature elution of the sorbed rhenium. Results from limited testing are also described which were intended to evaluate the physical stability of SuperLig® 639 resin during exposure to repeated temperature cycles covering the range of potential processing extremes.

1.1 Objectives

Primary test objectives included:

- Determine the impact of temperature on rhenium breakthrough profiles under column loading conditions with SuperLig® 639 resin and Hanford Tank 241-AN-105 (Envelope A) waste simulant.
- Evaluate SuperLig® 639 column performance under nominal conditions with Hanford Tank 241-AZ-102 (Envelope B) and 241-AN-107 (Envelope C) waste simulants.
- Evaluate the impact of eluting the SuperLig® 639 columns with water at 65 °C and compare the results to previous experiments in which the elution was conducted at ambient temperature.
- Identify competitors for sorption sites on SuperLig® 639 resin.
- Evaluate the physical stability of SuperLig® 639 resin after exposure to repeated thermal shock cycles.

These objectives are consistent with those prescribed in the relevant test specifications, task plans, and test exceptions for this work.

1.2 Conduct of Testing

Numerous column tests were performed with SuperLig® 639 resin using three Hanford waste simulants. Perrhenate ion was utilized as a surrogate for pertechnetate ion (the dominant form of technetium in actual waste solutions) so that the tests could be performed in a nonradiological fume hood at minimal cost. Variable temperature column tests were performed with AN-105 simulant using a 1.5 cm (nominal) ID column containing approximately 10 mL of SuperLig® 639 resin. Column tests were conducted at loading temperatures of 25, 35, and 45 °C. Due to concerns about degradation of the resin sample during the two-year storage period, the test series was repeated with a recently prepared SuperLig® 639 resin sample. In all cases, the columns were eluted with deionized water at 65 °C. On-line ICP-ES analysis was utilized for all tests to monitor rhenium breakthrough during loading and to track desorption of numerous species during feed displacement and elution.

Additional tests were performed under the nominal processing conditions with AZ-102 and AN-107 simulants using a 1 inch ID column containing approximately 74 mL of SuperLig® 639 resin. Both experiments were continually monitored with the on-line ICP-ES unit. The column was eluted with water at 65 °C after each rhenium loading test.

A separate study was conducted to evaluate the physical stability of SuperLig® 639 resin after exposure to 10 thermal shock cycles. These tests involved repeated and rapid transfer of resin between beakers of water at 25 and 65 °C. Optical microscopy and particle size analysis methods were then utilized to evaluate the impacts of thermal cycling.

1.3 Results and Performance Against Objectives

Column tests performed with AN-105 simulant revealed that rhenium breakthrough profiles from SuperLig® 639 columns are highly temperature dependent (see Figure 1-1). Increasing the column loading temperature from 25 to 45 °C, results in: 1) sharpening of the rhenium breakthrough profiles resulting from increased perrhenate sorption kinetics, and 2) an approximately 50% decrease in perrhenate loading. These trends in the data were consistent between the two resin batches tested and were expected. Across the temperature range tested with the more recently prepared resin batch, the 50% rhenium breakthrough point was observed after processing >100 BV of solution. Correlations derived from this work and separate tests specifically designed to determine fundamental diffusion parameters (both pore and film coefficients) for this system (Duffey, et al., 2003) will be utilized to optimize the RPP-WTP operating conditions during SuperLig® 639 column loading.

Column tests conducted with AN-105, AZ-102 and AN-107 simulants revealed that rhenium breakthrough profiles vary considerably with waste composition. The impact of changing the feed composition can be seen in Figure 1-2, where rhenium breakthrough profiles at 25 °C are plotted for each simulant. 50% rhenium breakthrough was observed with the AN-107 simulant after processing ~90 BV of solution. In contrast, only 30% rhenium breakthrough was observed after processing ~210 BV of AZ-102 simulant. Intermediate performance was observed with the AN-105 simulant.

Differences in the column loading performance are associated with the relative nitrate-to-perrhenate molar ratios for these simulant compositions, with lower values resulting in enhanced rhenium uptake. However, it was discovered for the first time in this work that the feed potassium concentration also significantly impacts rhenium uptake by SuperLig® 639 resin, with higher potassium resulting in higher rhenium uptake. Based on the trends in simulant potassium concentrations and nitrate-to-perrhenate molar ratios, column performance would be expected to decrease in the series: AZ-102, AN-105, AN-107; as was observed for these waste simulants.

After the completion of each column loading experiment, the feed was displaced from the columns with 0.1 M NaOH solution and the columns were eluted with deionized water at 65 °C. In all cases, the eluate rhenium concentration decreased to the design target (≤1% of the feed rhenium concentration) after processing <15 BV of solution. A comparison of the rhenium elution profile obtained at 65 °C after column loading with AN-105 simulant, to previous data obtained at ambient temperature is provided in Figure 1-3. High temperature elution results in a significant decrease in the processing time and eluent volume required to reach the design target for elution.

On-line monitoring (by Inductively Coupled Plasma - Emission Spectroscopy) of the solutions exiting the columns during feed displacement and elution yielded a highly significant and unique body of data that provides important information regarding species sorbed to SuperLig® 639 resin during contact with Hanford waste samples. The data was complimented with additional ion chromatography analysis of samples that were selected based on the trends observed in the on-line concentration profiles. The collective data revealed the presence of distinct nitrate and perrhenate desorption bands that were well separated. Nitrate ion desorbs from the resin almost immediately upon initiation of feed displacement with 0.1 M NaOH solution. In contrast, perrhenate desorption is more closely associated with the transition from NaOH solution to water and the simultaneous temperature increase to 65 °C. The degree of separation of the nitrate and perrhenate desorption bands is dependent upon the column temperature during feed displacement.

Highly time-resolved on-line analysis revealed the presence of peaks in the potassium concentration profiles which were associated with the desorption of nitrate and, for columns loaded with AZ-102 simulant, perrhenate salts. Figure 1-4 provides nitrate, sodium, potassium, and rhenium concentration profiles during feed displacement and elution following column loading with AZ-102 simulant. The trends in the concentration profiles indicate successive desorption of sodium nitrate, potassium nitrate, sodium perrhenate, and potassium perrhenate during liquid phase transitions from 5 M sodium simulant to 0.1 M feed displacement and, finally, to water eluate. The data indicates that both nitrate and perrhenate ions sorb to SuperLig® 639 resin during contact with Hanford waste simulants, with nitrate being the dominant sorbed species. The anionic species exist in the solid phase as neutral ion pairs composed of a mixture of sodium and potassium salts. The sorbed species are chromatographically separated during feed displacement and elution. If it is assumed that desorption rates for each species are nearly the same and are rapid relative to liquid phase diffusion, the separation of the desorption

bands may be attributed to varying selectivities (or affinities) of SuperLig® 639 resin for the neutral ion pairs. This implies that the resin selectivity increases in the series: $NaNO_3$, KNO_3, $NaReO_4$, $KReO_4$.

Loading levels for each ion pair on SuperLig® 639 resin were determined by integration of the desorption peaks in the concentration profiles. Comparison of the ratios of the various species in the eluate to the ratios in the simulants used for column loading reveals the selectivity of the resin for each species relative to other competitors. Selectivity coefficients for potassium versus sodium and for perrhenate versus nitrate are provided in Table1-1. The data indicates that the resin is selective for perrhenate sorption over nitrate and for potassium over sodium. The resin selectivity series implied in Table 1-1 is consistent with the series proposed above based on the observed desorption sequence for these species. The data in Table 1-1 indicates that selectivity varies depending on the simulant composition and the counter ion. This is not surprising, given that the sorption process is dependent upon the activities of the various ions in solution, which are, in turn, dependent upon the overall solution composition.

Prior to this time much of the above information was unknown. Highly time-resolved on-line analysis was essential in discerning the details of the competitor ion sorption/desorption mechanisms for this system. The observed preference of SuperLig® 639 resin for the potassium salt over the sodium salt was not recognized by the resin manufacturer prior to our disclosure. The potassium selectivity requires the addition of new mass transfer equations (Eqns. 1-2 and 1-4) to the fundamental conceptual model for sorption by SuperLig® 639 resin. Previously, the model only considered sorption of the sodium salts (Eqns. 1-1 and 1-3).

$$[\overline{L}] + [Na^+] + [Re\,O_4^-] \xleftrightarrow{K_{eq,1}} \left[\overline{L - Na\,Re\,O_4}\right], \quad (1\text{-}1)$$

$$[\overline{L}] + [K^+] + [Re\,O_4^-] \xleftrightarrow{K_{eq,2}} \left[\overline{L - K\,Re\,O_4}\right], \quad (1\text{-}2)$$

$$[\overline{L}] + [Na^+] + [NO_3^-] \xleftrightarrow{K_{eq,3}} \left[\overline{L - NaNO_3}\right], \quad (1\text{-}3)$$

$$[\overline{L}] + [K^+] + [NO_3^-] \xleftrightarrow{K_{eq,4}} \left[\overline{L - KNO_3}\right], \quad (1\text{-}4)$$

L represents active sorbing ligand sites in SuperLig® 639 resin.
K_{eq} represents the reaction equilibrium constants.
Bars represent species bound to the solid phase.

The selectivity coefficients provided in Table 1-1 represent the ratios of the equilibrium constants for the appropriate mass transfer equations.

The data in Table 1-1 indicates that SuperLig® 639 resin is ~25 times more selective for potassium perrhenate than for sodium perrhenate. Given the magnitude of the selectivity for the potassium salt, one would expect resin performance with regard to perrhenate (or pertechnetate) removal to be considerably enhanced in feeds containing high potassium concentrations. Recently after the discovery

of potassium selectivity, this information was utilized to explain exceptional performance observed in column tests with an actual waste sample from Tank 241-AP-101 (Burgeson, 2002). This waste sample contains 5.0 times more potassium than the AZ-102 sample. Column performance with the AP-101 sample was enhanced by a factor of ~2 relative to the performance anticipated without considering the potassium selectivity. This preliminary analysis indicates that SuperLig® 639 resin is also selective for potassium pertechnetate. Furthermore, it implies that significant improvements in technetium removal performance could be achieved by the addition of potassium salts to waste compositions containing low potassium levels. Modeling of the resin performance with these samples which takes into account the observed potassium selectivity, will be reported by L. L. Hamm (SRTC).

The column tests satisfied the primary objectives of this test program and provided much needed information regarding the impact of temperature and feed composition on column loading and elution. The identity and desorption behavior of previously unknown competitor species were also revealed.

Thermal shock testing revealed no evidence of physical degradation of the resin resulting from exposure to repeated temperature cycling in water.

1.4 Quality Requirements

This work was performed in accordance with the RPP-WTP QA requirements specified for work conducted by SRTC as identified in DOE IWO MOSRLE60. SRTC has provided matrices to WTP demonstrating compliance of the SRTC QA program with the requirements specified by WTP. Specific information regarding the compliance of the SRTC QA program with RW-0333P, Revision 10, NQA-1 1989, Part 1, Basic and Supplementary Requirements and NQA-2a 1990, part 2.7 is contained in these matrices.

This work was conducted according to the QA requirements in the following Test Specifications and Task Plans: TSP-W375-01-00023, Rev. 0 (Johnson, 2001a); TSP-W375-01-00021, Rev. 0 (Johnson, 2001b); TSP-W375-01-00022, Rev. 0 (Johnson, 2001c); WSRC-TR-2001-00202, Rev. 0 (McCabe, 2001a); WSRC-TR-2001-00204, Rev. 0 (McCabe, 2001b); and WSRC-TR-2001-00465, Rev. 0 (Saito, 2002). The work requirements described in the Task Plans were subsequently modified in test exceptions 24590-WTP-TEF-RT-02-016 and 24590-WTP-TEF-RT-02-010 Revision 1. This work was not required to comply with RW-0333P, Rev. 10. This work does comply with NQA-1 1989, Part 1, Basic and Supplementary Requirements and NQA-2a 1990, part 2.7.

The original Technical Specification QA Requirement drivers were to NQA-1-1994, Basic and Supplementary Requirements, and to RW-0333P Revision 8 (if applicable), which was in effect at the time the specifications were issued (2/01). The tasks, however, were conducted in accordance with the newer RPP-WTP QA requirements as specified in DOE IWO MOSRLE60, dated 6/2001.

SRTC has provided matrices to WTP demonstrating compliance of the SRTC QA program to the newer requirements as specified by WTP. Specific information regarding the compliance of the SRTC

QA program with RW-0333P, Revision 10, NQA-1 1989, Part 1, Basic and Supplementary Requirements and NQA-2a 1990, part 2.7 is contained in these matrices. The QA requirements specified in the Task Technical and Quality Assurance Plans were to these newer QA requirements. No additional QA requirements were required nor implemented in this work.

This testing was conducted for research purposes and the provisions of the RPP-WTP "Quality Assurance Project Plan for Testing Programs Generating Environmental Regulatory Data," PL-24590-QA00001, does not apply.

1.5 Issues and Recommendations

Issues of potential plant significance identified in this work include the following.

- Due to the dependence of rhenium (and presumably technetium) breakthrough profiles on temperature and the fact that the sorption kinetics is quite slow at 25 °C, optimal plant operation may involve technetium column loading at elevated temperatures. Temperature optimization balances the impacts of sorption kinetics and total loading. However, numerous factors will influence the ultimate design target for technetium column loading performance, and modeling efforts (currently underway at SRTC) will be needed to determine the optimal conditions.
- The dramatic dependence of rhenium breakthrough profiles on solution composition implies that SuperLig® 639 resin performance will vary significantly with Hanford waste samples. Column performance models accounting for changes in the liquid phase composition will be highly useful for the optimization of waste processing sequences based on anticipated performance in the design column carousel.
- ***Based on discoveries divulged herein, regarding preferred sorption of potassium perrhenate salts on SuperLig® 639 resin, potassium reagent additions to the waste samples after the completion of cesium removal processing should lead to dramatic improvements in technetium removal performance. The authors recommend that design personnel consider adding a potassium reagent addition step to the baseline process.***
- High potassium feeds may require longer elution times due to retardation of the potassium salts during elution. However, there was no indication in this study of unacceptable elution performance resulting from high potassium concentrations.

No other issues were identified.

Table 1-1. Selectivity Coefficients Calculated from Sodium, Potassium, Nitrate, and Perrhenate Loading Levels.

Simulant	$K_{KNO3/NaNO3}$	$K_{KReO4/NaReO4}$	$K_{ReO4/NO3}$
AN-105	7.0	NA	>443
AZ-102	15.9	25.1	>536
AN-107	3.8	NA	31.8

">" indicates bounding values calculated for columns not loaded to saturation

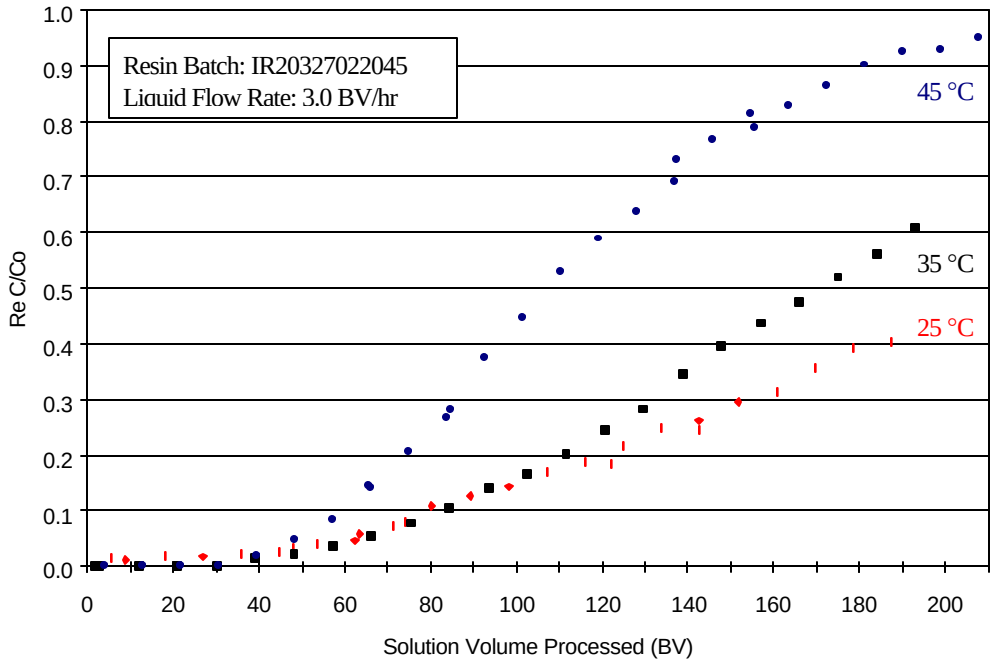

Figure 1-1. Rhenium Breakthrough Profiles Versus Temperature with AN-105 Simulant and SuperLig® 639 Resin.

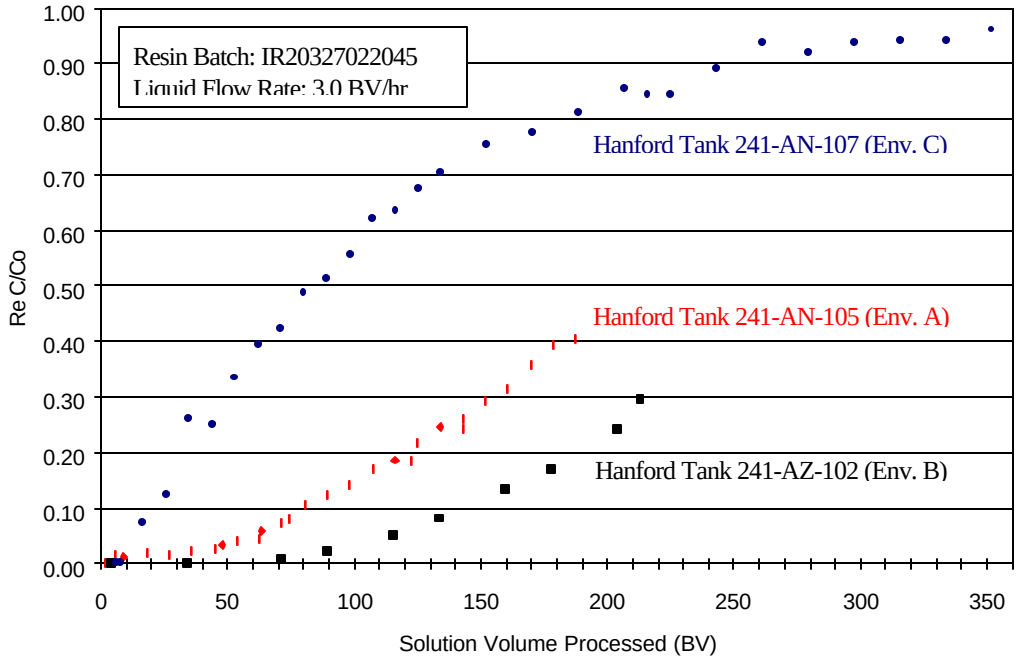

Figure 1-2. Rhenium Breakthrough Profiles Observed for Envelope A, B, and C Simulants.

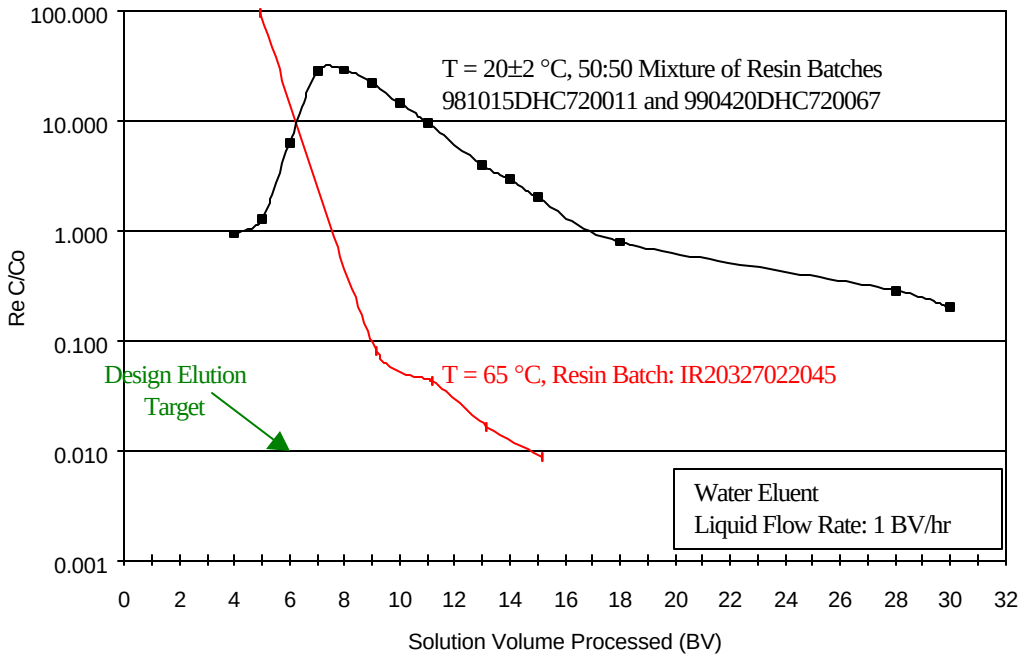

Figure 1-3. Rhenium Elution Profiles Versus Temperature from SuperLig® 639 Columns After Loading with AN-105 Simulant.

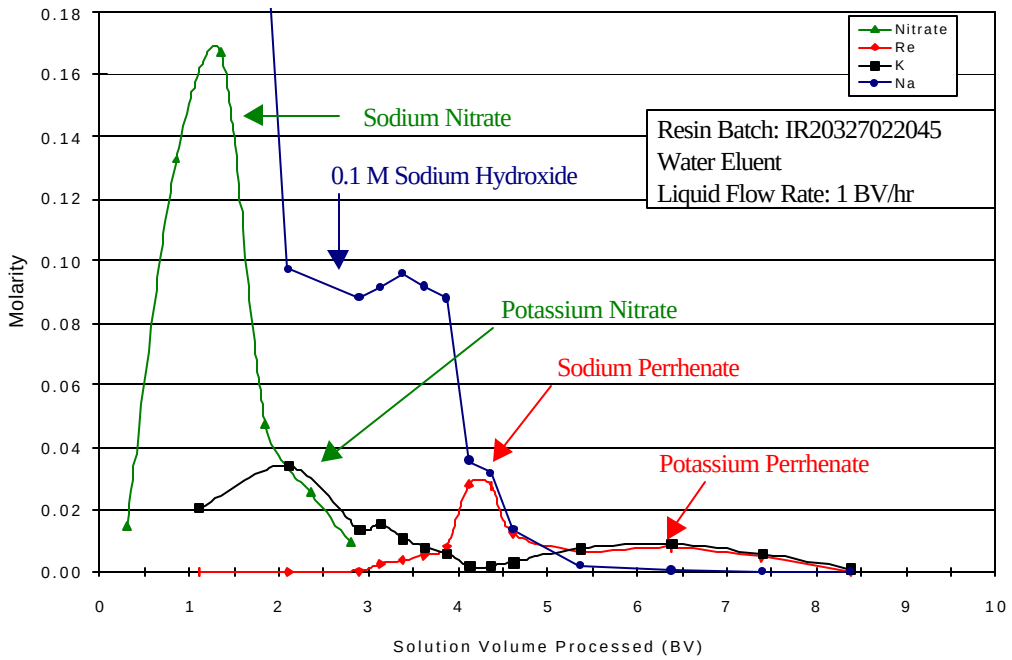

Figure 1-4. Concentration Profiles for Selected Species During 0.1 M NaOH Feed Displacement and Water Elution After Column Loading with AZ-102 Simulant.

(This Page Intentionally Left Blank)

2.0 Introduction and Background

Millions of gallons of radioactive waste were produced as a by-product of the production of nuclear weapons at various government sites across the United States. The current legacy waste inventory has essentially been reduced to two main sites (Hanford, WA and Aiken, SC) which are currently managed by the Department of Energy. Separate waste treatment processes have been developed for each site due to differences in waste composition and regulatory requirements for ultimate disposal. Development of the Hanford waste treatment strategy was originally contracted to BNFL, Inc. Based on limited initial testing and extensive nuclear waste processing experience, a treatment process was developed that included the following basic steps: 1) separation of low volume, high activity solids from high volume, lower activity supernate, 2) treatment of the supernate for the removal of specific radionuclides (strontium, transuranics, cesium, and technetium) using precipitation and ion exchange technologies, 3) evaporation of the bulk decontaminated low activity supernate, 4) vitrification of the decontaminated and concentrated supernate to generate low activity waste glasses, and 5) vitrification of high activity solids and ion exchange eluate solutions to generate concentrated high activity waste glasses. This treatment scheme was designed to minimize the volume of high activity waste requiring disposal.

Extensive testing was conducted in support of the original BNFL design for the Hanford waste treatment plant at the Savannah River Technology Center (SRTC) in Aiken, SC and at Pacific Northwest National Laboratory (PNNL) in Hanford, WA, during the period from 1998-2001. The test results indicated that the conceptual design plan was adequate and the Department of Energy subsequently contracted Bechtel National Inc. (BNI) to design, build, and perform initial operations of the waste treatment plant at Hanford. The River Protection Project - Waste Treatment Plant (RPP-WTP) for treatment of the Hanford radioactive waste is currently under construction. Final design validation and process optimization tests are continuing at SRTC and at PNNL during the design and construction phase.

The initial plant treatment schedule focuses on 10 waste storage tanks located at Hanford which have been categorized into four general waste types (or Envelopes). Envelopes A-C refer to liquid supernate samples that vary in chemical composition, while Envelope D refers to solids (sludge) primarily isolated from tank heels. Extensive testing has been conducted on actual samples in each waste category that were retrieved from the tanks. In order to minimize costs associated with sample isolation, transfer, and handling, recipes have been developed at SRTC to prepare nonradioactive simulants of various tank samples based on analysis data from actual samples. Supernate simulants have been developed for several specific waste tanks and are being used for testing throughout the RPP-WTP test program. All tank supernate compositions are caustic and are dominated by sodium salts (nitrate, nitrite, hydroxide, and aluminate are the dominant counter ions), which are generally present in high concentrations (2-10 M Na^+). All waste samples are caustic. Minor waste constituents are extensive in number and type and the targeted radionuclides for removal are present at concentrations that are several orders of magnitude lower than the concentrations of the primary constituents. These conditions require treatment

technologies that are highly selective. The baseline treatment methodology for the supernate involves evaporation or dilution to near 5 M Na^+ followed by precipitation and filtration for removal of radioactive strontium and transuranic elements (only needed for Envelope C) and ion exchange treatment for the removal of cesium and technetium.

This report summarizes the results of recent column tests with SuperLig® 639 resin in support of the RPP-WTP design. SuperLig® 639 resin is the chosen technology for removal of Tc-99 from the waste samples. Technetium primarily exists in the waste as pertechnetate ion, TcO_4^-. SuperLig® 639 resin is highly selective for pertechnetate ion and has previously been demonstrated to satisfy design requirements for the removal of technetium from actual Hanford waste samples. Extensive testing has also been conducted with SuperLig® 639 resin using waste simulants containing sodium perrhenate (ReO_4^-) as a chemical surrogate for sodium pertechnetate. Perrhenate and pertechnetate monoanions each have tetrahedral geometries resulting from symmetrical arrangement of four oxygen atoms around the central rhenium and technetium transition metal atoms. Previous studies have indicated that the two species are sufficiently similar in size to provide a reasonable basis for the substitution of perrhenate for pertechnetate (Schroeder, 1995). Previous testing with SuperLig® 639 resin has shown that pertechnetate ion uptake by SuperLig® 639 resin is higher than perrhenate uptake under identical conditions by approximately 70% (Hamm, et al., 2000). However, the diffusional properties of these two species in solution are known to be quite similar (Rard, 1991, Reid et al., 1977, Perry, 1973). Modeling efforts have demonstrated that simulant tests conducted with perrhenate ion can be utilized to predict resin performance with actual samples containing pertechnetate ion (Hamm, et al., 2000) after correction for the differences in loading levels between these two species.

Due to the proprietary nature of SuperLig® 639 resin, only limited information is available with regard to the chemical composition, structure, and function of the material. The current understanding of pertechnetate ion uptake by SuperLig® 639 resin includes the following concepts. The resin is prepared by attachment (presumably covalent molecular attachment) of a proprietary reagent to preformed, commercially-purchased polystyrene beads. The bound reagent is highly selective for pertechnetate ion in solutions (both caustic and acidic) containing high sodium ion concentrations. The number of ligand sites occupied is believed to be dependent upon the total ionic strength and the relative concentrations of various ions of interest in the liquid phase. The resin does not behave as a traditional ion exchange material. Rather, pertechnetate ion uptake occurs by extraction of neutral ion pairs from solution, with sodium pertechnetate presumably being the dominant bound species. The primary competitor for sorption sites on the resin is believed to be sodium nitrate, which is present at concentrations that are orders of magnitude larger than the pertechnetate ion concentration. Bound pertechnetate ion can be eluted from the resin with water. Sorption sites on the resin after elution are considered to be unoccupied by sorbing species. It should be noted that much of the above information was obtained through informal discussions with the resin manufacturer (IBC Advanced Technologies, Inc.). Knowledge of the molecular structure of the bound reagent would obviously allow for much greater insight with regard to the properties of this material and increase confidence in the above conceptual details of the sorption process.

Column tests have been performed with SuperLig® 639 resin using simulants of Hanford waste tanks 241-AN-105, 241-AZ-102, and 241-AN-107. These waste tanks have been categorized as Envelope A, B, and C waste types, respectively. Previous column testing (both lab-scale and pilot–scale) conducted with AN-105 simulant evaluated the impacts of solution flow rate and resin bed geometry upon rhenium breakthrough performance (King, et al., 2000, Steimke, et al., 2000). Additional tests are reported herein which evaluate the impact of temperature upon rhenium breakthrough performance during column loading with AN-105 simulant. The collective column test results, as well as additional tests recently performed at SRTC to determine fundamental diffusional parameters impacting sorption kinetics (Duffey, et al., 2003), will serve as primary data sources updating the model methodology used to predict full-scale column performance. To address compositional impacts on performance, additional tests were performed with Envelope B and C simulants. Results of these tests provide insights as to the impacts of solution composition on column performance. The data will be utilized to evaluate model predictions of column performance with these waste envelopes based on sorption isotherms developed from small-scale batch contact and sorption kinetics tests with various solution compositions.

All columns were eluted with water at 65 °C at the conclusion of the loading tests. Previous testing involved column elution at ambient temperature with water or 0.5 M nitric acid. Limited studies performed at SRTC in the past indicated that high temperatures significantly improve the elution performance of SuperLig® 639 resin (Steimke, et al., 2000). Elution of SuperLig® 639 resin with water at 65 °C is currently being considered due to slow pertechnetate desorption kinetics previously observed at ambient temperature. Comparison of the elution profiles obtained at 65 °C to previously reported data allows for evaluation of the impact of higher temperature on desorption kinetics. Limited testing was also conducted to determine whether high temperature column elution results in significant physical degradation of the resin particles due to thermal shock during the various processing cycles.

(This Page Intentionally Left Blank)

3.0 Experimental

3.1 Simulant and Reagent Preparation and History

0.1, 0.25, and 1.0 M NaOH solutions utilized for testing were prepared from NaOH pellets and filtered prior to use. Deionized (Millipore) water was used for all reagent preparations and for column elution. All simulant solutions were prepared according to procedures published by Eibling, et al. (2001). The simulant recipes were based on analysis data for Hanford waste tanks 241-AN-105, 241-AZ-102, and 241-AN-107. Reagent grade chemicals were utilized for all preparations.

The AN-105 and AZ-102 simulants were prepared in 2002 specifically for the RPP ion exchange test program and the simulant compositions included all RCRA hazardous recipe components. Prior to use, the solutions were filtered through 0.45 µm Nalgene® Nylon filter units and processed through SuperLig® 644 ion exchange columns for cesium removal (Hassan, et al., 2002a, Hassan, et al., 2002b). The composited cesium column effluents were then spiked with sodium perrhenate and utilized for SuperLig® 639 column testing. Since the SuperLig® 639 column tests were conducted months after the cesium column testing, the simulant solutions were filtered again prior to use to remove potential fine particulates that might lead to column fouling. Few solids were visually observed in the solutions prior to filtration or in the filter cups after filtration. The densities and viscosities of the filtered AN-105 and AZ-102 simulants at ambient temperature (20±2 °C) are provided in Table 3-1.

The AN-107 simulant was an archive sample generated in 1999 at the Thermal Fluids Laboratory (currently referred to as the Engineering Development Laboratory) at SRTC during testing conducted for the previous WTP contractor as part of the strontium/transuranics removal program (Duignan, 2000). The AN-107 sample was originally prepared at 5 M Na^+, but was subjected to caustic adjustment and strontium nitrate and sodium permanganate addition, followed by cross-flow filtration as part of the 1999 test program. The sample was subsequently stored in a 55 gallon drum and then retrieved for ion exchange testing. The sample did not contain RCRA hazardous components. Based on scoping tests conducted on a portion of the sample that had been spiked with RCRA metals, it was decided that inclusion of these species did not significantly impact ion exchange testing. Therefore, the archived sample was utilized for subsequent testing without the addition of RCRA hazardous components. The AN-107 sample was green in color (as opposed to the brown color typically observed prior to precipitation) and contained considerable amounts of white solids, which were removed by filtration through 0.45 µm Nalgene® Nylon filter units. The sample was processed through SuperLig® 644 ion exchange columns for cesium removal (Hassan, et al., 2002c). The composited effluent was then spiked with sodium perrhenate and filtered again prior to SuperLig® 639 column testing. Based on the known chemical properties of rhenium, it is assumed that all rhenium in the simulant exists as perrhenate ion, ReO_4^-. This contrasts with technetium, which is known to exist as a mixture of pertechnetate (TcO_4^-) and nonpertechnetate forms in actual Envelope C waste samples. Pertechnetate ion is more easily reduced than perrhenate ion and presumably reacts with organic species in the AN-

107 waste to form nonpertechnetate species. The density and viscosity of the filtered AN-107 simulant at ambient temperature (20±2 °C) are also provided in Table 3-1.

The concentrations of selected species added during initial simulant preparation based on the recipes reported by Eibling, et al. (2001) are provided in Table 3-2. Table 3-3 provides the average measured concentrations of selected species obtained for each simulant sample prior to SuperLig® 639 column testing, but after the completion of other testing (precipitation and cesium column tests). Note that differences in the data in Tables 3-2 and 3-3 may be due to compositional changes resulting from the cesium and or precipitation testing. In this study, a total of nine column tests were conducted using the simulants indicated in Table 3-3 (where each test has been assigned a number based on the order of completion). Individual sample analysis data for the feed solutions is provided in Appendix A.

3.2 Resin Handling, Properties and History

SuperLig 639 resin is manufactured by IBC Advanced Technologies, Inc. in American Fork, Utah. Individual resin batches were generally received from the manufacturer as essentially dry beads. More recent resin samples were received as water slurries. The composition of the material is considered proprietary.

3.2.1 Experiments 1-4

A sample of SuperLig® 639 resin from manufacturer batch #00082CTC-8-39 was received at SRTC prior to the initiation of simulant column testing for the RPP-WTP program. This resin batch was believed to have a higher density than previous resin batches used at SRTC. The higher density form was the product of a research effort (conducted by IBC and funded by BNFL) that was specifically intended to minimize resin floating in 5 M Na^+ waste solution (Breuning, 2001). Initial evaluation of this material at SRTC revealed that this "high density" form actually had a lower material density than previous resin batches and exhibited a greater propensity to float in 5 M Na^+ simulant solutions. Table 3-4 summarizes the physical and chemical properties measured for a number of SuperLig® 639 resin batches tested at SRTC. Distribution coefficients, K_d, were calculated as indicated in Equation 3-1.

$$K_d = [(C_i/C_f)-1]*[V/M] \qquad \text{Eqn. 3-1}$$

C_i = initial solution rhenium concentration
C_f = final solution rhenium concentration
V = solution volume
M = dry resin mass

The bulk dry bed density of batch #00082CTC-8-39 was actually higher than previous batches due to a change in the particle size distribution for this sample. Presumably, the resin manufacturer mistakenly

assumed that higher bulk bed density necessarily implied a higher material density. This lead to the claim that a higher density form had been prepared. Particle size distributions determined by chord length analysis for various manufacturer batches are provided in Figure 3-1.

Based on this information, the RPP-WTP customer requested that simulant column testing be conducted with an archived SuperLig® 639 resin sample that had been used in previous testing at SRTC (batch #990420DHC720067). A single sample of resin from batch #990420DHC720067 was subsequently used for four column tests conducted with AN-105 simulant (Experiments 1-4). Table 3-5 provides the characterization data and processing history for each resin sample used for column testing during the laboratory-scale simulant test program. SuperLig® 639 resin batch #990420DHC720067 was originally received from the manufacturer as essentially dry beads (typical f-factor for as-received resin >0.95; f-factor = [vacuum dried resin mass]÷[original resin mass]). The archived resin sample was stored dry at SRTC. Prior to use, the resin was wetted with deionized water, heated overnight in a 10:1 (water:resin) volume mixture of deionized water at 65 °C, filtered on a 0.45 μm Nalgene® Nylon filter, and vacuum dried to constant weight (26.4 °C,–29 in. Hg). The resin was then stored in a polyethylene bottle until use.

F-factor determinations conducted on duplicate samples of resin batch #990420DHC720067, which were collected at the same time as the sample used for experiments 1-4, indicated no detectable desorption of water (i.e. no mass correction needed for adsorbed water, f-factor = 1.0). The dry resin sample to be used for the column experiments was weighed and transferred to a polyethylene bottle. The resin was soaked in a 10:1 volume mixture of deionized water for 8 hours. Most of the water was decanted away and 1.0 M NaOH solution was added to the bottle to give a 10:1 volume mixture. The resin was again allowed to soak in solution for 8 hours before the slurry was carefully transferred into the test column. During transfer the slurry was intermittently swirled in the polyethylene bottle to maintain a homogeneous sample. Free-fall of the resin beads into the column under static flow conditions resulted in the formation of a packed bed. The bed height did not change significantly during subsequent drainage of excess fluid from the column. Due to the relatively high material density of this resin batch and the fact that this material had previously been shown not to float in AN-105 simulant, the resin bed was not restrained with quartz wool and glass beads as described below for tests with more recent resin batches.

3.2.2 Experiments 5-9

Due to concerns that resin batch #990420DHC720067 had degraded (arising from lower than expected column and batch contact performance after storage), the RPP-WTP customer requested that the AN-105 column tests be repeated with a resin batch that had been received at SRTC after the initiation of the first series of column tests. Three column tests (Experiments 5-7) were subsequently conducted with AN-105 simulant using separate samples of SuperLig® 639 batch #IR20327022045. Chord length analysis of each resin sample (conducted after the samples were removed from the column) confirmed that the particle size distributions were virtually identical, indicating that sampling

variability was minimal (Figure 3-4). The mean particle diameter calculated from the chord length distributions was 481 µm. A single sample of resin from batch #IR20327022045 was used for column tests with the AZ-102 and AN-107 waste samples (Exp. 8-9). The estimated mean particle diameter for this sample was 475 µm and the distribution was virtually identical to the distributions shown in Figure 3-4.

SuperLig® 639 resin batch #IR20327022045 was received from the manufacturer as a water slurry in a 1 gallon polyethylene bottle. Before collecting a subsample of the bulk slurry sample for testing, the 1 gallon bottle was gently and repeatedly tumbled end-over-end to homogenize the sample. A subsample of resin was then collected by repeatedly dipping a 50 mL beaker into the sample to give a final volume near 150 mL. The 1 gallon bottle was also gently tumbled at random times between sampling events. Prior to use, the bulk of the shipping liquid was decanted from the material and the resin was washed several times with deionized water, while being careful to continually maintain the resin in a wetted state. The resin was then heated overnight at 65 °C in a ten-fold volume excess of deionized water. The bulk of the water was immediately decanted away prior to cooling of the slurry. The sample was then washed several times and stored in water.

Resin samples used for testing were never fully dried prior to use. Samples to be used for column testing were collected by transferring the water/resin slurry to a disposable Nalgene® Nylon filter unit and applying vacuum (-20 in. Hg) to drain the free-flowing liquid from the resin. Air was then aspirated through the wet resin sample for ~60 seconds. The top of the filter unit was covered with a piece of latex rubber that was attached to the filter with a rubber band. The sample was then exposed to static (very low flow) vacuum conditions for a total of 10 minutes. The sample of resin to be used for column testing was then quickly transferred from the center of the filter unit to a small beaker and weighed. Immediately following isolation of the column sample, duplicate, small resin samples (~0.1 g) were collected from the filter and weighed for f-factor determination. This procedure allowed for accurate measurement of the sample mass without fully drying the sample. Sample f-factors were determined by placing the duplicate 0.1 g resin samples in the vacuum oven at 50 °C and -20 in. Hg. The samples were periodically removed from the oven, cooled in a dessicator, and weighed, until a constant value was observed. F-factors obtained for resin samples handled in this way were consistently 0.70 ±0.01. The wet resin sample for testing was quantitatively transferred to the column as described above for Experiments 1-4. Due to the low material density of resin batch #IR20327022045 and the known bouyancy of the material in 5 M Na^+ simulant, it was necessary to restrain the resin bed for each test by carefully placing quartz wool and 2 mm glass beads above the bed after column packing.

3.2.3 Thermal Shock Testing (Exp. 10)

A subsample (~120 mL) of SuperLig® 639 resin was collected from batch #IR20327022045 using the sampling procedure described above for Experiments 5-9. The sample was kept under water during collection and thereafter. The bulk of the shipping liquid was decanted away and the resin was washed 6 times with separate 100 mL samples of deionized water prior to use.

3.3 Equipment

3.3.1 Columns

Jacketed, borosilicate glass columns were prepared by glass blowers at SRTC for testing. Nominal 1.5 cm ID columns were utilized for experiments 1-7 (Figure 3-3). The actual measured inside diameter of each column used for testing is provided in Table 3-5. The inner portion of the column apparatus containing the ion exchange material was prepared from 17 mm OD standard wall tubing and the outer jacket was prepared from 38 mm OD medium wall tubing. A scale was placed on the inner tubing to monitor the height of the resin bed and the liquid level. The total height of the resin bed reservoir was ~10 cm. Recirculator lines were attached to the jacketed portion of the column using machined polyethylene bushings with Viton® O-ring seals. The head was attached to the column using a Rudivis-type ground-glass joint. The column head was prepared from medium wall 19 mm OD glass tubing. The column head contained attachments for the inlet feed line, a thermocouple, and a spring-activated pressure relief valve. The thermocouple extended through the center of the column head to just above the surface of the resin bed. The thermocouple was calibrated by the Standards Laboratory at SRTC. The pressure relief valve was set to activate at 5 PSI. All glass components of the apparatus were coated with a clear layer of polyvinyl chloride for safety reasons. After assembly, the column headspace was airtight and the columns were generally operated with a slight positive pressure (<1.5 PSI).

The bottom portion of the small column apparatus was specifically designed to minimize liquid mixing and hydraulic end (dispersive) effects, since the resin bed path length was quite short (~6 cm) in experiments 1-7. A 100-mesh stainless steel screen that was attached to a stainless steel ring was placed in the bottom of the column to support the resin bed. The column was designed and the screen was sized such that the bottom of the resin bed only contacted screen that was unobstructed by the support ring. This design minimized disturbance of the liquid flow patterns at the bottom of the resin bed. The void space below the screen was filled with 1 mm diameter glass beads to reduce dead spaces within the liquid phase. Utilizing a glass bead size similar to the resin bead diameter should minimize perturbation of the liquid flow properties as fluid exits the bottom of the resin bed. The beads and screen were supported by a custom-machined polyethylene bushing with a taper in the inner flow cavity which constricted the diameter from ~10 mm to ~2 mm across a vertical distance of ~1 cm. This design feature allowed for smooth, gradual constriction of the fluid stream exiting the column and discouraged the formation of flow eddies. A small stainless steel mesh funnel was placed inside the taper to prevent pluggage of the opening by the glass beads. A three-way Whitey 40 Series $^{1}/_{16}$" ID stainless steel ball valve was attached to the bottom of the bushing for flow control.

Jacketed 1 inch ID columns were prepared for tests with AZ-102 and AN-102 simulants using 28 and 44 mm OD standard wall tubing for the inner and outer column walls, respectively. A photograph of the large column is provided in Figure 3-4. The large column design was the same as described above except as noted below. The column head contained additional attachments for a pressure gauge and a

vent (located on the back). The total height of the resin bed reservoir was ~30 cm. Since end effects should not be as pronounced in a large column being operated at a relatively slow flow rate (3 BV/hr) and assembly of the smaller column was tedious, a simpler design was utilized for the large column. The resin in the large column was supported by a 100 mesh stainless steel screen that was held in place by a polyethylene bushing. The column design allowed for minimal mixing volume below the resin bed. The bushing was not tapered as described above for the small column and was attached to a $^{1}/_{8}$" ID stainless steel valve to stop liquid flow as needed.

3.3.2 Supporting Equipment

The photograph provided in Figure 3-5 shows the general layout for experimental equipment used during the column testing. All solutions were passed through the columns in the downflow direction using Fluid Metering Incorporated QG50 positive displacement pumps with ¼" and $^{3}/_{8}$" piston sizes. Solution was transferred to the column head through $^{1}/_{8}$" OD polyethylene tubing. $^{1}/_{16}$" OD polyethylene or PEEK® brand tubing was used for column effluent lines. The effluent solution was transferred through the ICP-ES sampling apparatus followed by a Spectrum Chromatography IS-95 Interval Sampling system. Digital balances used during the testing were calibrated by the SRTC Standards Laboratory and the calibration was checked in the lab prior to use each day. The column temperature was maintained during all tests using a Haake DC-5 recirculating unit. Column feed solutions were also preheated as needed by immersing the feed bottle in a temperature-controlled water bath.

3.3.3 Analysis Equipment and Methods

Selected samples collected during testing were submitted for analysis to the Analytical Development Section (ADS) at SRTC. Analysis methods included Inductively Coupled Plasma – Emission Spectroscopy (ICP-ES), Ion Chromatography – Anion (IC Anion), Total Base, Free OH^-, Total Inorganic Carbon (TIC), Total Organic Carbon (TOC), and Microtrac particle size analysis. Quality assurance and control procedures and blank and standard results for each analysis set are documented and maintained by ADS and are not reported here.

Non-ADS analysis methods included density, viscosity, optical microscopy, chord-length analysis, and on-line ICP-ES (discussed below). Liquid density measurements were conducted in duplicate by measuring the mass of sample required to fill a 100 mL volumetric flask at ambient temperature (20±2 °C). Simulant viscosity measurements were also conducted in duplicate at ambient temperature using a Cannon-Fenske Viscometer. Solid bulk dry densities were measured for the resin samples by transferring at least 20 mL of dry resin into a 1 inch ID graduated cylinder. Resin material density measurements were conducted using a pycnometer filled with water. 2-3 mL of resin was used for each test and the total volume of the vessel was 10 mL. All pycnometer measurements were conducted in duplicate at ambient temperature. The wetted resin samples were exposed to repeated vacuum cycles to remove entrapped air prior to each material density determination. Photographs were taken of the

resin under magnification using an optical microscope fitted with a digital camera to evaluate the impact of thermal cycling.

Chord length analysis was conducted using a Lasentec FBRM (Focused Beam Reflectance Measurement) M400L. Raw chord length distributions are complicated by the fact that any given particle contains a number of measurable chords depending upon the particle shape. For samples with essentially spherical particles, like SuperLig® 639 resin, the probability of measuring chords that are not representative of the true particle diameter is known and standard corrections can be applied to the data to correct for this effect. Specifically, the chord length data can be converted to a form that is nearly equivalent to the particle spherical equivalent diameter (SED), which is a standard output from more traditional particle size analysis methods. All of the chord length data was converted to the SED-like form, which is referred to as the "square-weighted chord" in the Lasentec software. (Note: Even though the Lasentec software term is "square-weighted", it actually refers to a cubic or volume-type correction.)

3.3.4 On-line ICP-ES Analyzer

A detailed description of the on-line ICP-ES system is provided in a separate report (Spencer, 2003). The monitor included a Thermo Jarrell Ash IRIS echelle spectrometer with a fiber optic interface connected to a remote plasma torchbox. On-line ICP-ES data was collected at 15-minute intervals throughout each column experiment. The basic sampling mechanism involved diversion of a small subsample (~70 µL) of column effluent solution through a collection loop that was injected into a plasma torch for analysis. During each sampling event a volume of yttrium standard solution comparable to the sample size was injected into the effluent stream. Dilution of the composited effluent should have been <1% as a result of ICP-ES sampling events during column loading.

3.4 Procedures

3.4.1 Column Testing (Experiments 1-9)

For Experiments 1-4, the SuperLig® 639 columns were pretreated with 6 bed volumes (BV, 1 BV = resin bed volume measured after column packing) of 1.0 M NaOH solution at a flow rate of 3 BV/hr just prior to column loading. 1.0 M NaOH had been used for resin pretreatment during testing conducted for the previous WTP contractor. After completion of Experiments 1-4, the column pretreatment solution was changed to 0.25 M NaOH at a flow rate of 1 BV/hr for 6 hours in order to be more consistent with current plant design processing conditions. Column pretreatment for all subsequent tests (Experiments 5-9) used the new plant design protocol.

The solution liquid level during the column tests was generally maintained at a height above the resin that was approximately half the resin bed height. The resin bed height, liquid level, column temperature, and head pressure were monitored throughout the experiments. No changes were observed in the resin bed height for any experiments during column operation. The nominal flow rate during column loading was 3

BV/hr. Column loading was considered to begin at the moment that simulant solution contacted the NaOH solution above the resin. Upon initial contact, the head space was visually monitored for the formation of solids that could lead to column fouling. Solids were not observed for any experiments. Analysis samples were generally collected either manually or with the IS-95 autosampler after processing 5 and 10 BV of simulant, and at ~9 BV increments throughout the remainder of column loading. Loading sample volumes were typically 4 mL. Liquid flow rates were checked for each sampling event by measuring the mass of the sample collected in a known time period. Periodic flow rate checks were also performed using larger collection volumes for higher accuracy. These flow rate checks were utilized to monitor the flow during column operation and adjust the pump speed as necessary. The final flow rate value for each column run was calculated from the volume of the bulk effluent solution (after correction for the samples collected) and the processing time. Flow rate and temperature data for each experiment are provided in Table 3-6.

After completion of column loading, the liquid level was decreased to within 1 cm of the top of the resin bed or the glass beads by briefly pumping air into the column. 0.1 M NaOH was then pumped into the column to restore the liquid to the original level. This required closing the valve at the bottom of the column and venting the column head momentarily. 0.1 M NaOH solution was then pumped through the column at a flow rate of 3 BV/hr for one hour in order to displace the simulant from the column. The column temperature during feed displacement was maintained at the temperature of the previous column loading phase. Column effluent samples were collected during the feed displacement phase in 10 or 20 minute increments (0.5-1.0 BV increments) depending on the experiment. During the final twenty minutes of feed displacement the column temperature was increased to 65 °C in preparation for column elution.

The elution phase was considered to begin at the moment that deionized water contacted the 0.1 M NaOH feed displacement solution above the resin bed. The nominal liquid flow rate during elution was 1 BV/hr for all experiments. The actual measured flow rates are provided in Table 3-6 for all experiments. 2 mL samples of eluate were collected at ~2 BV increments for ICP-ES analysis (ADS). For selected experiments, ~4 mL samples were collected for IC anion analysis in order to identify competitor species in the eluate. The columns were generally eluted for 24 hours before the experiments were stopped.

ADS results for individual samples from Experiments 1-9 which were collected during column loading, feed displacement, and elution are provided in Appendices B-J, respectively. The raw ICP-ES data was provided in a separate report (Spencer et al., 2003). Table 3-6 identifies which experiments correspond to the file names provided in the Spencer report. Calibrated on-line ICP-ES data is also provided in Appendices B-J, along with the cumulative bed volumes of solution processed at each sampling event. Rhenium data from the on-line monitor for Experiments 1-3 was calibrated based on the instrument response with a 50 mg/L rhenium standard. For Experiments 5-9, the raw, on-line ICP-ES data was calibrated using analytical results for carefully selected samples that were submitted to ADS.

3.4.2 Thermal Shock Testing (Exp. 10)

A sample of SuperLig® 639 resin that had been washed repeatedly with deionized water at ambient temperature (22±2 °C) was transferred to a jacketed beaker containing ~400 mL of deionized water at 25±1 °C. After 30 minutes, duplicate 2 mL samples were collected for analysis by optical microscopy and Microtrac particle size analysis. An additional 5 mL sample of resin was collected for chord length analysis. Care was taken not to crush or otherwise abrade the resin particles. Samples were collected with a small glass ladle that was used to gently stir the resin prior to sampling. Each sample was the composite of several collection events with the ladle. A volume of liquid was collected with each sample to give a liquid height that was approximately twice the resin height. Most of the water was then decanted away from the bulk resin sample. The resin was transferred over a time period of ~1 minute directly into a second jacketed beaker containing ~400 mL of deionized water at 65±1 °C. A minimal amount of deionized water was utilized to transfer resin beads that could not be poured into the second beaker. The temperature of the slurry was measured with a calibrated digital thermocouple immediately after all of the resin was transferred. The resin was left in the second beaker for a total of thirty minutes. The slurry temperature was measured again after 5 and 30 minutes of contact. The bulk of the water was then decanted from the beaker. The resin was immediately transferred back to the original jacketed beaker, which again contained ~400 mL of deionized water at 25±1 °C. The slurry temperature was measured after 0, 5, and 30 minutes of contact. After the 30 minute time period, samples were collected as described above. This completed Cycle 1 of the thermal shock testing. A total of 10 cycles were conducted with the same resin sample. 5 mL samples were collected for chord length analysis from each cycle. 2 mL samples for Microtrac and optical microscopy analysis were collected after cycles 1, 5, and 10.

Table 3-1 Density and Viscosity Data for Hanford Waste Simulants.

Simulant	Experiment #	Density[1] (g/mL)	Viscosity[1] (cP)
AN-105	1-7	1.234 (0.0014)	2.98 (0.015)
AZ-102	8	1.232 (0.0000)	3.05 (0.060)
AN-107	9	1.255 (0.0099)	3.37 (0.065)

[1] Density and viscosity data determined at ambient temperature (20±2 °C)

Table 3-2. Expected Concentrations of Selected Species in Original Hanford Simulants Based on Reagents Added.

Simulant	AN-105 [M]	AZ-102 [M]	AN-107[1] [M]
Na	5.000	5.000	5.000
K	0.090	0.153	0.027
Al	0.687	0.053	0.008
S	0.004	0.325	0.051
P	0.003	0.009	0.007
Cr	0.012	0.037	0.000[3]
Mg	1.04E-04	6.94E-05	6.07E-04
Ca	4.66E-04	5.08E-03	1.59E-03
Sr	0.000[2]	4.34E-06	4.46E-05
Ba	0.000[2]	1.08E-05	3.20E-05
Cd	1.37E-05	3.26E-05	0.000[3]
B	2.21E-03	1.08E-05	1.91E-03
Si	3.51E-03	3.75E-02	0.000[2]
Mn	0.000[2]	6.94E-05	6.01E-03
Fe	0.000[2]	3.79E-04	1.79E-02
Ni	0.000[2]	6.94E-05	5.32E-03
Mo	4.00E-04	1.14E-03	2.20E-04
Pb	1.20E-04	5.43E-05	0.000[3]
Nitrate	1.243	0.515	2.188
Nitrite	1.126	1.243	0.784
Sulfate	0.004	0.325	0.051
Phosphate	0.003	0.009	0.007
Chloride	0.120	0.013	0.030
Fluoride	0.005	0.101	0.004
Oxalate	3.24E-03	0.061	0.006
Formate	2.99E-02	0.000[2]	0.136
Added Hydroxide	1.60	0.206	0.012
Carbonate	0.098	0.964	0.825
TIC	0.098	0.964	0.825
TOC	0.140	0.949	1.981

[1] The AN-107 simulant solution was significantly altered from the original composition during strontium/transuranics precipitation testing.

[2] Indicates species absent from the Eibling recipe (Eibling et al., 2001) and not added to simulant.

[3] Indicates species included in the Eibling recipe (Eibling et al., 2001) but not added to simulant.

Table 3-3. Measured Molar Concentrations of Selected Species in Hanford Simulants Used for SuperLig® 639 Column Testing.

Simulant (Experiment #)	AN-105 (1-4)	AN-105 (5-7)	AZ-102 (8)	AN-107 (9)
Na	4.959	4.866	4.665	5.742[1]
K	0.095	0.094	0.147	0.035
Al	0.548	0.556	0.048	0.009
S	0.006	0.006	0.310	0.055
P	0.003	0.002	0.009	0.010
Cr	0.011	0.011	0.026	3.65E-06
Mg	<6.23E-06	<6.23E-06	<6.23E-06	<6.23E-06
Ca	4.82E-04	1.50E-05	1.71E-03	3.56E-03
Sr	4.36E-07	<7.99E-07	6.88E-06	1.04E-03[1]
Ba	1.62E-06	1.75E-06	1.95E-06	<1.75E-07
Cd	2.64E-05	2.02E-05	<1.04E-06	<1.04E-06
B	2.19E-03	2.25E-03	9.12E-04	1.92E-03
Si	4.42E-03	3.69E-03	1.34E-04	3.43E-04
Mn	<1.48E-06	<1.48E-06	<1.48E-06	4.50E-05[2]
Fe	3.23E-05	3.23E-05	8.52E-06	3.11E-04[2]
Ni	2.88E-05	6.54E-06	<4.60E-06	0.011
Mo	3.82E-04	3.86E-04	1.05E-03	2.21E-04
Pb	8.18E-04	8.07E-04	<5.11E-05	<5.11E-05
Re	7.32E-05[3,4]	6.27E-05[4]	2.07E-04[4]	3.06E-05[4]
Nitrate	1.183	1.073	0.472	2.564[1]
Nitrite	1.130	1.124	1.131	0.847
Sulfate	0.006	0.005	0.280	0.051
Phosphate	0.002	0.002	0.011	0.027
Chloride	0.100	0.100	<5.64E-04	0.028
Fluoride	NM[5]	NM[5]	0.072	0.094
Oxalate	0.002	0.002	0.013	0.011
Formate	0.032	0.031	0.168	0.143
Total Base	2.375	2.325	1.215	1.240
Free Hydroxide	1.41	1.345	0.1835	0.553[1]
TIC (mg/L)	3245	3820	NM[5]	NM[5]
TOC (mg/L)	1540	1420	NM[5]	NM[5]

[1] Indicates species whose concentrations were expected to increase due to precipitation processing

[2] Indicates species whose concentrations were expected to decrease due to precipitation processing

[3] Average [Re] excluding Experiment 1

[4] Perrhenate concentration assumed to be equal to total rhenium concentration

[5] Not measured for this sample.

Table 3-4. Chemical and Physical Property Data for SuperLig® 639 Batches.

Resin Batch	K_d[1] (mL/g)	Final [Re] (mg/L)	Particles Floating[2] (%)	Bulk Dry Density[3] (g/mL)	Material Density[4] (g/mL)	Mean Particle Diameter[5] (mm)
980624001DC	199	2.40	0-10	0.489	1.219	NM[6]
981015DHC720011	390	1.41	30-50	0.468	1.147	670
990420DHC720067	512	1.16	0	NM[6]	1.237	670
00082CTC-8-39	425	3.38	100	0.534	1.128	510
IR20327022045	409[7]	4.75	100	NM[6]	NM[6]	481

[1] distribution coefficients determined in AN-105 simulant; orbital shaker 24-hour contact; phase ratio 100:1; T = 20 ±2 °C; unless otherwise indicated

[2] visually estimated in 5 M Na^+ AN-105 simulant (solution density 1.23 g/mL)

[3] grams dry solid/bulk bed volume of dry packed solid measured in a graduated cylinder

[4] grams dry solid/volume wet resin particles (in water); determined by pycnometer

[5] mean determined by Lasentec chord length analysis (analogous to volume-based mean determined by traditional methods)

[6] not measured for this batch

[7] measured by kinetics test method after 24-hour contact, phase ratio 200:1 (Duffey, et al., 2003)

Table 3-5. SuperLig® 639 Resin Bed Characterization Data and Processing History.

Expt	Date[1] (2002)	Resin Batch	Resin Mass[2] (g)	Column ID (cm)	Column Bed Volume (mL)	Column Bed Density (g/mL)	Initial Conditioning/ History	NaOH Pretreatment Solution [M]
1	1/8	990420DHC720067	4.8736	1.60	10.10	0.4825	vacuum dried	1.0
2	1/15	990420DHC720067	4.8736	1.60	10.10	0.4825	used for Exp. 1	1.0
3	1/21	990420DHC720067	4.8736	1.60	10.10	0.4825	used for Exp. 2	1.0
4	2/5	990420DHC720067	4.8736	1.60	10.10	0.4825	used for Exp. 3	1.0
5	7/17	IR20327022045	6.3283	1.45	10.07	0.6286	not dried	0.25
6	7/29	IR20327022045	6.3285	1.45	10.15	0.6235	not dried	0.25
7	8/19	IR20327022045	6.3286	1.45	10.40	0.6086	not dried	0.25
8	9/3	IR20327022045	46.2471	2.50	74.58	0.6201	not dried	0.25
9	9/17	IR20327022045	46.2471	2.50	74.58	0.6201	used for Exp. 8	0.25

[1] indicates date that the experiment was started

[2] mass corrected for water content

Table 3-6. Flow Rate and Temperature Data for SuperLig® 639 Column Experiments.

Expt.	Loading Temp. (°C)	Loading Flow Rate (BV/hr)	Elution Temp. (°C)	Elution Flow Rate (BV/hr)	Spencer Report Filename[1]
1	25.0	2.98	64.8	1.17	wkjan7b
2	44.5	3.05	64.8	1.07	wkjan14a
3	35.0	3.01	65.0	1.02	wkjan21a
4	25.3	2.92	64.6	0.98	WKFeb5Run4
5	25.8	2.99	63.5	1.15	k071702a
6	35.1	3.02	64.7	0.95	wkjul29
7	44.8	2.95	65.0	0.94	wkAug18_2002run1
8	25.1	2.95	65.1	0.99	RunSept42002wkdata
9	25.0	3.02	64.9	1.07	wksep162002

[1] see Spencer et al., 2003

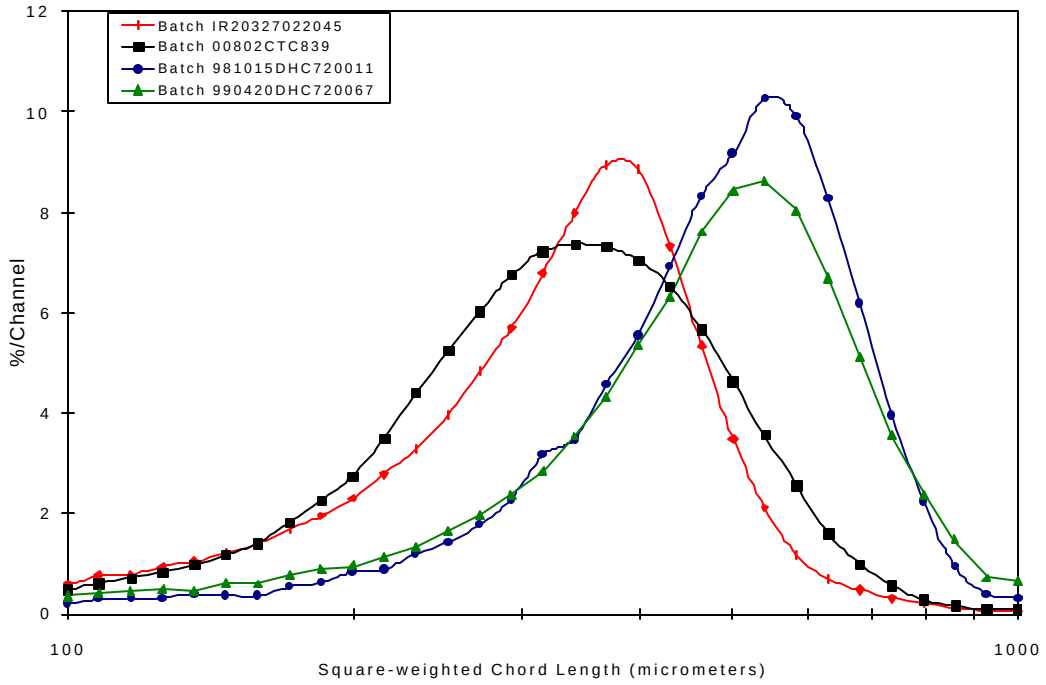

Figure 3-1. Particle Size Distributions Determined by Chord Length Analysis for Various SuperLig® 639 Batches.

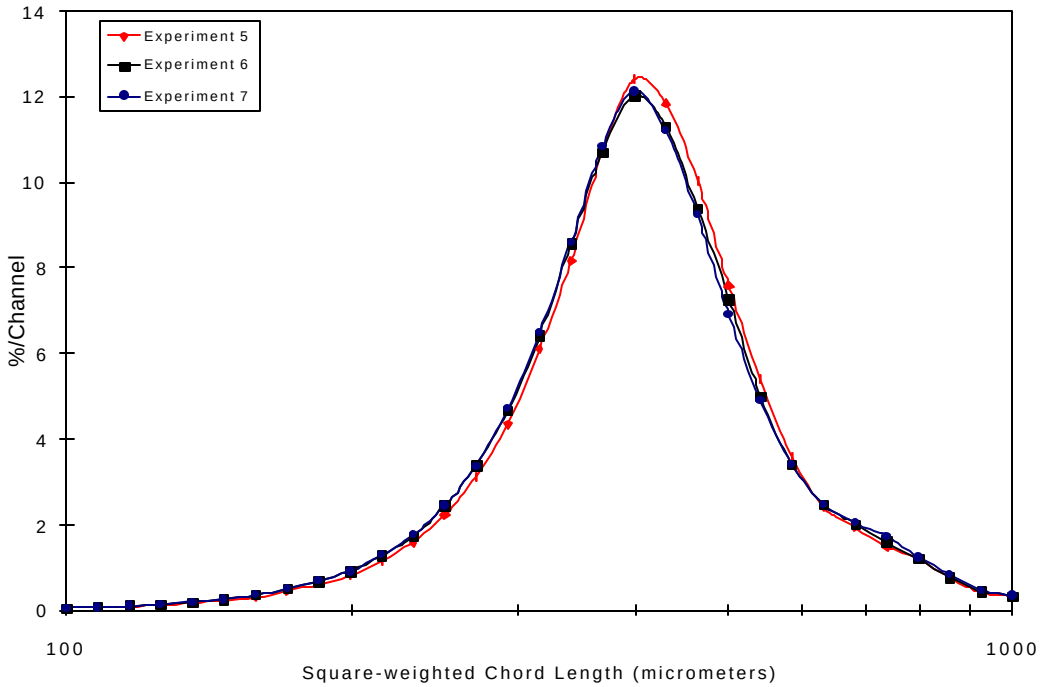

Figure 3-2. Particle Size Distributions Determined by Chord Length Analysis for SuperLig® 639 Samples from Batch IR20327022045 Used for Experiments 5-7.

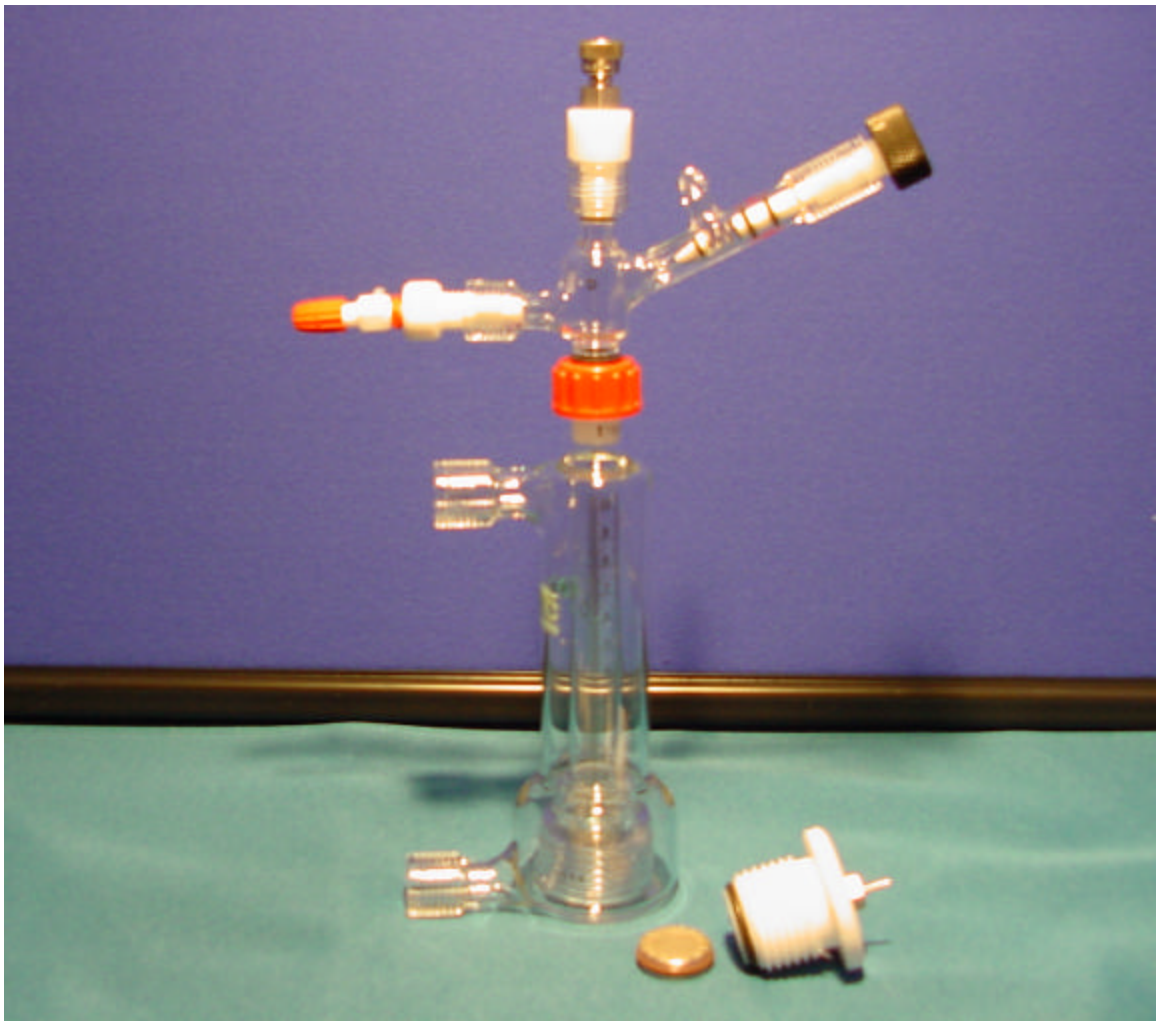

Figure 3-3. Photograph of the 1.5 cm (nominal) ID Column Used for Experiments 1-7.

Figure 3-4. Photograph of the 1 inch ID column Used for Experiments 8-9.

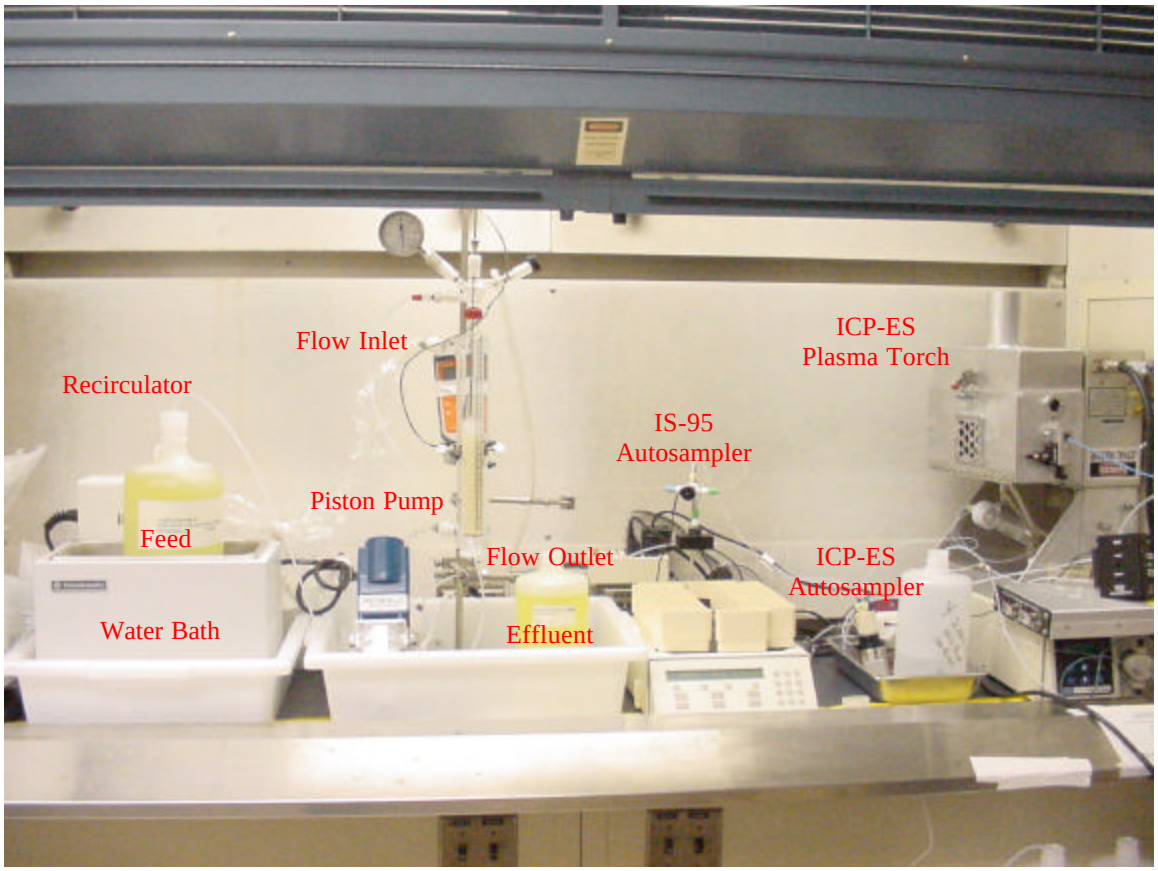

Figure 3-5. Photograph of the Experimental Equipment Used for SuperLig® 639 Column Testing.

4.0 Results and Discussion

4.1 Experiments 1-4: Variable Temperature Column Tests with AN-105 Simulant and Resin Batch #990420DHC720067

4.1.1 Loading

Rhenium (or, more specifically, perrhenate) loading tests were conducted at 25, 35, and 45 °C with AN-105 simulant to determine the impact of temperature on column loading. The same resin sample from batch #990420DHC720067 was utilized for all tests after thorough elution of the resin bed at the conclusion of each loading experiment. The resin sample had been received at SRTC approximately two years prior to this testing and had been stored in air in a polyethylene bottle without protection from light. In order to evaluate resin degradation during repeated processing cycles, the 25 °C rhenium loading test (Expt. 1) was repeated (Expt. 4) with limited sampling at the conclusion of the test series. Rhenium breakthrough profiles determined for Experiments 1-3 from ICP-ES analysis (ADS) are provided in Figure 4-1. A target flow rate of 3 BV/hr (0.330 cm/min) was utilized for all tests. Table 4-1 summarizes the column performance data for each experiment. The feed sample used for Experiment 1 was inadvertently spiked to a lower initial rhenium concentration (C_o) than the feed samples used for the other tests. However, a SuperLig® 639 column performance model developed at SRTC (Hamm et al., 2000) indicates that in this concentration range (2E-05 to 8E-05 M), the sorption isotherm is essentially linear. Therefore, the inlet rhenium concentration does not impact the breakthrough profile. The 50% rhenium breakthrough point of 85 BV observed for Experiment 4 agreed to within 5% with the value observed for Experiment 1. This indicates that neither resin degradation throughout the test series nor the low feed Re concentration in Experiment 1 greatly impacted the breakthrough profiles.

Expected trends were observed in the rhenium breakthrough profiles as a function of temperature. A stepwise, 25-35% decrease in the number of bed volumes of solution processed to reach 50% rhenium breakthrough was observed as the temperature was increased by 10 °C increments. The data indicates that rhenium equilibrium loading levels decrease by approximately 56% when the temperature is increased from 25 to 45 °C. In addition to earlier rhenium breakthrough at higher temperatures, the loading profiles are characterized by sharper breakthrough at higher temperatures. The breakthrough profile at 25 °C was nearly linear in shape with a relatively flat slope. 10% rhenium breakthrough was observed at ~25 BV, while 90% rhenium breakthrough (estimated by extrapolation) was not expected until ≥140 BV of solution had been processed. In contrast, at a loading temperature of 45 °C the rhenium breakthrough increases from 10 to 90% over a range of only 60 BV. This indicates that the rate of rhenium sorption to SuperLig® 639 resin increases with temperature. Direct measurement of fundamental diffusion parameters (pore and film diffusion coefficients) to describe the uptake of perrhenate by the resin as a function of both temperature and particle size will be reported separately

(Duffey et al., 2003). The column test results reported herein will be utilized to confirm VERSE model predictions based on the data generated by Duffey.

4.1.2 Feed Displacement and Elution

At the conclusion of each loading experiment, the feed was displaced from the columns using 0.1 M NaOH solution at the temperature utilized for column loading. The feed displacement solution was passed through the columns at a flow rate of 3 BV/hr for a period of one hour. During the last 20 minutes of processing, the column temperature was gradually increased to 65 °C. (Note: The current plant design does not involve a temperature ramp at the end of feed displacement. The eluate solution is heated to 65 °C prior to column entry and the column is not jacketed for temperature control.) Water was then passed through the columns at 65 °C using a flow rate of 1 BV/hr. On-line ICP-ES analysis with a 15-minute sampling frequency was utilized to track the concentration profiles of numerous species during feed displacement and subsequent elution. Figure 4-2 through 4-5 provide the on-line data for sodium, potassium, and rhenium collected during Experiments 1-4, respectively. The raw ICP-ES data is plotted versus bed volumes of solution processed. The profiles provided in the figures are not calibrated and do not represent absolute concentrations or relative concentrations between the various species analyzed. The instrument response for any given element is dependent on the intensity of the emission line selected for analysis. Therefore, the data should only be utilized to track trends in the concentration profiles. Zero bed volumes corresponds to the beginning of feed displacement. The temperature ramp occurred after processing 2±0.25 BV of solution and the water elution started at 3±0.5 BV.

The following trends were observed in the on-line ICP-ES data:

- The sodium concentration decreased rapidly after processing 1-2 BV of solution. This feature was immediately followed by a plateau in the sodium response that was ~3 BV in duration and corresponded to the passage of the 0.1 M NaOH feed displacement solution through the resin bed.
- Two features were associated with the plateau in the sodium response. A large peak was observed in the potassium signal that generally just preceded the end of the sodium plateau. The rhenium response initially increased gradually while processing the feed displacement solution. A step increase in the rhenium response was then observed which was associated with the temperature ramp to 65 °C near the end of the feed displacement.
- A second step decrease in the sodium response was typically observed after processing 4-6 BV of solution.
- The end of the sodium plateau, which is associated with the transition from NaOH to water, was invariably associated with a sharp increase in the rhenium response to a peak at 5-6 BV.
- The concentrations of all three species (Na, K, Re) had decreased to nearly undetectable levels (by on-line analysis) after 10 BV of solution had been processed.

Based on these observations, it is apparent that significant rhenium desorption occurs during feed displacement and that raising the temperature increases rhenium desorption in 0.1 M NaOH solution. However, the primary rhenium elution peak is associated with the water eluate front, as indicated by the sodium signal decrease at the end of the plateau in the sodium response. The impact of temperature on rhenium desorption during feed displacement, can be seen by observing the onset of the initial rhenium response. At a temperature of 25 °C, the onset of rhenium desorption occurs after processing 4-5 BV of solution (Figures 4-2 and 4-5). At 35 and 45 °C (Figures 4-3 and 4-4), the onset of rhenium desorption occurs near 1 BV. The data indicates that maximum separation of the rhenium desorption peak from the residual feed solution occurs at a loading temperature of ≤25 °C. (It should be noted, however, that for Experiment 1 the column was not loaded near rhenium saturation, which probably also impacts the onset of rhenium desorption during feed displacement.) In all cases, after processing 6-8 BV of solution the rhenium signal decreases below the detectable limits (0.2 mg/L) for the on-line monitor (Spencer et al., 2003). The observed trends are quite consistent with the concept of a sorption model for the relevant mass action equations, where increased desorption results from decreasing the ionic strength (i.e. sodium concentration decrease) and increasing the temperature (i.e. a decrease in the thermodynamic equilibrium constants).

The observation of a strong peak in the potassium signal just prior to the primary rhenium elution peak was unexpected. To our knowledge, there is no previous evidence of sorption of potassium salts to SuperLig® 639 resin. It is possible that the potassium is associated with the beginning of the rhenium desorption peak, with the remaining rhenium desorption being associated with, for instance, the sodium perrhenate salt. It would be difficult to observe desorption of sodium due to the high background signal from the 0.1 M NaOH feed displacement solution. Alternatively, the potassium signal peak may be associated with desorption of some other anion from the resin. It has long been assumed that nitrate ion is the primary competitor for absorption sites on SuperLig® 639 resin, although there has not been direct evidence that this is the case. (Limited competitor studies were conducted by the resin manufacturer; see IBC Advanced Technologies, Inc., 1996). The potassium peak could be associated with the desorption of nitrate ion during feed displacement.

Due to budget constraints and customer desires to repeat the AN-105 column tests with a more recently prepared resin batch, ADS-calibration of the raw ICP-ES data was not conducted for Experiments 1-4. However, at the conclusion of Experiments 1-3, a standard (50 mg/L) rhenium spike solution was analyzed with the on-line monitor for calibration purposes. The rhenium profiles for these experiments were then corrected using the observed response for the standard. The calibrated rhenium concentration profiles are provided in Figures 4-6 and 4-7, where the rhenium concentrations are plotted in units of molarity and C/C_o, respectively. Significantly less rhenium was loaded on the column during Experiment 1, due to the fact that the feed rhenium concentration was low. As a result, the rhenium desorption profile observed for this experiment is considerably smaller when plotted on a molar basis. Normalization of the elution data with respect to the feed rhenium concentrations (Figure 4-7) allows for observation of the impacts of temperature on column loading. As expected based on the rhenium breakthrough data, the rhenium loading levels decreased with increasing temperature.

The peak rhenium concentration for Experiment 1 was delayed by nearly 2 BV relative to the peak concentrations observed for Experiments 2 and 3. This feature is presumably associated with the fact that the passage of the water eluate front from the column in Experiment 1 was delayed relative to Experiments 2 and 3. As mentioned above, the primary rhenium peak is invariably associated with the decrease in the sodium hydroxide concentration to below 0.1 M. These observations might be useful to design personnel when establishing the timing and duration of valve closures, solution displacement steps, and temperature ramps in the full-scale plant operation.

Appendix K provides the raw ICP-ES response during feed displacement and elution for additional species measured during Experiment 2. Peaks were observed in the concentration profiles for calcium, silicon, and silver. It is not known whether the source of the silicon during elution is sorbed silicate species added to the simulant or silicon leaching from the glass columns during the transition from 0.1 M NaOH to water. Appendix L lists all species monitored with the on-line unit. No desorption peaks were observed for any species other than those shown in Appendix K.

4.2 Experiments 5-7: Variable Temperature Column Tests with AN-105 Simulant and Resin Batch #IR20327022045

4.2.1 Loading

Rhenium loading tests were conducted at 25, 35, and 45 °C (Experiments 5-7, respectively) with AN-105 simulant and resin batch #IR20327022045 to determine the impact of temperature on column loading. Rhenium breakthrough profiles at each loading temperature determined from ICP-ES analysis (ADS) are provided in Figure 4-8. A flow rate of 3 BV/hr was utilized for all tests. Table 4-1 provides column performance data for each experiment. Trends in the rhenium breakthrough profiles were similar to those observed in Experiments 1-4. A stepwise, 20-30% decrease in the number of bed volumes of solution processed to reach 50% rhenium breakthrough was observed as the temperature was increased by 10 °C increments. The data indicates that rhenium equilibrium loading levels decrease by approximately 51% when the temperature is increased from 25 to 45 °C. As was observed in Experiments 1-4, the loading profiles are characterized by sharper rhenium breakthrough at higher temperatures. At 25 °C the rhenium breakthrough profile is nearly linear indicating that resin performance at this temperature is significantly impacted by perrhenate sorption kinetics.

Figures 4-9 and 4-10 provide breakthrough profiles obtained by ADS and on-line analysis, respectively, for several species during initial column loading for Experiment 5. The on-line data is plotted in the coordinate C/C_a, where C_a represents the average instrumental response after the breakthrough profiles have stabilized to constant levels (presumably representative of the original feed concentration). This coordinate is assumed to be equal to C/C_o. The breakthrough profiles for nearly all species analyzed increased to ~100% of the feed concentration prior to processing 5 BV of solution. Mixing of the feed solution with the column pretreatment solution (0.25 M NaOH) results in the gradual increase in the concentration profiles while processing the first few bed volumes of solution.

Interestingly, breakthrough of potassium from the column is retarded relative to all other species analyzed. This indicates that potassium salts are sorbed to SuperLig® 639 resin during column loading, which is consistent with the observation of a potassium desorption peak in Experiments 1-4. Calcium is initially observed during column loading at levels significantly higher than the feed concentration. This observation indicates that SuperLig® 639 resin contains calcium, either as a material component or as a sorbed species. The trends described above in the initial column breakthrough data for Experiment 5 are consistent with the trends observed for Experiments 1-4 and 6-7.

4.2.2 Feed Displacement and Elution

At the conclusion of each loading experiment, the feed was displaced from the columns using 0.1 M NaOH solution at the temperature utilized for column loading. The feed displacement solution was passed through the columns at a flow rate of 3 BV/hr for a period of one hour. During the last 20 minutes of processing, the column temperature was gradually increased to 65 °C. Water was then passed through the columns at 65 °C using a flow rate of 1 BV/hr. On-line ICP-ES analysis with a 15-minute sampling frequency was utilized to track the concentration profiles of numerous species during feed displacement and elution. Figures 4-11 through 4-13 provide the on-line data for sodium, potassium, and rhenium collected for Experiments 5-7, respectively. The on-line data was calibrated using ADS ICP-ES analysis results for carefully selected samples. The rhenium elution profiles for all three experiments are plotted together in Figure 4-14. The amount of rhenium desorbed based in visual inspection of the elution profiles does not appear to correlate with the trends observed during column loading. The rhenium desorption profile observed for Experiment 6 (25 °C loading) is smaller than expected. Based on the column loading profiles, one would expect the total rhenium eluted from the columns to follow the following trend: Expt. 5 ≥ Expt. 6 > Expt. 7. The reason for this inconsistency in the data is unknown.

ADS analysis of selected elution samples was conducted to determine the time required for complete elution of the SuperLig® 639 columns at elevated temperature. The plant design target for complete elution of the columns is 1% of the rhenium feed concentration. The rhenium detection limit for the on-line monitor was too high to measure 1% of the feed rhenium concentration for the AN-105 simulant. Figure 4-15 provides Re C/C_o values for selected elution samples from Experiments 5-7. In all cases the rhenium concentration decreases to ≤1% of the feed after processing <15 BV of solution. A review of historical laboratory-scale tests conducted at SRTC with AN-105 simulant and different SuperLig® 639 resin batches, revealed that high temperature elution results in significant improvements in rhenium elution efficiency. A comparison of water elution profiles obtained at ambient temperature (20±2 °C) and 65 °C is provided in Figure 4-16. At ambient temperature, eluate rhenium concentrations reached the design elution target after processing 15-30 BV of solution, depending primarily on the degree of column loading. It is believed that a low rhenium loading level led to significantly faster elution for Experiment 2 in the 1999 report. In contrast, 65 °C elution resulted in achievement of the design target prior to processing 15 BV of eluate.

The trends observed in the on-line ICP-ES data were generally consistent with those discussed for Experiments 1-4. However, the instrumental sensitivity was considerably lower for these experiments than for Experiments 1-4. The reasons for the lower sensitivity are discussed in a separate report (Spencer et al., 2003) Due to the instrumental differences, the peak in the potassium concentration during feed displacement was not observed in every experiment. Since the on-line data is plotted on a molar basis (Figures 4-11 to 4-13), the concentration profiles represent the relative amounts of sodium, potassium, and rhenium at each sampling time. As would be expected, residual sodium from the simulant and the feed displacement solutions is the dominant species.

Samples were collected during feed displacement for Experiments 5-7 and submitted to ADS for analysis. Table 4-2 provides ICP-ES analysis data of composite samples collected during the processing intervals indicated. Since the effluent concentrations of all species are changing rapidly during feed displacement, it is most informative to compare concentrations relative to the original levels in the simulant. The values calculated for several species that are generally considered not to absorb to SuperLig® 639 resin are shown in Table 4-2 in order to track residual feed displacement efficiency. The final samples analyzed for each experiment indicate that <5% residual feed remains in the effluent at the conclusion of feed displacement. The sodium concentration for the final sample in each experiment also approaches 5% of the feed, although the decrease in the sodium concentration is impacted by the fact that the feed displacement solution contains 0.1 M sodium (2% of the feed concentration). In contrast, both the potassium and rhenium concentrations remain near 30% of the initial values in the feed, indicating that some process such as desorption from the resin is leading to higher concentrations for these species. IC anion analysis of these samples also indicates that nitrate desorption may be occurring during feed displacement. Relative nitrate levels are consistently higher than nitrite and chloride levels throughout feed displacement (Table 4-2). Figure 4-17 provides concentration profiles for several species during feed displacement and elution for Experiment 6. The trends in the data clearly indicate desorption of rhenium, potassium, and nitrate ion from the resin. Furthermore, nitrite, phosphate, sulfate, chloride, and formate ions appear not to desorb from the resin at levels that are observable above the residual feed background signal (although a small peak was observed in the formate concentration profile near 3.75 BV).

Although the trends in the data indicate that potassium and nitrate levels are high in the feed displacement solutions relative to other species analyzed, no distinct desorption peaks were observed for sodium, potassium or nitrate in the ADS data. However, highly time-resolved on-line data clearly and repeatedly indicated that potassium desorption occurs during feed displacement. Subtraction of background residual feed contributions in the ADS data (and, for the sodium concentration, subtraction of contribution from the 0.1 M NaOH feed displacement solution) for Experiment 6, based on the trends observed for the nonadsorbing species, revealed the presence of distinct desorption peaks for nitrate, sodium, and potassium. Figure 4-18 provides the matrix background corrected concentration profiles for these species during feed displacement. Presumably, the peaks correspond to desorption of sodium and potassium salts from the resin. The onset of nitrate desorption occurs after processing <1BV of 0.1 M NaOH solution, indicating that nitrate salts are desorbed rapidly from the resin during

the initial decrease in ionic strength associated with the transition from feed to NaOH solution. The nitrate anion composition appears to be dominated by the sodium salt, which elutes from the column prior to the potassium salt. The tail of the nitrate desorption profile is associated with the potassium salt which elutes from the resin in a broad band.

Integration of the nitrate and potassium desorption profiles allowed for calculation of the nitrate loading on the resin and the contribution of potassium nitrate to the total. Loading levels calculated by this method are shown in Table 4-3. The nitrate loading of 0.703 mmol NO_3^-/g resin is in the total capacity range of 0.347 to 0.880 mmol/g calculated previously for SuperLig® 639 resin batches (Hamm et al., 2000). The sodium concentration profile for Experiment 6 (and for other experiments discussed below) was slightly higher than expected. Presumably, mixing of the 0.1 M NaOH feed displacement solution with residual 5 M Na^+ feed cannot be adequately accounted for by the simple background subtraction method utilized. As a result, the contribution of the sodium salt to the total nitrate loading was calculated by subtraction of the potassium loading from the total. Comparison of the ratio of sodium nitrate to potassium nitrate levels for the eluate to the Na^+/K^+ mole ratio of these species in the feed, indicates that the eluate is enriched in potassium by a factor of 7.0 relative to the feed solution.

Perrhenate loading levels on SuperLig® 639 resin were calculated by two different methods. Analysis of the composited column effluent solution for each experiment provided the total rhenium breakthrough for each experiment. The perrhenate loading was then calculated by subtracting the total rhenium in the effluent from the total in the feed. Table 4-4 provides the perrhenate loading for Experiments 5-7 calculated by this method (A). Total perrhenate loading levels were also calculated as described above for nitrate loading by integration of the rhenium desorption profiles. Loading levels calculated in this way are also provided in Table 4-4 (B). Loading levels calculated by the methods described above were consistent except for Experiment 5, where the calibrated ICP-ES concentration profile was lower than expected (as discussed earlier). Based on the calculations, rhenium loading levels on the resin for Experiments 5-7 ranged from 0.011 to 0.016 mmol/g resin. Loading levels calculated for Experiments 5 and 6 do not represent the effective capacity of the resin for perrhenate under the processing conditions, since the column loading tests were stopped well before rhenium saturation.

Appendix K provides the raw ICP-ES response during feed displacement and elution for additional species measured during Experiment 5. A broad calcium desorption peak was frequently observed (Experiments 5-7) following the rhenium desorption peak during column elution. As mentioned earlier, calcium was also observed to desorb from the resin during initial processing of AN-105 simulant. The source of the calcium is unknown. A small silicon peak was consistently observed to occur near the rhenium desorption peak. It is not known whether the source of the silicon during elution is sorbed silicate species added to the simulant or silicon leaching from the glass columns. Small peaks were also occasionally observed in the concentration profiles for chromium, magnesium and silver. Appendix L lists all species analyzed with the on-line monitor. No desorption peaks were observed for any species other than those shown in Appendix M.

4.3 Experiment 8: Column Test with AZ-102 Simulant and Resin Batch #IR20327022045

4.3.1 Loading

A single column experiment was conducted with AZ-102 simulant using ~74 mL of SuperLig® 639 resin from batch #IR20327022045 (column ID: 2.50 cm). Simulant was processed through the column at 25 °C using a flow rate of 3 BV/hr (superficial velocity: 0.758 cm/min). Figure 4-19 provides the rhenium breakthrough profile obtained with the AZ-102 simulant during column loading. Only 30% rhenium breakthrough was obtained after processing 213 BV of simulant solution. Based on the current conceptual model for perrhenate sorption with SuperLig® 639 resin, the exceptional breakthrough performance observed for this sample might be attributed to the low nitrate concentration and the low nitrate/perrhenate ratio (NO_3^-/ReO_4^-: AZ-102 – 2488, AN-105 – 19825).

Initial breakthrough profiles for the AZ-102 sample obtained from ADS and on-line analysis are provided in Figures 4-20 and 4-21, respectively, for numerous species during column loading with the AZ-102 simulant. The concentration profiles for nearly all species analyzed stabilize near 100% of the feed concentrations within 4 BV after the start of column loading. As was observed during column loading with AN-105 simulant, potassium breakthrough is retarded with respect to all other species measured (except for rhenium). Based on the on-line data, 50% potassium breakthrough is estimated to occur ~1 BV after breakthrough of the feed solution.

Column tests were conducted with SuperLig® 639 resin on an actual sample from Tank 241-AZ-102 during previous testing at SRTC (Hassan, et al., 2001). The test conducted with the actual sample differed from the AZ-102 simulant test in the following ways. Different resin batches were used for each test. SuperLig® 639 resin batch #981015DHC720011 was used for the actual waste test. The actual waste sample was treated for cesium removal testing with SuperLig® 644 resin prior to testing with SuperLig® 639 resin. Due to poor cesium ion exchange performance and the need to generate a sufficiently decontaminated product for vitrification testing, only the first portion of the cesium column effluent was used for technetium removal testing. The as-received waste sample was only 2.7 M Na^+, and the sample used for SuperLig® 639 column testing was further diluted by the cesium column pretreatment solution (0.25 M NaOH) to 2.2 M Na^+. Low ionic strength is expected to have a negative impact on SuperLig® 639 loading performance. Comparison of the breakthrough performance data for the simulant and the actual sample is further complicated by the fact that pertechnetate loading levels on SuperLig® 639 resin are known to be 70% higher than perrhenate levels (Hamm et al., 2000). The nitrate/pertechnetate mole ratio, which is also believed to be a primary factor influencing SuperLig® 639 loading performance, was 32% lower in the actual waste sample (NO_3^-/ReO_4^-: 1685) than in the simulant. Despite the numerous differences between the simulant and actual waste samples, one common feature between the column tests is exceptional loading performance, presumably resulting from relatively low NO_3^-/XO_4^- (X = Tc or Re) ratios in these samples. Only 10% technetium breakthrough was observed with the actual AZ-102 sample after processing 170 BV of feed solution.

Modeling of the breakthrough data for the actual and simulated waste samples will be needed to fully evaluate and compare the column performance with each material.

4.3.2 Feed Displacement and Elution

At the conclusion of the loading experiment with AZ-102 simulant, the feed was displaced from the column using 0.1 M NaOH solution at 25 °C. The feed displacement solution was passed through the columns at a flow rate of 3 BV/hr for a period of one hour. During the last 20 minutes of processing, the column temperature was gradually increased to 65 °C. Water was then passed through the columns at 65 °C using a flow rate of 1 BV/hr. On-line ICP-ES analysis with a 15-minute sampling frequency was utilized to track the concentration profiles of numerous species during feed displacement and elution. Figure 4-22 provides the on-line data for sodium, potassium, and rhenium collected for Experiments 8. The on-line data was calibrated using ADS ICP-ES analysis results for carefully selected samples.

The trends observed in the on-line data are generally consistent with those described for Experiments 1-7. The sodium concentration profile decreases to near 0.1 M during feed displacement and then rapidly decreases again after processing 4 BV of solution. The second step decrease corresponds to the water eluate front passing through the columns and is associated with the peak rhenium concentration, as has been described previously for elution following loading tests with AN-105 simulant. The molar concentrations of sodium and rhenium at the peak in the rhenium concentration profile are nearly identical, indicating that the primary desorbing species at this processing point is the sodium perrhenate salt. Surprisingly, the primary rhenium desorption peak is immediately followed by a large, broad rhenium desorption peak, although the sodium concentration continues to decrease rapidly. As can be seen in Figure 4-22, the rhenium concentration in the secondary desorption peak corresponds almost exactly with a similar broad peak observed in the potassium concentration profile. Based on these observations, it appears that the sorbed perrhenate ion is a mixture of the sodium and potassium salts. Furthermore, it is apparent that elution of the potassium perrhenate salt is retarded and the profile is broadened with respect to the profile for the sodium perrhenate salt. These trends in the sodium and potassium perrhenate desorption profiles are consistent with those observed for the sodium and potassium nitrate salts during feed displacement following AN-105 column loading. There was no indication in the on-line data of desorption of potassium perrhenate salts during feed displacement and elution for any experiments following column loading with AN-105 simulant (Experiments 1-7). However, perrhenate loading levels on the resin are much lower than nitrate loading levels (Table 4-4) and the potassium concentration in the AN-105 simulant is 41% lower than in the AZ-102 simulant. The rhenium concentration in the eluate solution decreases to 1% of the AZ-102 feed concentration after processing 9.5 BV of solution.

Figure 4-23 provides ADS ICP-ES and IC anion data for samples collected during feed displacement. The concentration profiles for fluoride, formate, nitrite, phosphate, sulfate, and chromium are presumably representative of feed displacement efficiency. There is no indication of nitrite desorption

from the resin even though nitrite levels in the feed (1.24 M) are 2.4 times higher than nitrate levels. As was observed with the AN-105 simulant, there is evidence in the concentration profiles for desorption of rhenium, nitrate, and potassium during feed displacement. Correction of the concentrations of these species for residual feed based on the concentration profiles for the nonadsorbing species, reveals the presence of nitrate and potassium desorption peaks (Figure 4-24). ADS analysis of samples collected during column elution confirmed the trends described above in the on-line data for the sodium and potassium perrhenate salts (Figure 4-24 and 4-25).

Integration of the total nitrate and the potassium nitrate desorption profiles obtained from samples collected during AZ-102 feed displacement allowed for calculation of the nitrate loading on the resin and the contribution of potassium nitrate to the total. Loading levels calculated by this method are shown in Table 4-3. The total nitrate loading of 0.303 mmol NO_3^-/g resin is 57% lower than the nitrate loading calculated for AN-105 simulant. Lower nitrate loading was somewhat expected based on the fact the AZ-102 simulant contains 59% less nitrate than the AN-105 simulant. The current conceptual model of SuperLig® 639 resin uptake includes the idea that the available number of sorption sites varies with total ionic strength and total nitrate. These observations confirm that nitrate is the primary competitor for sorption sites on SuperLig® 639 resin and the data is in agreement with the idea of variable effective resin capacity. Comparison of the ratio of sodium nitrate to potassium nitrate levels for the eluate to the Na^+/K^+ molar ratio in the feed, indicates that the sorbed nitrate salt is enriched in potassium by a factor of 15.6 relative to the feed solution. Potassium enrichment in the nitrate salts for AN-105 simulant was only 7.0. The selectivity of the resin for potassium over sodium is dependent upon the activities of the various ions in solution. This may explain the different selectivities observed for the AN-105 and AZ-102 simulants.

Perrhenate loading levels on SuperLig® 639 resin following column loading with AZ-102 simulant were calculated by two different methods, as described above for the AN-105 sample. Table 4-4 provides the perrhenate loading levels calculated for Experiment 8 by each method. Loading levels calculated based on effluent and eluate compositions were 0.065 and 0.076 mmol ReO_4^-/g resin. Integration of the concentration profile for the potassium perrhenate salt allowed for calculation of the contribution of the potassium salt to the total sorbed perrhenate. Simple subtraction provided the contribution of the sodium perrhenate salt. Comparison of the sodium and potassium perrhenate levels to the Na^+/K^+ molar ratio in the feed indicates that the perrhenate salt is enriched in potassium relative to the feed by a factor of 25.1. Total perrhenate loading with AZ-102 simulant was larger than any values observed with AN-105 simulant, even though the column was only loaded to 30% rhenium breakthrough with AZ-102 simulant. Based on the previous conceptual model of SuperLig® 639 sorption, the high perrhenate loading with AZ-102 presumably arises from the small nitrate to perrhenate ratio for this simulant. However, given the fact that the resin appears to be significantly more selective for potassium perrhenate than for sodium perrhenate, the significantly higher potassium concentration in the AZ-102 sample likely significantly impacts the column performance as well. Table 4-5 provides selectivity coefficients calculated based on the loading levels in Tables 4-3 and 4-4.

Based on the observation of potassium selectivity with SuperLig® 639, the conceptual sorption model for this material must be modified. The previous conceptual model only considered dynamic equilibrium for sodium nitrate and perrhenate salts between the liquid and solid phases. The model must now be expanded to include analogous exchange of potassium salts. For a rhenium based waste solution in contact with SuperLig® 639 resin the following four mass-action processes would apply:

$$[\overline{L}] + [Na^+] + [Re\,O_4^-] \xleftrightarrow{K_{eq,1}} \left[\overline{L - Na\,Re\,O_4}\right], \quad (4\text{-}1)$$

$$[\overline{L}] + [K^+] + [Re\,O_4^-] \xleftrightarrow{K_{eq,2}} \left[\overline{L - K\,Re\,O_4}\right], \quad (4\text{-}2)$$

$$[\overline{L}] + [Na^+] + [NO_3^-] \xleftrightarrow{K_{eq,3}} \left[\overline{L - NaNO_3}\right], \quad (4\text{-}3)$$

$$[\overline{L}] + [K^+] + [NO_3^-] \xleftrightarrow{K_{eq,4}} \left[\overline{L - KNO_3}\right], \quad (4\text{-}4)$$

where the bars imply the solid surface phase. Four similar mass-action processes apply for technetium based waste solutions. The thermodynamic equilibrium constants are reasonably temperature dependent, which is consistent with the significant shifts observed for the rhenium breakthrough profiles during the variable temperature column tests with AN-105 simulant. As indicated by the mass-action equations shown above, elution of the SuperLig® 639 resin should be predominately controlled by the eluate total ionic strength and liquid temperature. Equations 4-2 and 4-4 become increasingly important as the liquid potassium concentration increases. It is likely that SuperLig® 639 performance with high potassium feeds, such as Tanks 241-AP-101 and 241-AW-101, will be significantly improved due to the large potassium selectivity of this material.

Based on the above observations, the authors suggest that the RPP-WTP program consider an additional step in the basic plant flowsheet design. We predict that addition of potassium salts to tank wastes containing relatively low potassium concentrations (≤0.1 M K^+ on a 5 M Na^+ basis) will substantially improve pertechnetate removal performance. The addition should not be made prior to cesium ion exchange treatment. Potassium is a substantial competitor for sorption sites on SuperLig® 644 resin and there would be negative impacts on the cesium removal process. In contrast, increasing the total potassium concentration to levels greater than the concentration in the AZ-102 sample (~0.15 M K^+) should significantly increase technetium uptake levels with SuperLig® 639 resin. Modeling efforts, currently underway at SRTC, will be able to predict the magnitude of added reagent required to enhance technetium removal performance for a given waste composition.

Obviously, the impacts of potassium reagent addition upon downstream treatment processes such as evaporation and vitrification will have to be evaluated prior to implementation. The preferred counter ion to use for potassium reagent addition would have to be determined. Nitrate and nitrite salts may be good candidates for addition since these species are burned off during the waste vitrification process (assuming offgas NO_x thresholds are not exceeded). Significant nitrate ion addition would negatively

impact SuperLig® 639 resin performance. However, depending on the waste composition, the amount of nitrate salt required to reach the desired potassium concentration may have an insignificant impact on the nitrate/pertechnetate molar ratio. Any changes in the nitrate and nitrite concentrations must also be evaluated with regard to impacts on the melter redox chemistry. Potassium hydroxide may also be a viable candidate for addition, although the impact on the viscosity of resulting melter feeds may need to be examined.

Appendix N provides the raw ICP-ES response during feed displacement and elution for additional species measured during Experiments 8. Small magnesium, calcium, strontium and silicon peaks were observed during elution. Appendix L lists all species analyzed with the on-line monitor. No desorption peaks were observed for any species other than those shown in Appendix N.

4.3 Experiment 9: Column Test with AN-107 Simulant and Resin Batch #IR20327022045

4.3.1 Loading

A single column experiment was conducted with AN-107 simulant using the same resin sample from batch #IR20327022045 (column ID: 2.50 cm) that was used for the AZ-102 column test. AN-107 simulant was processed through the column at 25 °C using a flow rate of 3 BV/hr (superficial velocity: 0.758 cm/min). Figure 4-26 provides the rhenium breakthrough profile obtained with the AN-107 simulant during column loading. 50% rhenium breakthrough was observed after processing only 82 BV of simulant. Based on the current conceptual model for perrhenate sorption with SuperLig® 639 resin, the poor breakthrough performance observed for this sample might be attributed to the high nitrate/perrhenate ratio (NO_3^-/ReO_4^-: AN-107 – 83791). However, the potassium concentration in the AN-107 simulant of 0.027 M is quite low relative to the AN-105 and AZ-102 simulants. Based on the observation of preferred potassium perrhenate uptake with the AZ-102 simulant, low potassium levels would also be expected to negatively impact SuperLig® 639 resin performance.

Initial breakthrough profiles obtained from ADS and on-line analysis are provided in Figures 4-27 and 4-28, respectively, for selected species during column loading with the AN-107 simulant. The concentration profiles for sodium and molybdenum stabilize near 100% of the feed concentrations within 3 BV after the start of column loading. Potassium breakthrough is slightly retarded (by ~0.25 BV) with respect to sodium and molybdenum.

Column tests were conducted with SuperLig® 639 resin on an actual sample from Tank 241-AN-107 during previous testing at SRTC (Hassan et al., 1997). The test conducted with the actual sample differed from the AN-107 simulant test in the following ways. Different resin batches were used for each test. A resin batch number was not provided in the report for the actual waste testing. The actual waste sample used for column testing had not been subjected to strontium/transuranics precipitation testing. The actual sample was caustic adjusted prior to cesium removal testing to 0.3 M free hydroxide by the addition of NaOH solution. The sample contained approximately 5.5 M Na^+, 0.026 M K^+, and 2.48 M NO_3^-. The technetium concentration in the actual sample was 2.96 E-05 M. However, only

~34% of the technetium existed as pertechnetate ion, and the remaining technetium was not extractable with SuperLig® 639 resin. The pertechnetate ion concentration was 1.01 E-05 M and the nitrate/pertechnetate mole ratio was 246,340. Comparison of the breakthrough performance data for the simulant and the actual sample is further complicated by the fact that pertechnetate loading levels on SuperLig® 639 resin are known to be 70% higher than perrhenate levels (Hamm et al., 2000). Approximately 23% pertechnetate (as opposed to total technetium) breakthrough was observed with the actual AN-107 sample after processing 12 BV of solution, although there was considerable scatter in the breakthrough data. This poor column performance is generally consistent with the AN-107 simulant, for which 20% perrhenate breakthrough was observed after processing 35 BV of solution Modeling of the breakthrough data for the actual and simulated waste samples will be needed to fully evaluate and compare the column performance with each material.

4.3.2 Feed Displacement and Elution

At the conclusion of the loading experiment with AN-107 simulant, the feed was displaced from the column using 0.1 M NaOH solution at 25 °C. The feed displacement solution was passed through the column at a flow rate of 3 BV/hr for a period of one hour. During the last 20 minutes of processing, the column temperature was gradually increased to 65 °C. Water was then passed through the columns at 65 °C using a flow rate of 1 BV/hr. On-line ICP-ES analysis with a 15-minute sampling frequency was utilized to track the concentration profiles of numerous species during feed displacement and elution. Figure 4-29 provides the on-line data for sodium, potassium, and rhenium collected for Experiment 9. The on-line data was calibrated using ADS ICP-ES analysis results for carefully selected samples. The trends observed in the on-line data are generally consistent with those described for Experiments 1-8. There was no indication in the on-line data of desorption of potassium perrhenate salts during feed displacement and elution.

Figure 4-30 provides ADS ICP-ES and IC anion data for samples collected during feed displacement. The concentration profiles for fluoride, formate, nitrite, phosphate, sulfate, and chloride are presumably representative of feed displacement efficiency. As was observed with the AN-105 simulant, there is evidence in the concentration profiles for desorption of rhenium, nitrate, and potassium during feed displacement. Correction of the concentrations of these species for residual feed based on the concentration profiles for the nonadsorbing species, provided distinct nitrate and potassium desorption peaks (Figure 4-31). ADS analysis of samples collected during column elution confirms the trends described above in the on-line data (Figure 4-31 and 4-32).

Integration of the total nitrate and the potassium nitrate desorption profiles obtained from samples collected during AZ-102 feed displacement allowed for calculation of the nitrate loading on the resin and the contribution of potassium nitrate to the total. Loading levels calculated by this method are shown in Table 4-3. Comparison of the ratio of sodium nitrate to potassium nitrate levels for the eluate to the Na^+/K^+ molar ratio in the feed, indicates that the nitrate salt is enriched in potassium by a factor of 3.8 relative to the feed solution. This potassium selectivity is lower than was observed for both the AN-

105 and the AZ-102 simulants. The total rhenium loadings calculated based on effluent (Type A) and eluate (Type B) compositions agree very well. The total rhenium loading of 0.0065 mmoles/g is representative of the effective perrhenate capacity of the resin in AN-107 simulant at 25 °C since the column was loading to near rhenium saturation. The rhenium loading is smaller than was observed for the AN-105 or AZ-102 column tests at loading temperatures of 25 °C, even though the columns were not loaded to complete rhenium breakthrough for either of these samples. The low potassium concentration in the AN-107 simulant and the poor performance of SuperLig® 639 resin with this sample make the AN-107 sample a prime candidate for pertechnetate removal enhancement by the addition of relatively low levels of potassium salts.

Appendix O provides the raw ICP-ES response during feed displacement and elution for additional species measured during Experiments 9. Small magnesium, calcium, strontium and silicon peaks were observed during elution. Appendix L lists all species analyzed with the on-line monitor. Desorption peaks were not observed for any species other than those shown in Appendix O.

4.3 Experiment 10: Thermal Shock Testing With SuperLig® 639 Resin Batch #IR20327022045

A sample of SuperLig® 639 resin was exposed to repeated temperature cycles in water to evaluate the impacts of thermal shock upon the physical stability of the resin. This testing did not measure impacts upon the resin chemical performance (such as rhenium uptake) resulting from repeated thermal cycles. Furthermore, since all temperature cycles were conducted in water, synergistic effects from temperature cycling and chemical degradation (associated with chemical exposure during column loading, feed displacement, elution, and regeneration) on the physical properties of the resin were not evaluated.

The test methodology involved rapid transfer of resin between beakers containing water at 25 and 65 °C. Care was taken to minimize damage to the resin beads due to handling during transfer and sampling. Resin samples were collected for optical microscopy, Microtrac particle size analysis, and Lasentec chord length analysis. Appendix P provides the resin/water slurry temperatures measured after specific contact times at each temperature. 30-minute contact times at each temperature allowed for thorough temperature stabilization. The average measured slurry temperature immediately after resin transfer to beaker #1 (target temperature: 25 °C) was 29.7 °C. The average measured slurry temperature immediately after resin transfer to beaker #2 (target temperature: 65 °C) was 58 °C. After 5 minutes of contact, the average slurry temperatures for beakers 1 and 2 were 26.5 and 62.2 °C, respectively. After 30 minutes of contact the slurry temperatures were stabilized near the target temperatures. Based on the temperature data, the resin slurry temperature changed rapidly (within 30 seconds or less) from 25 to 58.0 °C and from 65 to 29.7 °C. Therefore the magnitude of the temperature change during initial contact was 33-35 °C on average. The rapid temperature changes utilized in this study were intentionally more harsh than SuperLig® 639 resin would be expected to experience in the plant operation.

An optical micrograph (magnification: ~16X) of a SuperLig® 639 resin sample (batch #IR20327022045), which was collected just prior to the first thermal cycle is provided in Figure 4-33. SuperLig® 639 resin is composed of tan beads that are highly spherical. A small fraction (<5%) of the beads was observed to contain fissures, prior to thermal shock testing. In some cases the beads were fractured into two separate crescent-shaped pieces. Optical micrographs were obtained for the as-received (AR) resin sample, prior to thermal shock testing, and for samples collected after thermal shock cycles 1, 5, and 10. Appendix P provides particle count data obtained from each photograph. The percentage of fissured particles ranged from 1-6% for all samples. The measured percentages of fissured particles are probably biased high, since the tendency during analysis was to photograph areas that contained at least some cracked particles. There was no indication in the micrographs that repeated exposure of the resin to thermal shock cycles led to physical degradation of the particles.

Particle analysis data obtained by Microtrac and Lasentec methods indicated that there were no significant differences in the distributions for all samples collected during thermal cycle testing (plots and data are provided in Appendix P). Chord length distributions obtained for resin samples collected after each temperature cycle were virtually indistinguishable when overlayed (Appendix P). The average number-weighted particle diameter determined by Microtrac analysis was 430.9 μm (st. dev.: 5.0 μm). The average square-weighted chord length determined by Lasentec analysis (which approximates the spherical equivalent diameter measured by Microtrac) was 426.3 μm (st. dev.: 5.9 μm). The percentages of measured chord lengths <100 μm and <10 μm averaged 10.3% and 1.8% (st. dev.: 0.5 and 0.1%, respectively) in the Lasentec data. There was no indication in the data of generation of fine particulates during exposure of the resin to repeated thermal cycles.

Based on the above observations, we conclude that physical degradation of SuperLig® 639 resin resulting from thermal shock across the temperature range of 25-65 °C is negligible.

Table 4-1. Overall Performance Data for SuperLig® 639 Column Experiments.

Expt.	Simulant	Loading Temp. (°C)	Feed [Re], C_o (M)	Feed Vol. Processed[1] (BV)	Effluent [Re][2] (C/C_o)	Eluent Vol. at Peak [Re] (BV)	Eluent Vol. at £1% of Re C_o[3] (BV)
1	AN-105	25.0	2.95E-05	127	0.70[4]	5.6	NM[5]
2	AN-105	44.5	7.25E-05	179	1.04	4.6	NM[5]
3	AN-105	35.0	7.38E-05	144	0.89	4.7	NM[5]
4	AN-105	25.3	7.63E-05	195	0.95[4]	6.3	NM[5]
5	AN-105	25.8	6.24E-05	199	0.45[4]	5.1	15.2
6	AN-105	35.1	6.15E-05	200	0.66[4]	5.2	13.5
7	AN-105	44.8	6.42E-05	209	0.96[4]	5.5	11.5
8	AZ-102	25.1	2.07E-04	213	0.30	4.3	9.5
9	AN-107	25.0	3.06E-05	352	0.96	4.5	NM[5]

[1] total volume of simulant processed
[2] rhenium breakthrough at conclusion of loading
[3] minimum volume
[4] estimated by extrapolation
[5] not measured for this test

Table 4-2. ADS Analysis Data for Samples Collected During 0.1 M NaOH Feed Displacement for Experiments 5-7.

Expt.	Solution Volume Processed[1] (BV)	Concentration (% of Feed)								
		Na	K	Re	Al	P	S	NO_3^-	NO_2^-	Cl^-
5	0-1	9.7	95.3	38.7	97.1	99.2	88.0	100.9	101.0	112.8
5	1-2	55.1	48.3	49.6	39.3	39.0	38.6	75.8	50.4	47.1
5	2-3	6.8	23.2	27.2	2.9	3.5	3.2	13.2	3.2	2.4
6	0-0.5	83.8	82.7	55.5	91.7	87.0	86.5	104.5	88.8	106.7
6	0.5-1.0	90.8	88.7	55.9	97.0	91.7	89.1	110.2	93.7	40.4
6	1.0-1.5	85.7	81.6	58.6	83.1	73.4	75.2	109.2	88.6	97.8
6	1.5-2.0	31.1	27.0	94.5	15.8	15.1	14.6	73.2	25.9	17.1
6	2.0-2.5	7.7	25.6	61.5	3.8	3.5	3.7	18.8	4.1	3.9
6	2.5-3.0	3.5	28.6	37.2	1.7	2.4	1.7	5.2	1.7	1.6
7	0-1	96.7	95.3	38.7	97.1	99.2	88.0	97.4	91.3	106.1
7	1-2	55.1	48.3	49.6	39.3	39.0	38.6	77.1	51.1	48.7
7	2-3	6.8	23.2	27.2	2.9	3.5	3.2	5.3	2.5	2.0

[1] samples were composited over the processing ranges indicated

Table 4-3. Sodium and Potassium Nitrate Loading Levels Determined from Desorption Profiles for Experiments 6, 8, and 9.

Expt.	Simulant	Feed $[NO_3^-]$ [M]	Feed [Na]/[K]	Total NO_3^- Loading[1] (mmol/g)	$NaNO_3$ Loading[2] (mmol/g)	KNO_3 Loading[1] (mmol/g)	Sorbed $[NaNO_3]/[KNO_3]$
6	AN-105	1.243	55.6	0.703	0.624	0.079	7.9
8	AZ-102	0.515	32.7	0.303	0.204	0.099	2.1
9	AN-107	2.188	164.1	0.698	0.682	0.016	42.6

[1] loading values determined by extrapolation and integration of the desorption profiles
[2] loading values calculated by subtraction of the potassium nitrate loading from the total

Table 4-4. Sodium and Potassium Perrhenate Loading Levels Determined from Desorption Profiles for Experiments 5-9.

Expt	Simulant	Feed $[NO_3^-]/[ReO_4^-]$	Feed [Na]/[K]	Total ReO_4^- Loading A[1] (mmol/g)	Total ReO_4^- Loading B[2] (mmol/g)	$NaReO_4$ Loading[2] (mmol/g)	$KReO_4$ Loading[2] (mmol/g)	Sorbed $[NaReO_4]/[KReO_4]$	Sorbed $[NO_3^-]/[ReO_4^-]$
5	AN-105	19825	55.6	0.016	0.009	NA	NA	NA	44.7
6	AN-105	19825	55.6	0.015	0.015	NA	NA	NA	48.3
7	AN-105	19825	55.6	0.011	0.011	NA	NA	NA	64.3
8	AZ-102	2488	32.7	0.065	0.076	0.043	0.033	1.3	4.64
9	AN-107	83791	164.1	0.006	0.007	NA	NA	NA	2636

[1] loading values calculated based on total rhenium in the effluent
[2] loading values determined by extrapolation and integration of the desorption profiles

Table 4-5. Selectivity Coefficients Calculated from Sodium, Potassium, Nitrate, and Perrhenate Loading Levels.

Expt.	Simulant	$K_{KNO3/NaNO3}$	$K_{KReO4/NaReO4}$	$K_{ReO4/NO3}$
5	AN-105	7.0	NA	>443
6	AN-105	7.0	NA	>411
7	AN-105	7.0	NA	308
8	AZ-102	15.9	25.1	>536
9	AN-107	3.8	NA	31.8

">" indicates bounding values calculated for columns not loaded to saturation

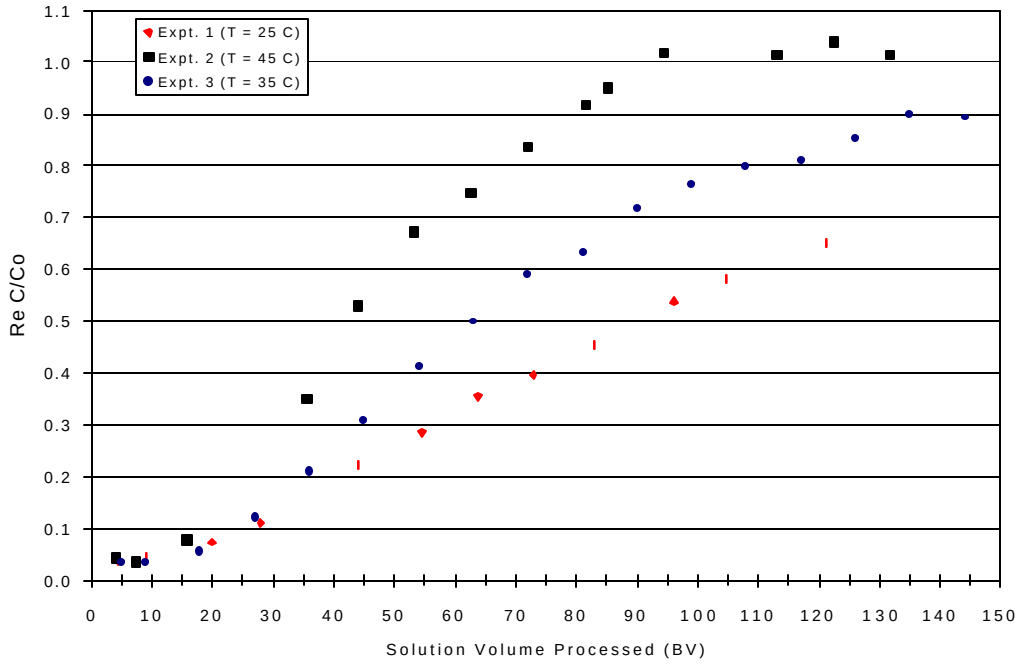

Figure 4-1. Rhenium Breakthrough Profiles Versus Temperature with AN-105 Simulant and SuperLig® 639 Batch #990420DHC720067 (Experiments 1-3).

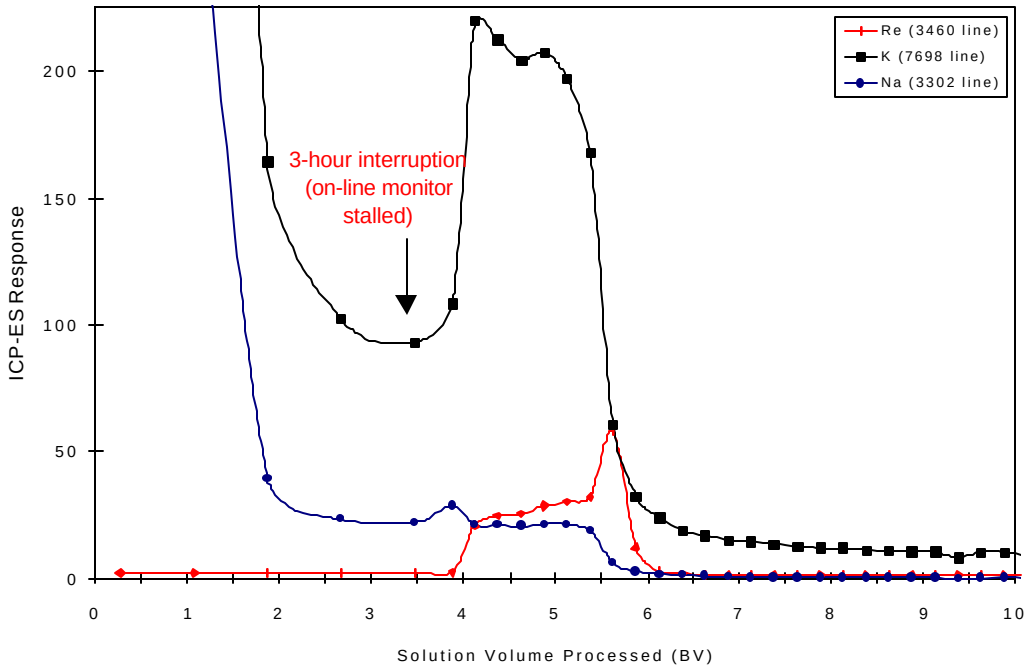

Figure 4-2. Uncalibrated On-line Data Collected During Feed Displacement (25 °C) and Elution (65°C) for Experiment 1.

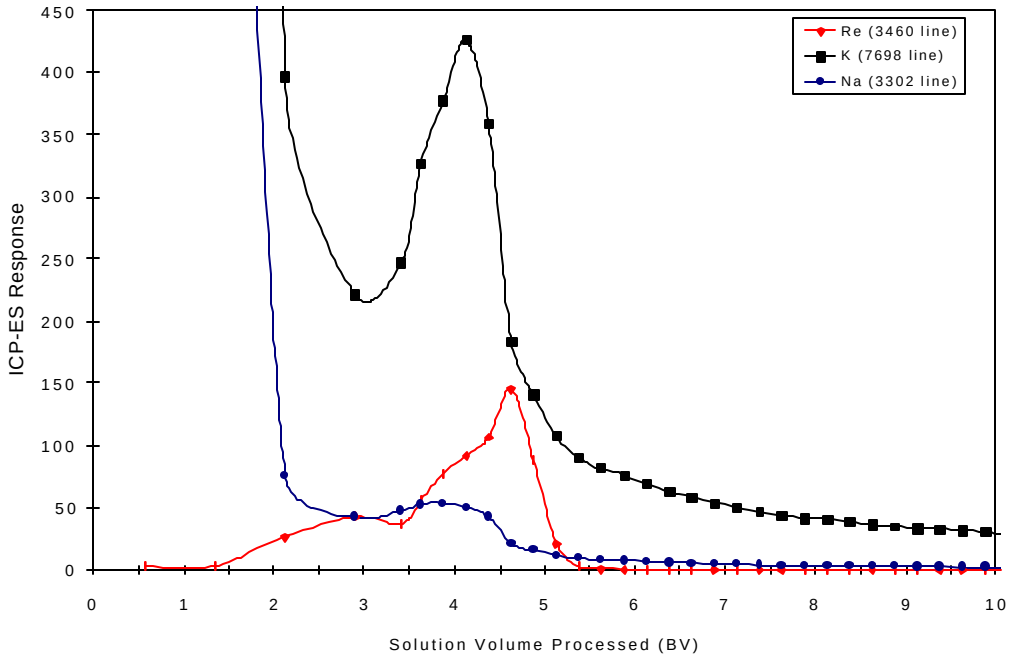

Figure 4-3. Uncalibrated On-line ICP-ES Data Collected During Feed Displacement (45 °C) and Elution (65°C) for Experiment 2.

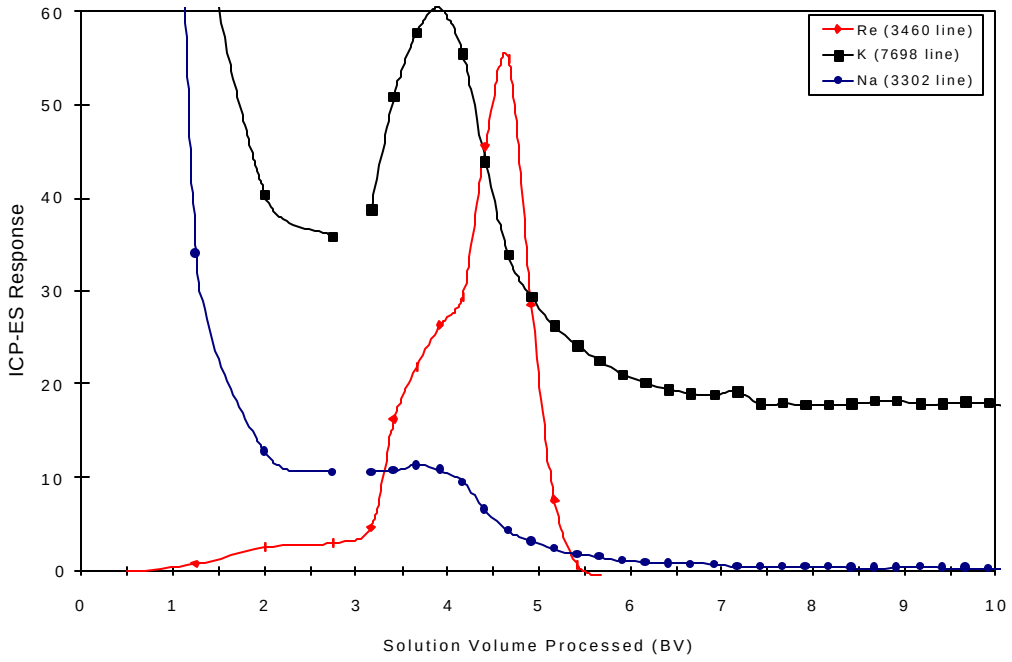

Figure 4-4. Uncalibrated On-line ICP-ES Data Collected During Feed Displacement (35 °C) and Elution (65°C) for Experiment 3.

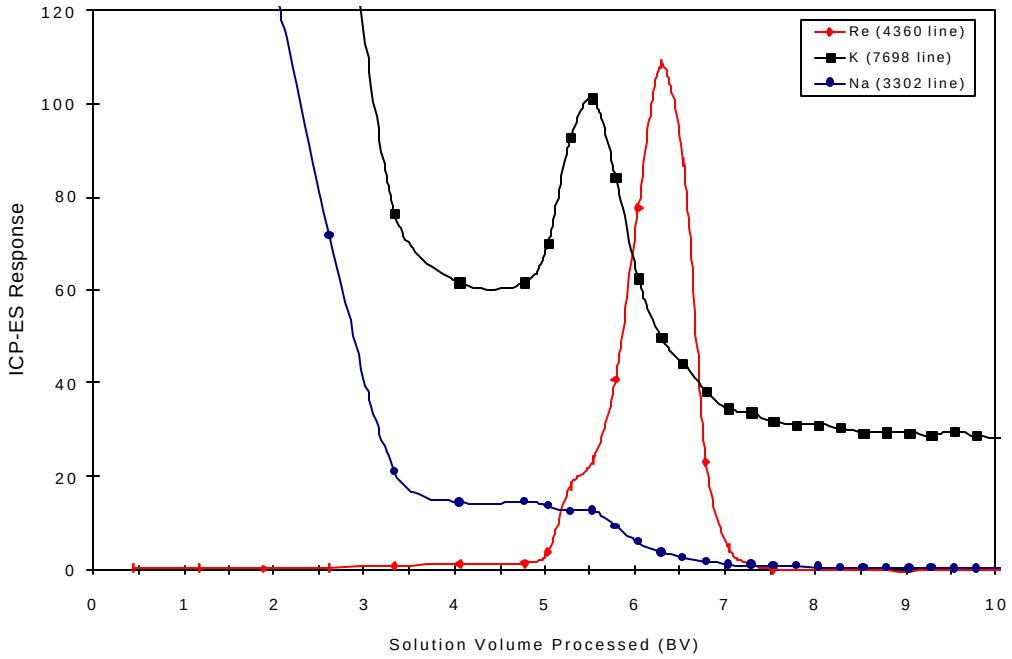

Figure 4-5. Uncalibrated On-line Data Collected During Feed Displacement (25 °C) and Elution (65°C) for Experiment 4.

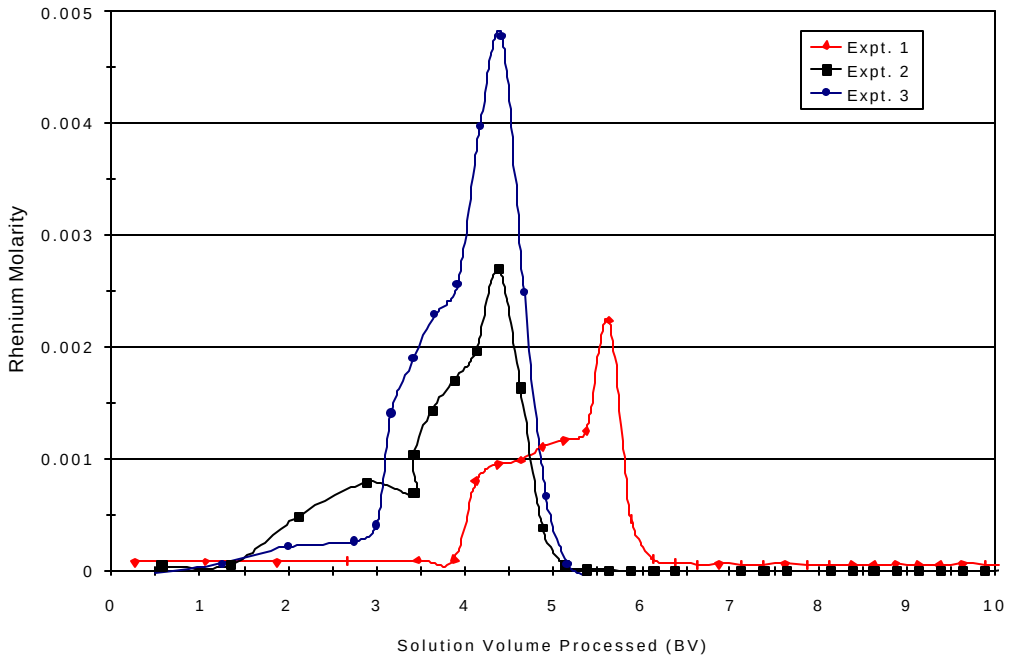

Figure 4-6. Calibrated On-line ICP-ES Rhenium Data Collected During Feed Displacement and Elution (65°C) for Experiments 1-3.

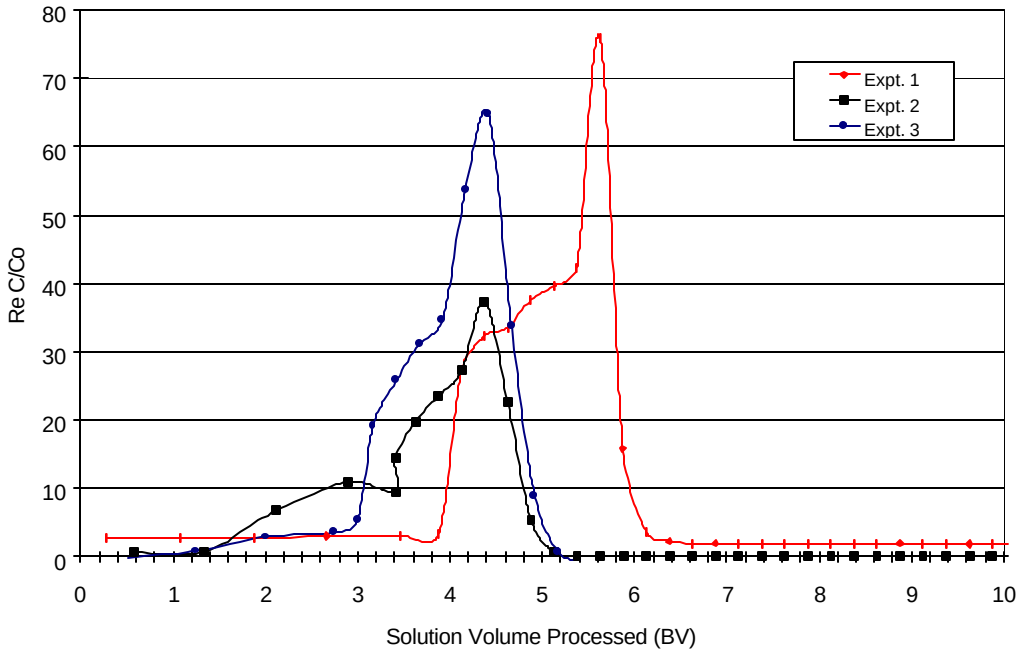

Figure 4-7. Normalized On-line ICP-ES Rhenium Data Collected During Feed Displacement and Elution (65°C) for Experiments 1-3.

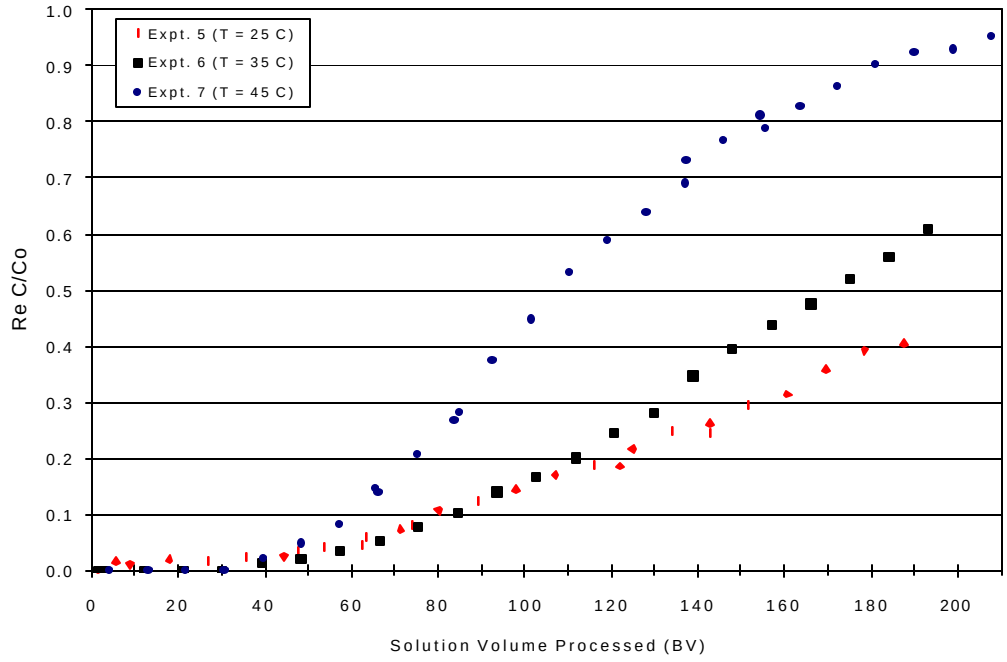

Figure 4-8. Rhenium Breakthrough Profiles Versus Temperature with AN-105 Simulant and SuperLig® 639 Batch # IR20327022045 (Experiments 5-7).

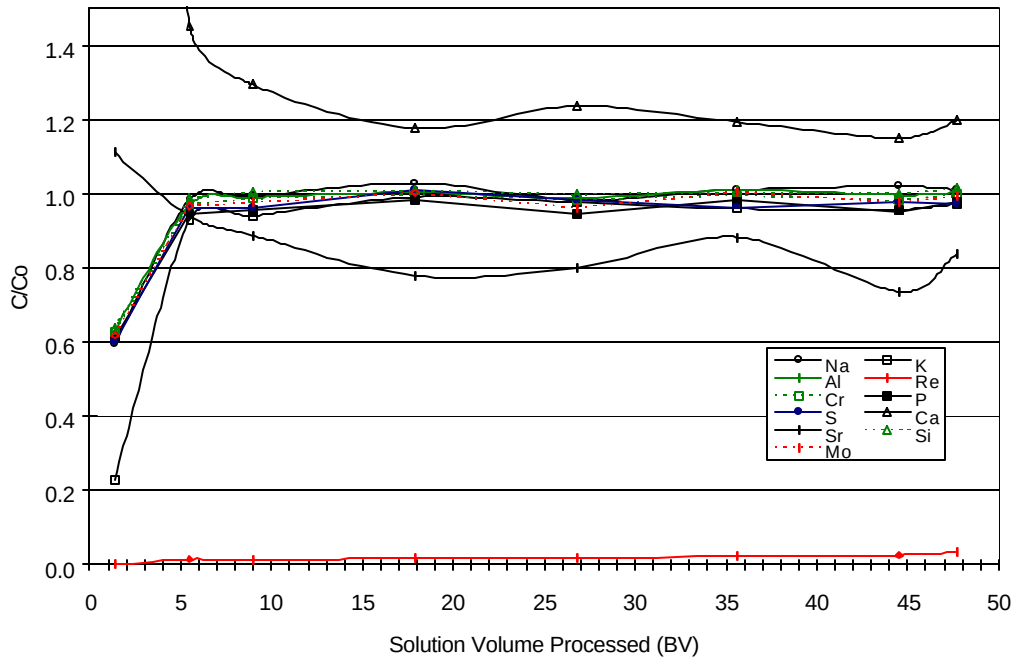

Figure 4-9. Breakthrough Profiles Obtained from ADS Analysis for Numerous Species during Column Loading for Experiment 5.

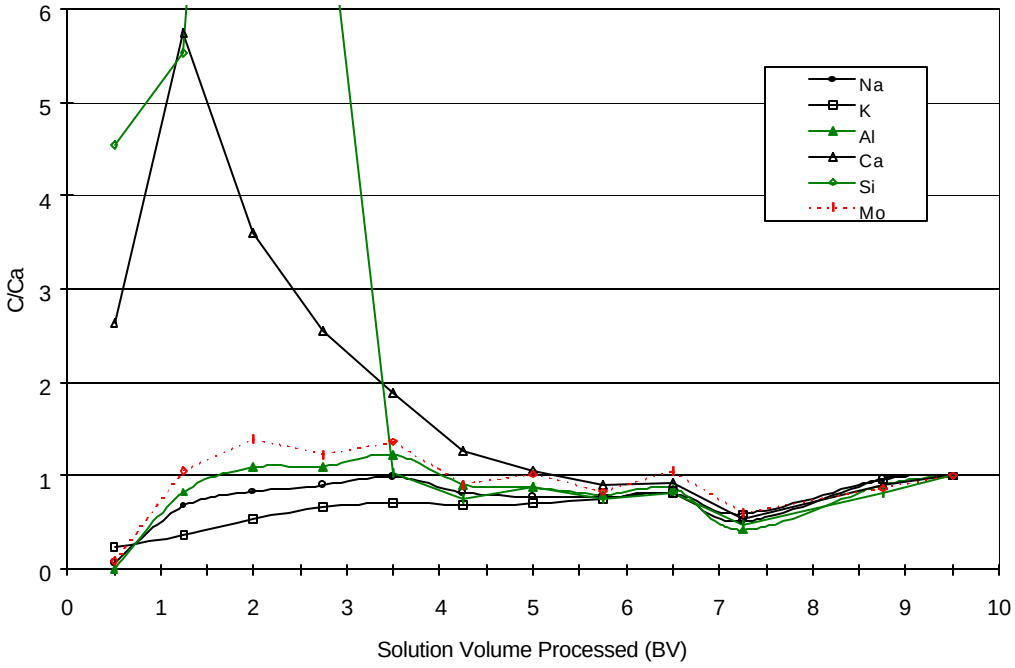

Figure 4-10. Breakthrough Profiles Obtained from On-line Data for Numerous Species during Column Loading for Experiment 5.

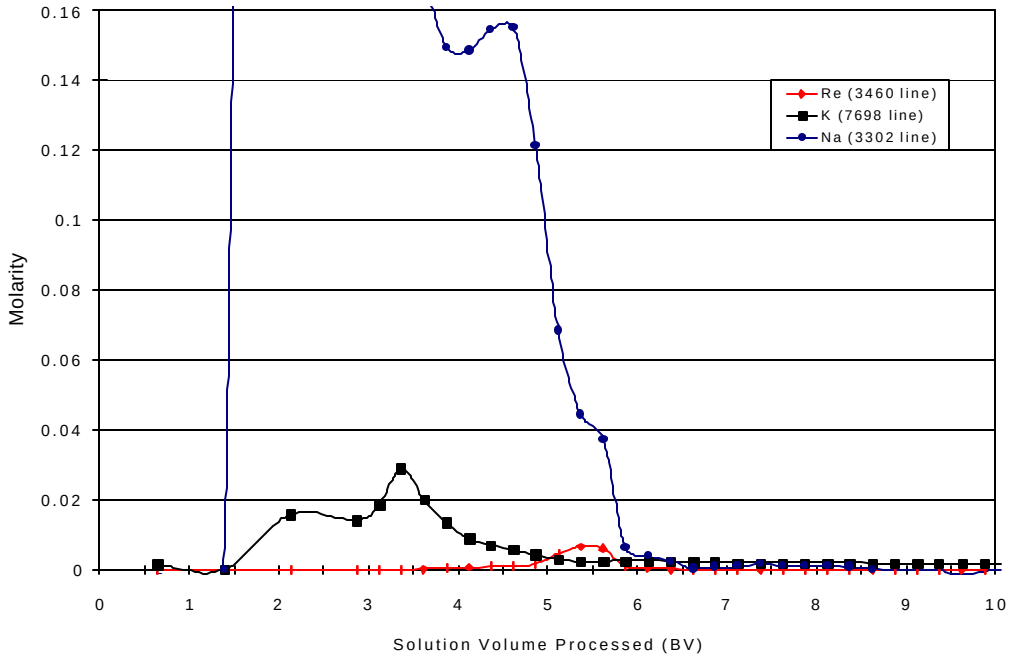

Figure 4-11. Calibrated On-line Data Collected During Feed Displacement (25 °C) and Elution (65°C) for Experiment 5.

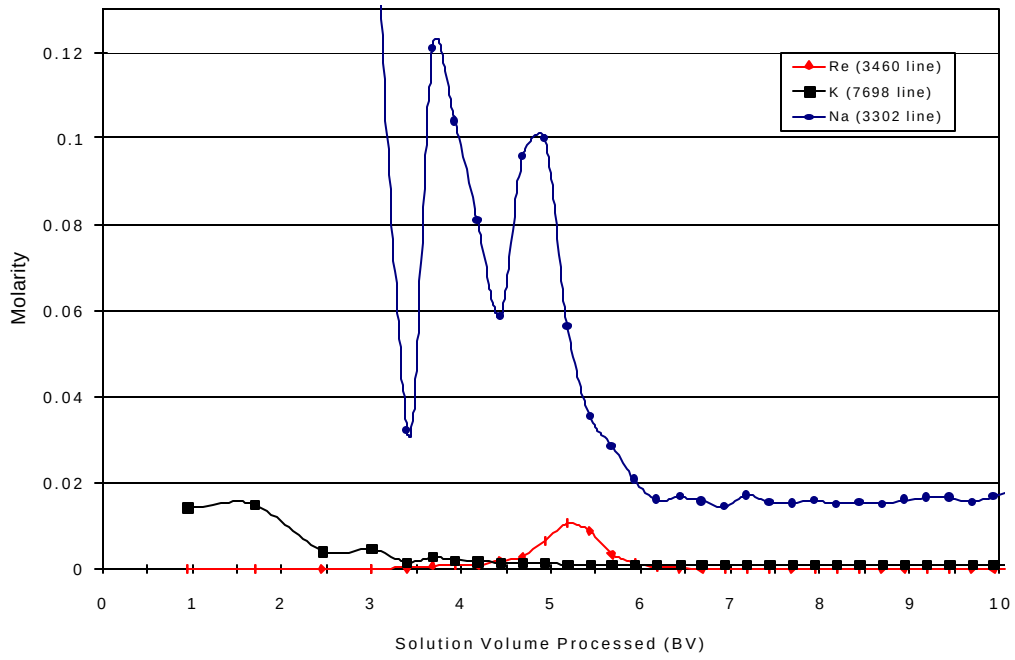

Figure 4-12. Calibrated On-line Data Collected During Feed Displacement (35 °C) and Elution (65°C) for Experiment 6.

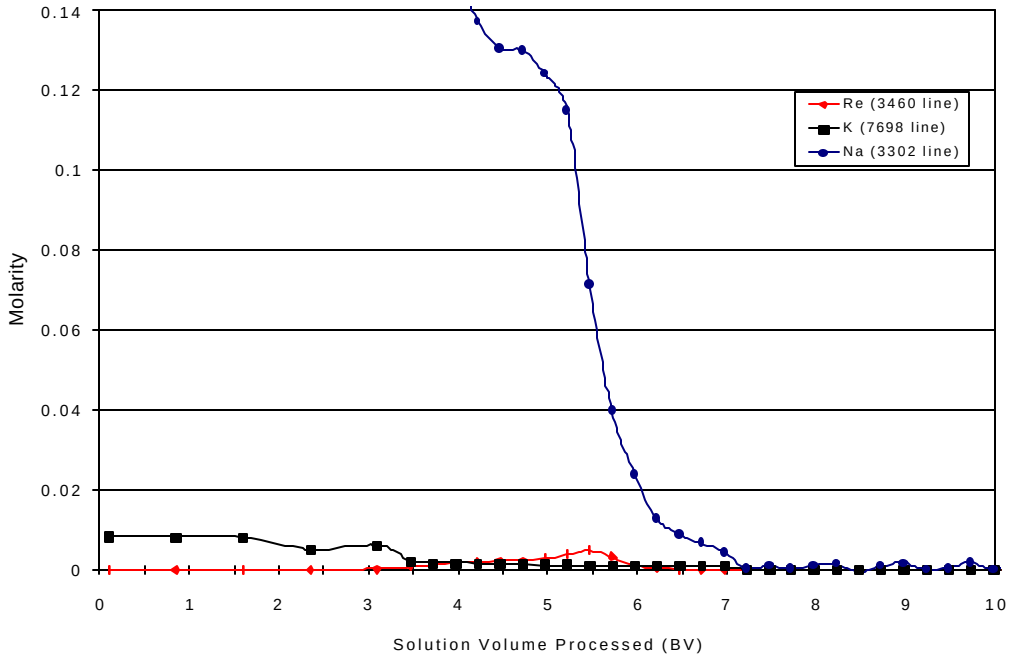

Figure 4-13. Calibrated On-line Data Collected During Feed Displacement (45 °C) and Elution (65°C) for Experiment 7.

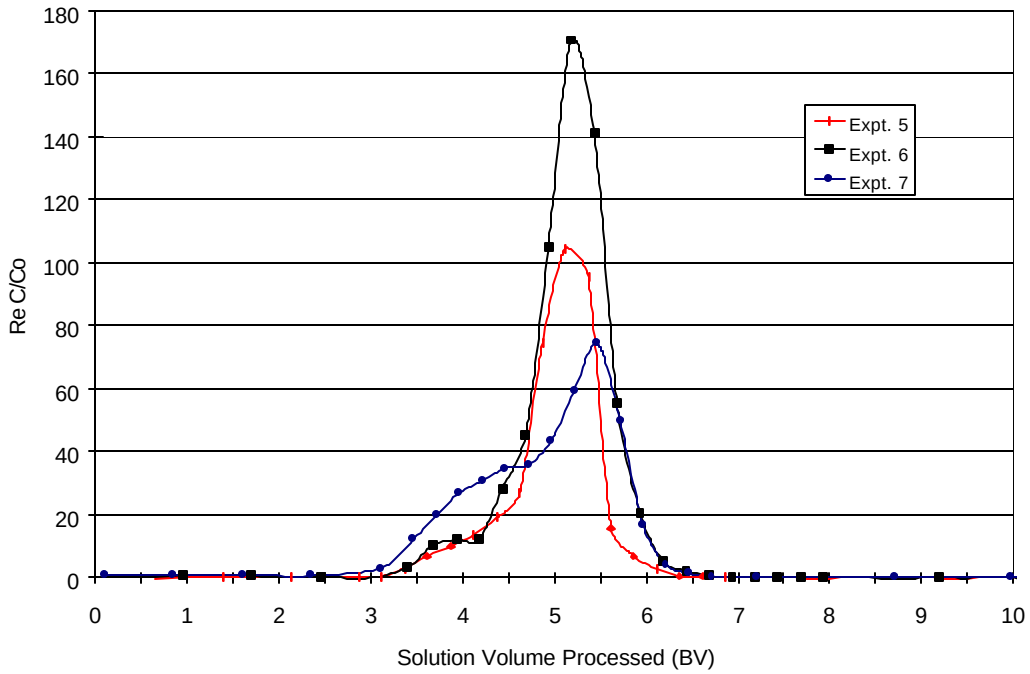

Figure 4-14. Calibrated On-line Rhenium Data Collected During Feed Displacement (25 °C) and Elution (65°C) for Experiments 5-7.

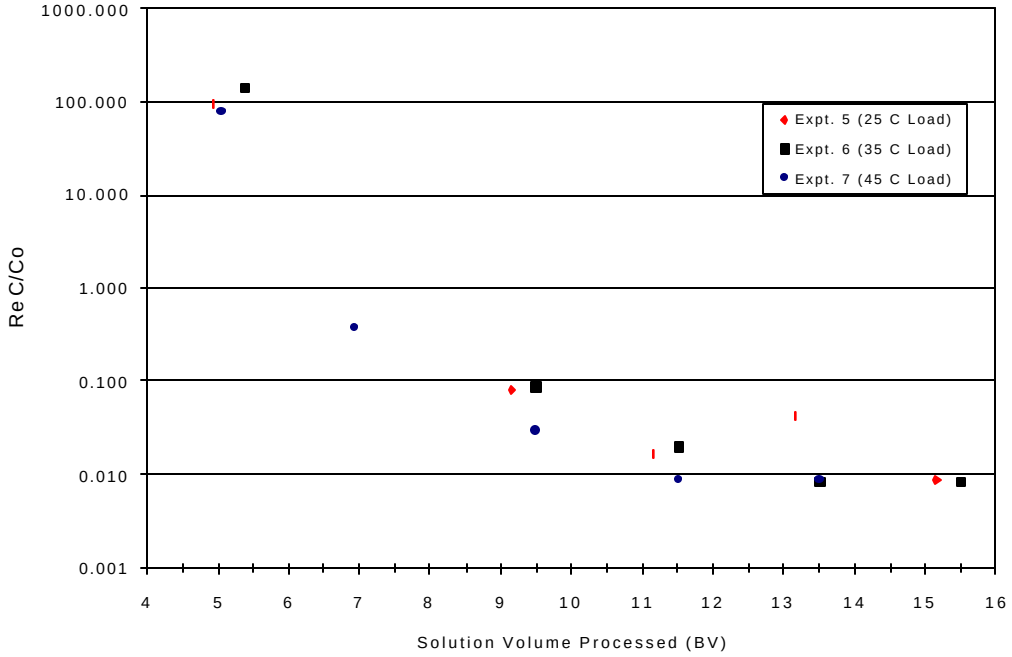

Figure 4-15. ADS Rhenium Data for Samples Collected During Water Elution (65°C) for Experiments 5-7.

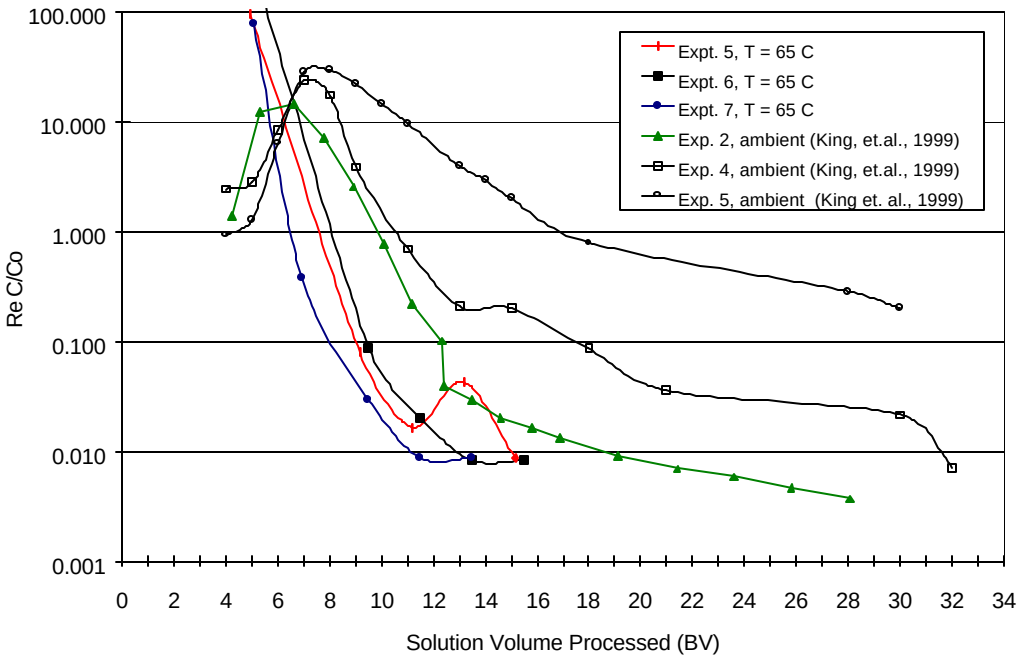

Figure 4-16. Rhenium Water Desorption Profiles for Samples Collected During Water Elution (65°C) for Experiments 5-7.

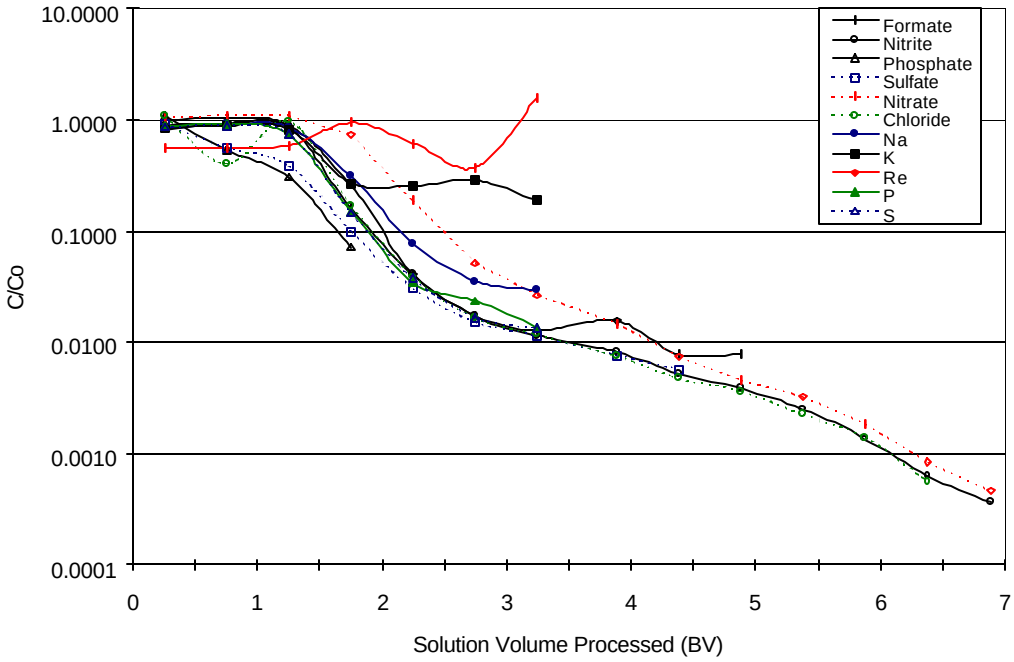

Figure 4-17. Concentration Profiles for Selected Species during Feed Displacement and Elution for Experiment 6.

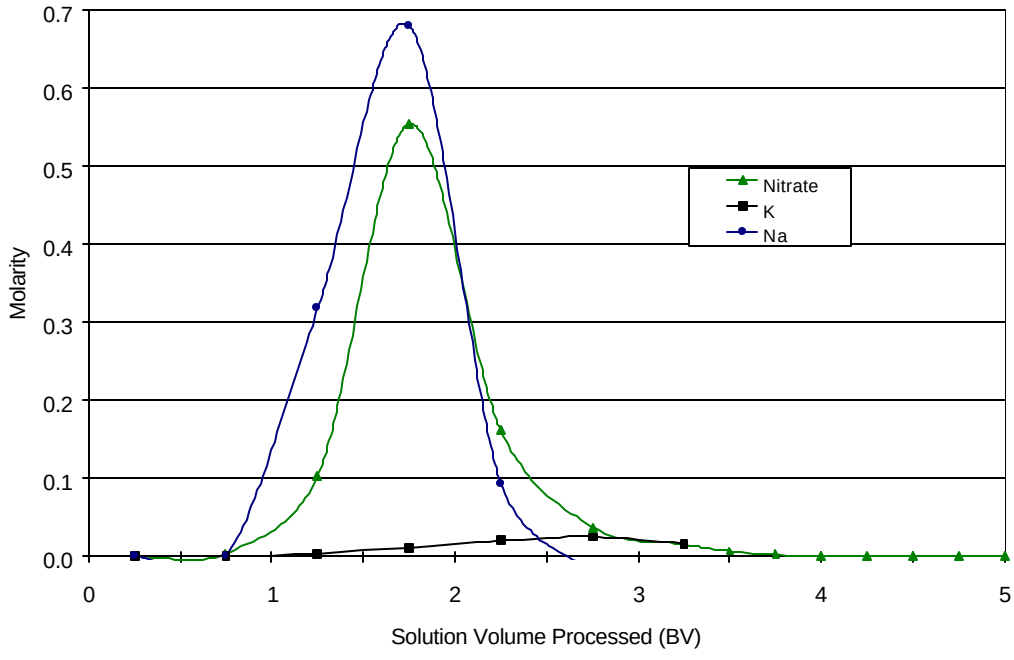

Figure 4-18. Matrix Background Corrected Nitrate Data for Samples Collected During Feed Displacement (35 °C) and Elution (65°C) for Experiment 6.

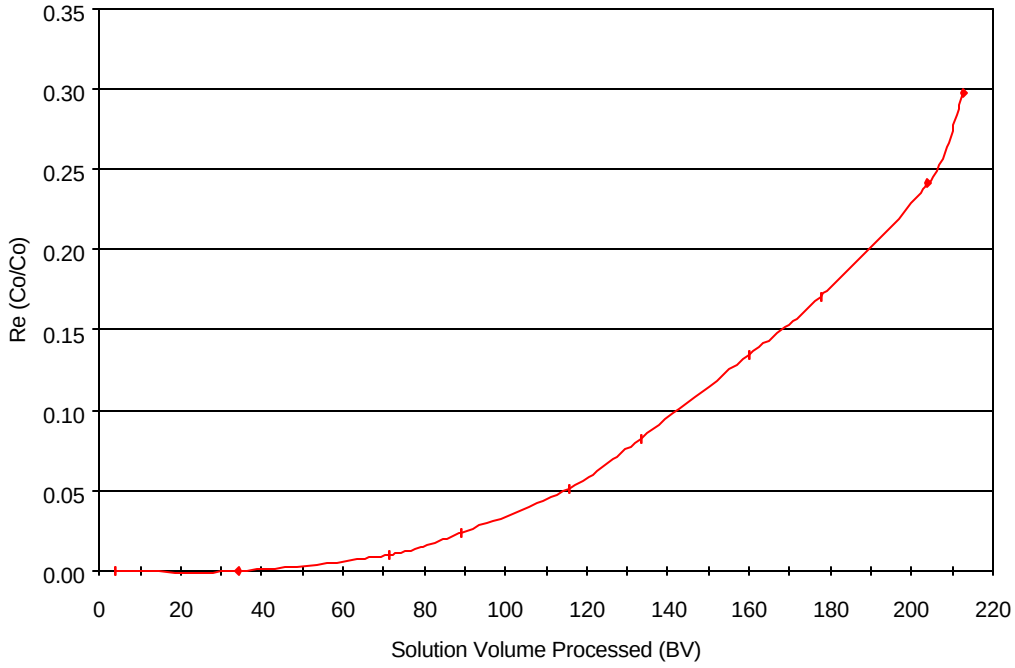

Figure 4-19. Rhenium Breakthrough Profile (25 °C) with AZ-102 Simulant and SuperLig® 639 Batch # IR20327022045 (Experiment 8).

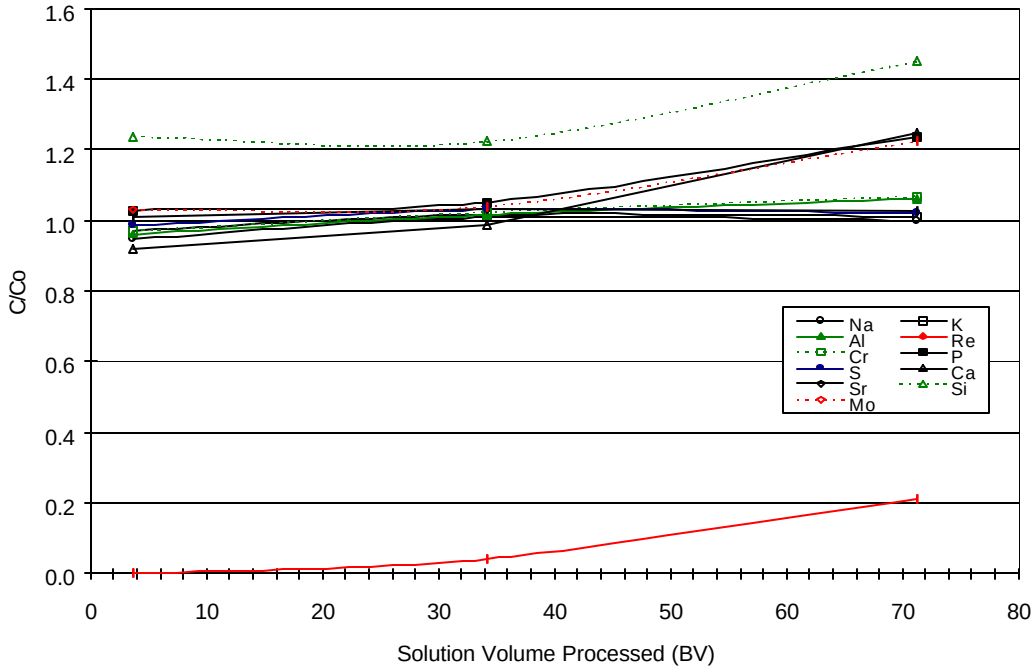

Figure 4-20. Breakthrough Profiles Obtained from ADS Analysis for Numerous Species during Column Loading for Experiment 8.

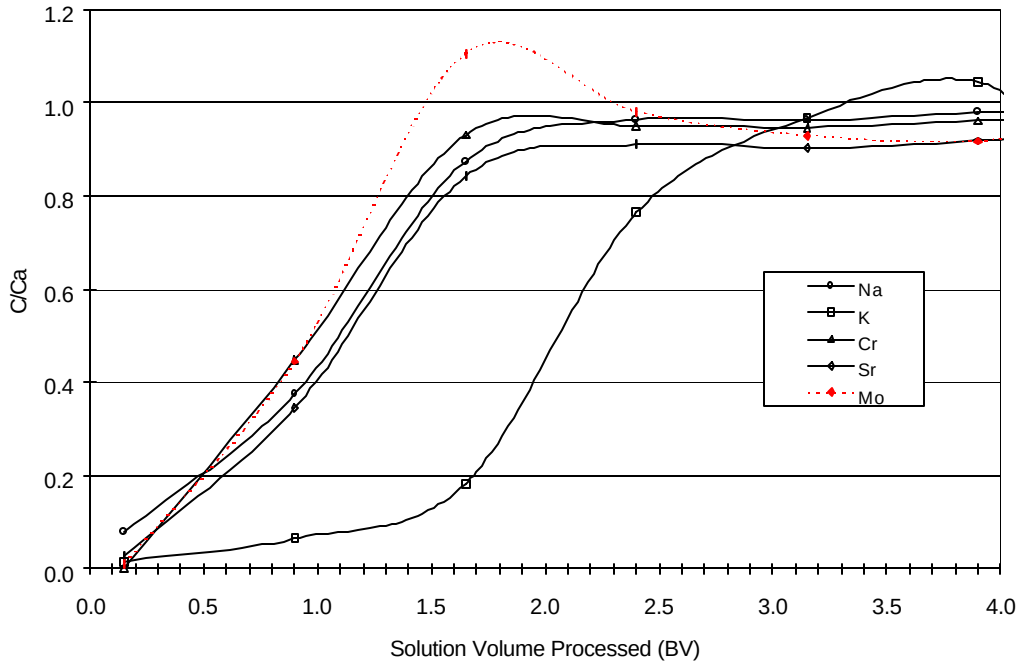

Figure 4-21. Breakthrough Profiles Obtained from On-line Data for Numerous Species during Column Loading for Experiment 8.

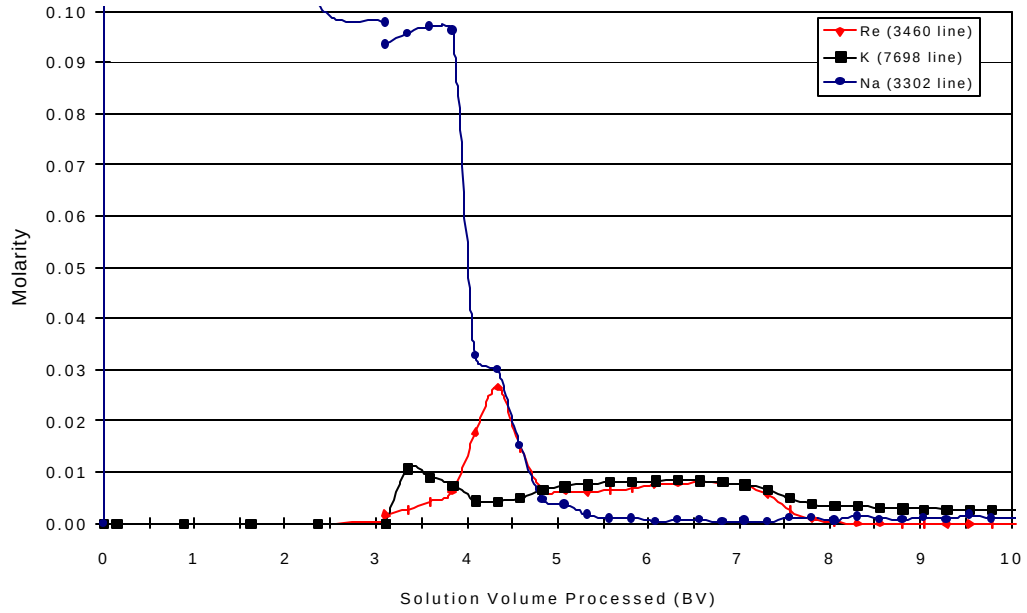

Figure 4-22. Calibrated On-line Data Collected During Feed Displacement (25 °C) and Elution (65 °C) after Loading with AZ-102 Simulant (Experiment 8).

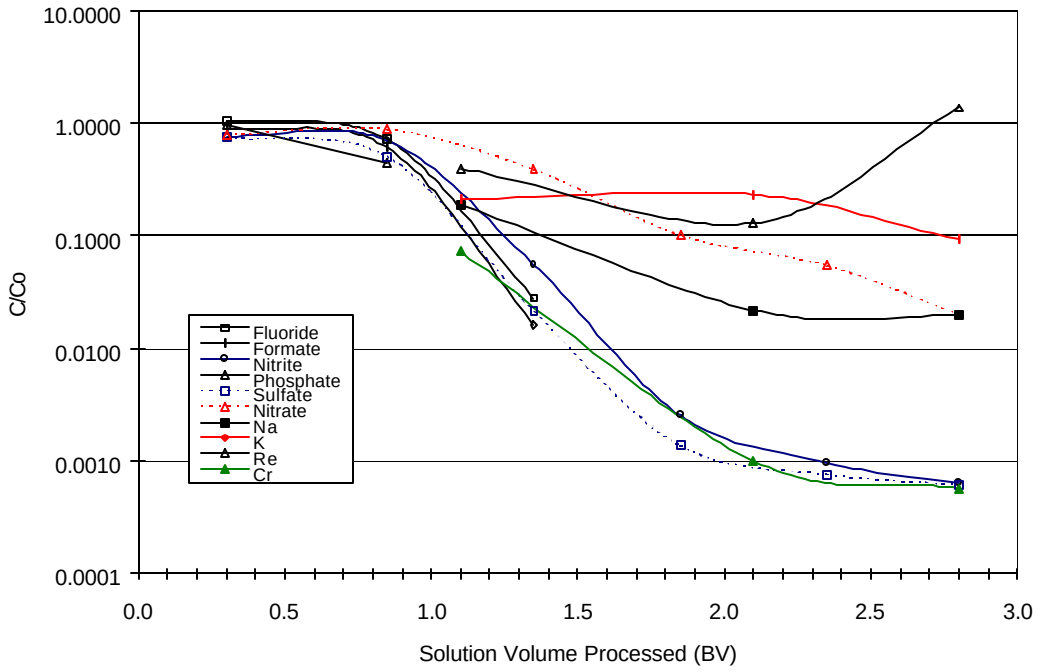

Figure 4-23. Concentration Profiles for Selected Species during Feed Displacement and Elution for Experiment 8.

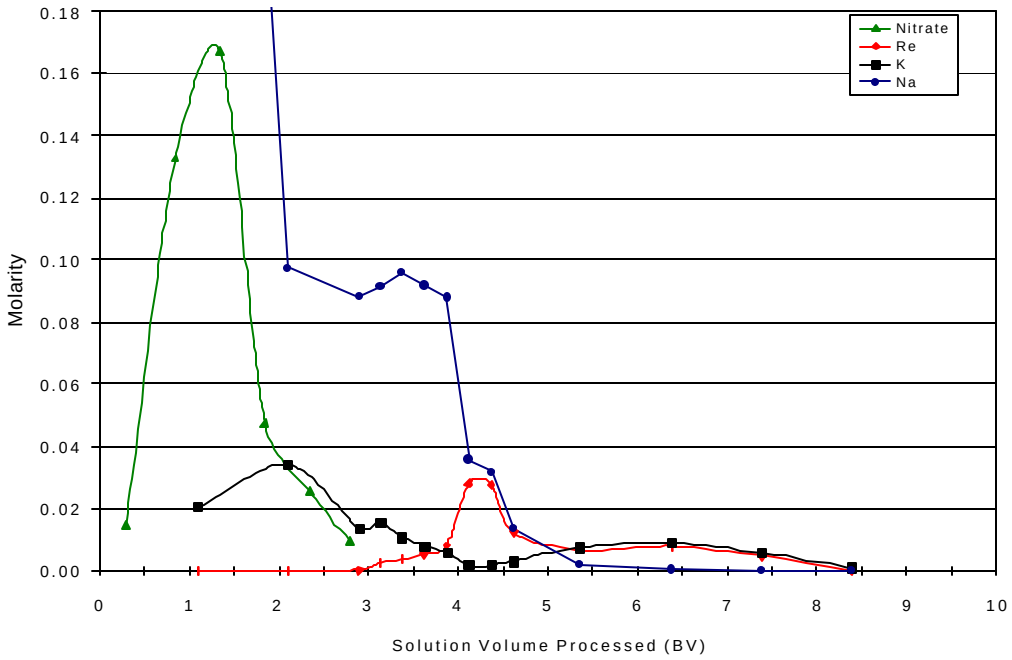

Figure 4-24. Matrix Background Corrected ADS Data for Samples Collected During Feed Displacement and Elution after Loading with AZ-102 Simulant (View 1).

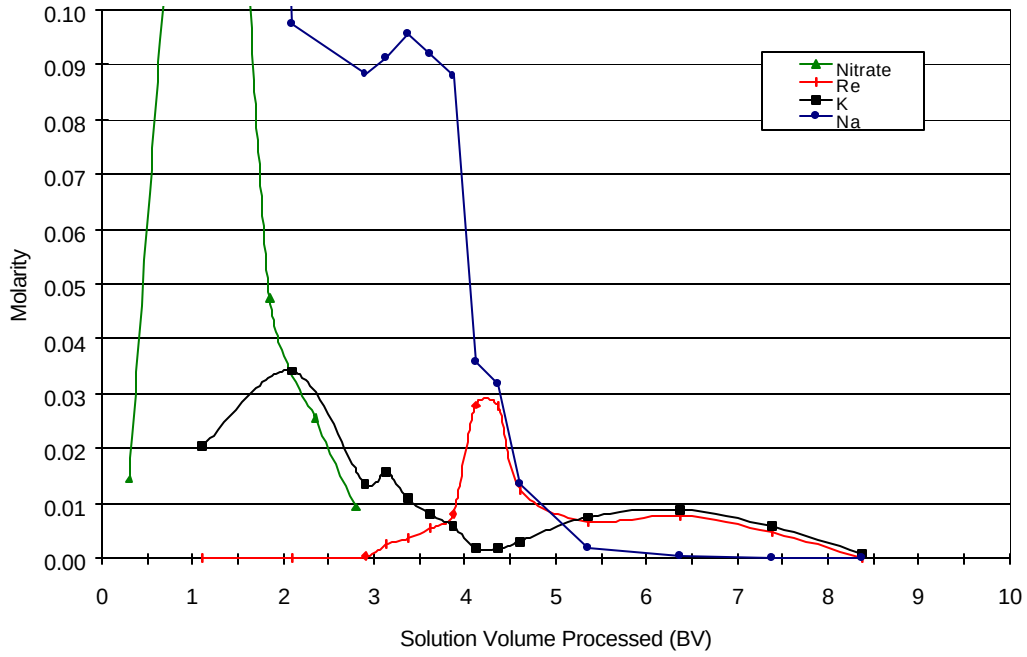

Figure 4-25. Matrix Background Corrected ADS Data for Samples Collected During Feed Displacement and Elution (65 °C) after Loading with AZ-102 Simulant (View 2).

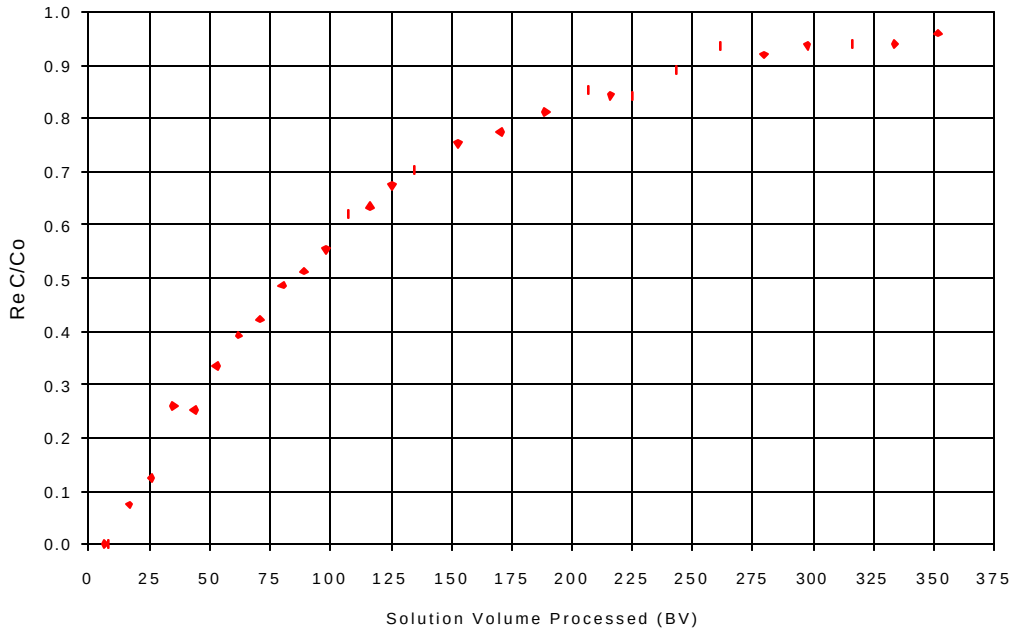

Figure 4-26. Rhenium Breakthrough Profile (25 °C) with AN-107 Simulant and SuperLig® 639 Batch # IR20327022045 (Experiment 9).

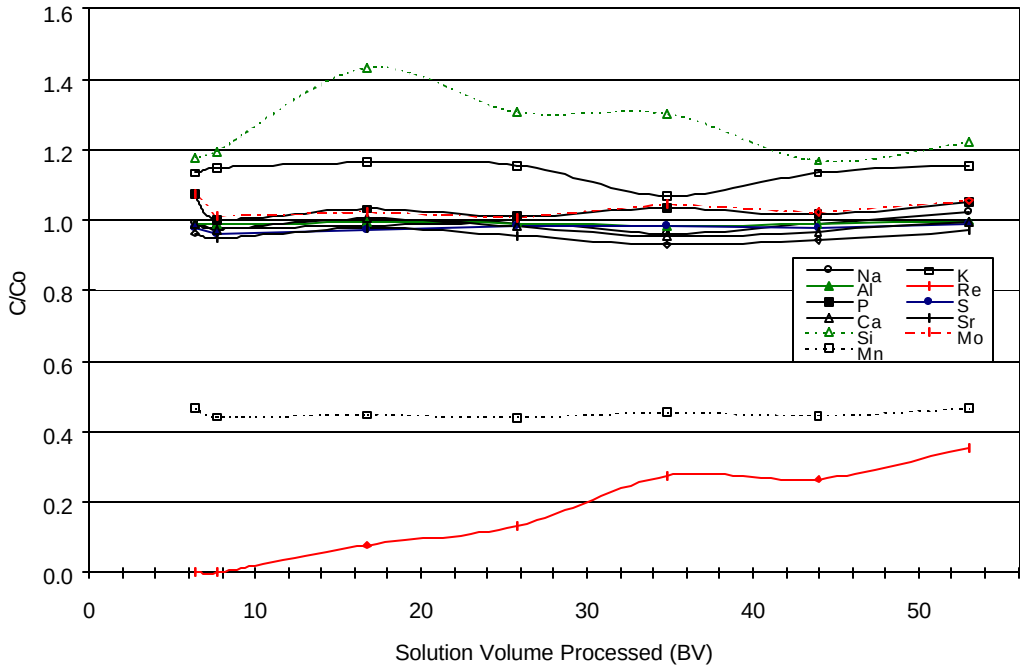

Figure 4-27. Breakthrough Profiles Obtained from ADS Analysis for Numerous Species during Column Loading for Experiment 9.

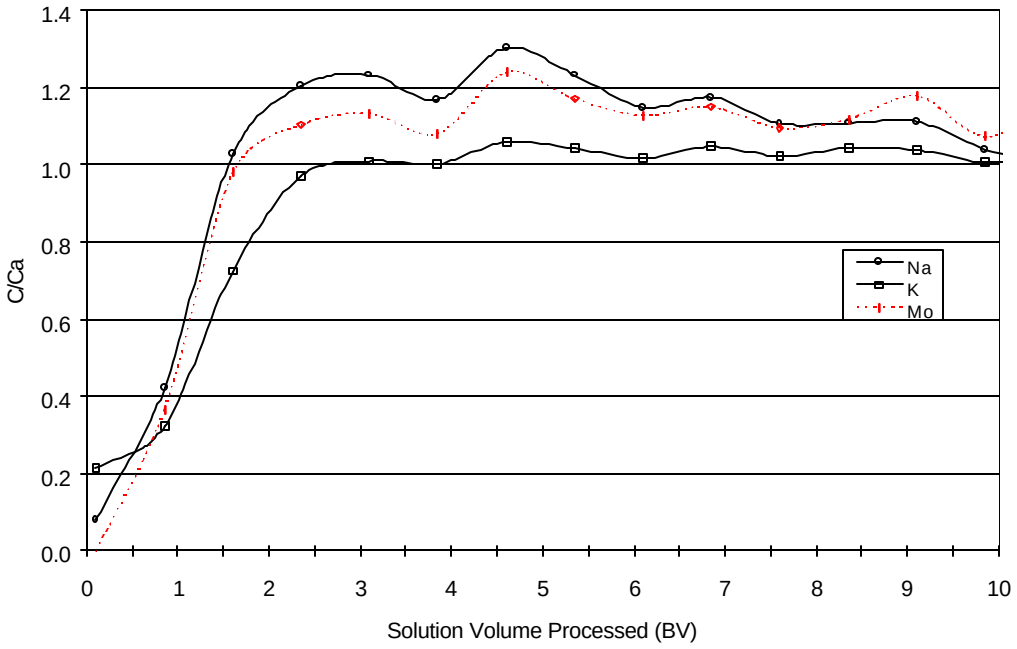

Figure 4-28. Breakthrough Profiles Obtained from On-line Data for Numerous Species during Column Loading for Experiment 9.

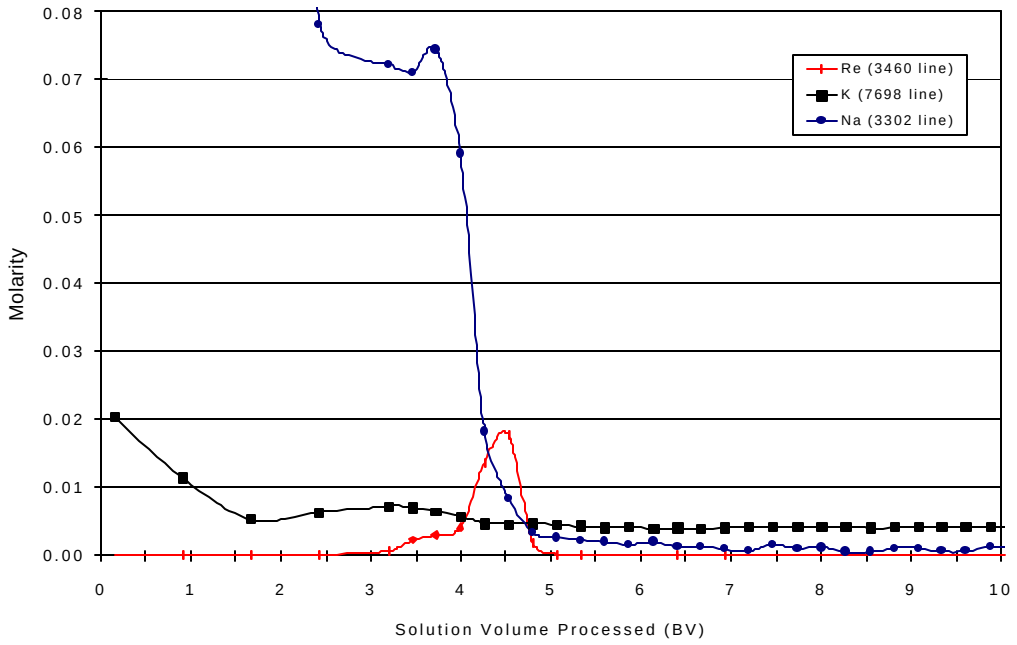

Figure 4-29. Calibrated On-line Data Collected During Feed Displacement (25 °C) and Elution (65 °C) after Loading with AN-107 Simulant (Experiment 9)

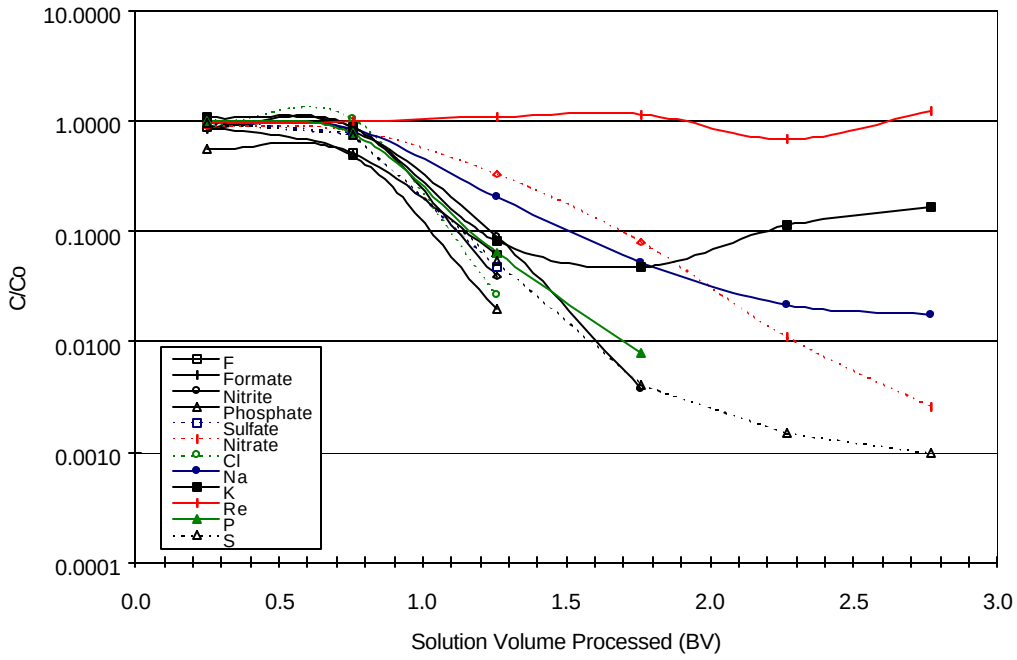

Figure 4-30. Concentration Profiles for Selected Species during Feed Displacement and Elution for Experiment 9.

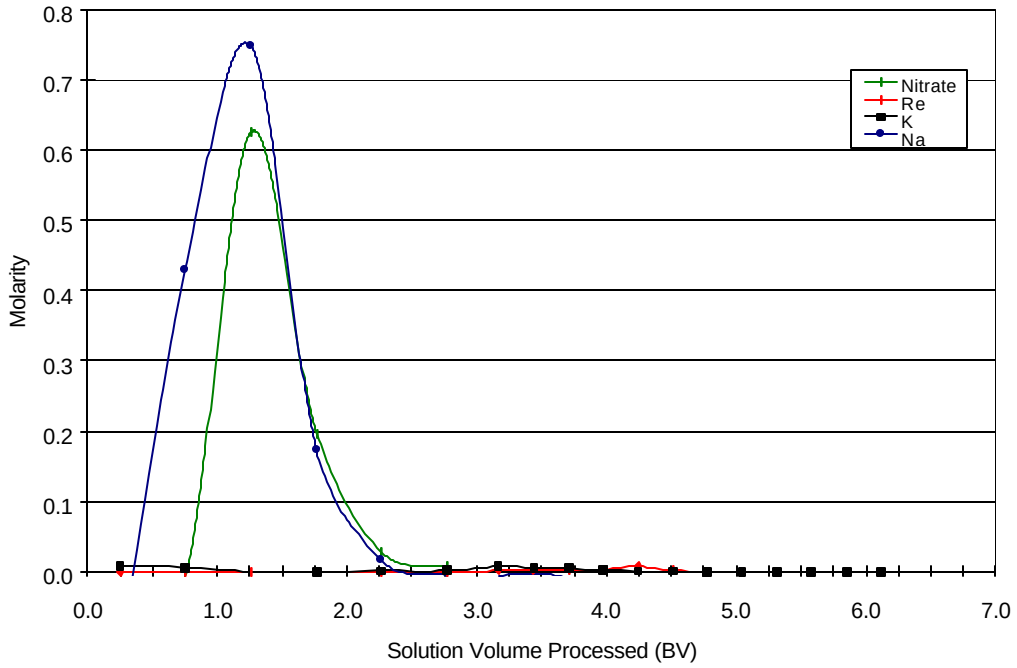

Figure 4-31. Matrix Background Corrected ADS Data Collected During Feed Displacement (25 °C) and Elution (65 °C) after Loading with AN-107 Simulant (Experiment 9).

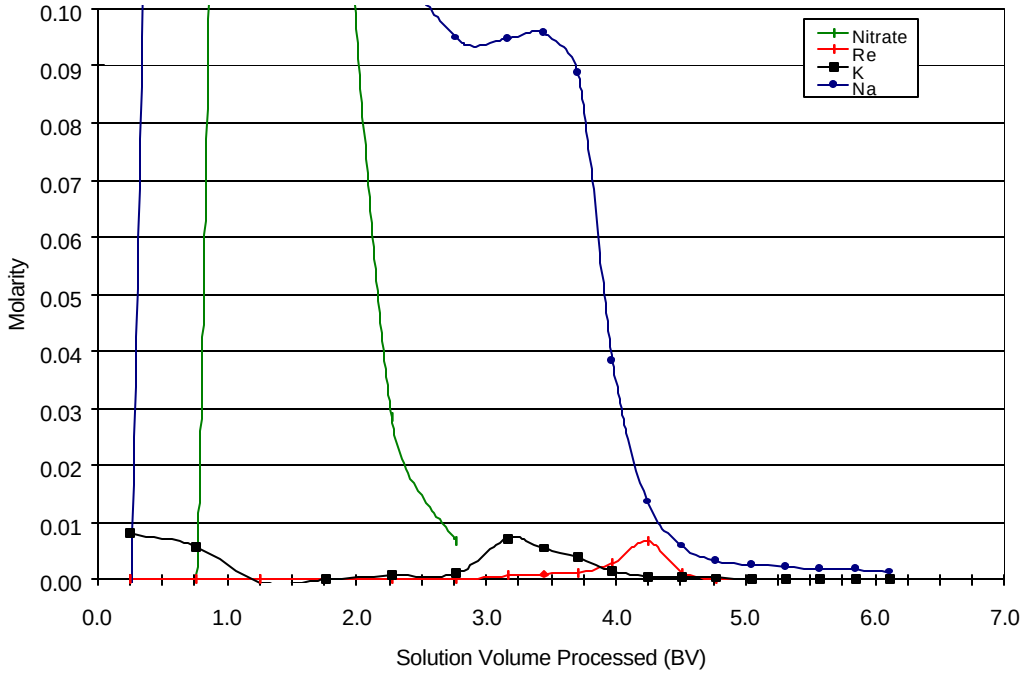

Figure 4-32. Matrix Background Corrected ADS Data Collected During Feed Displacement (25 °C) and Elution (65 °C) after Loading with AN-107 Simulant (Experiment 9).

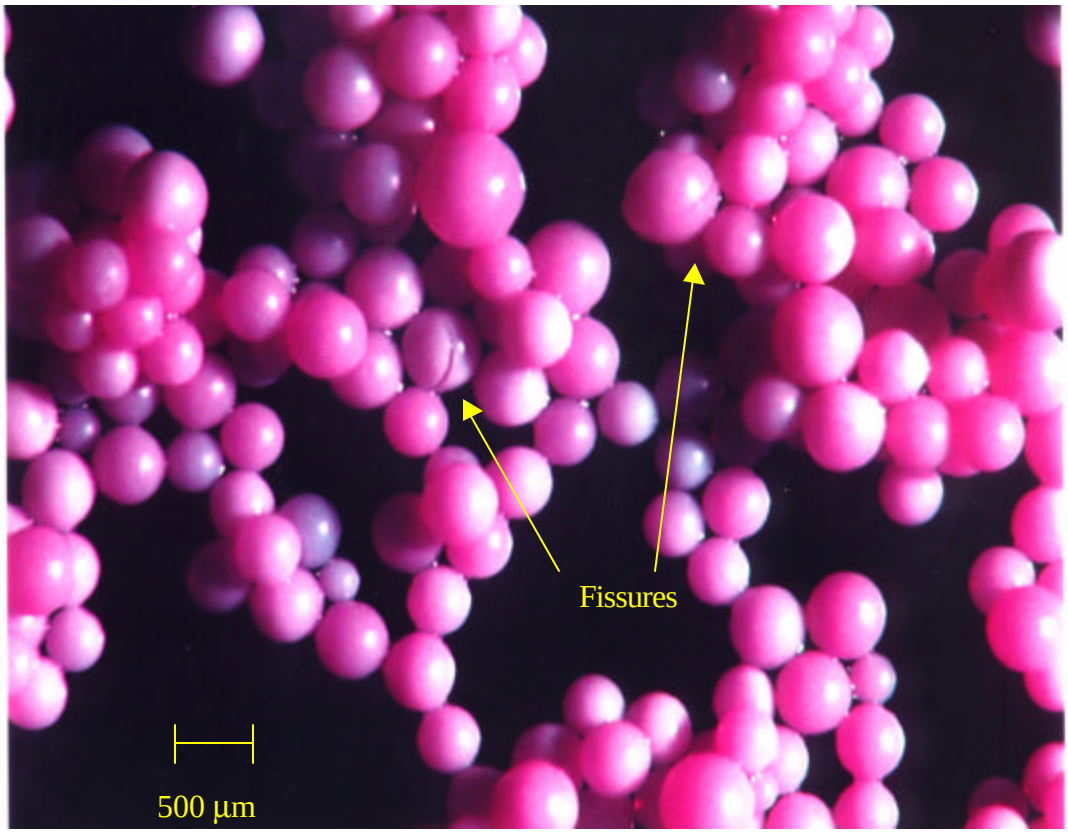

Figure 4-33. Optical Micrograph of SuperLig® 639 Resin from Batch #IR20327022045.

5.0 Conclusions

Significant information has been obtained in this work with regard to the performance of SuperLig® 639 resin. Perrhenate removal has been characterized as a function of loading temperature and solution composition. The resin performs exceptionally well for the removal of perrhenate ion from Hanford waste simulants, and performance is known to be enhanced for actual waste samples containing pertechnetate ion (Hamm, 2000). Elution performance was significantly improved by increased temperature. Furthermore, thermal shock tests conducted in this study indicate that no significant physical degradation of the resin results from exposure to the maximum potential process temperature range over a short time span. Highly time resolved on-line analysis resulted in the discovery of previously unknown competitors for sorption sites on SuperLig® 639 resin. In addition, it was discovered that the resin is very selective for potassium perrhenate over sodium perrhenate. The potassium selectivity was discovered in a timely fashion, in the sense that this information was quickly utilized to explain SuperLig® 639 column performance with actual waste samples containing exceptionally high potassium. Without knowledge of the potassium selectivity, the technetium breakthrough performance with these samples would have been unexplained. The authors proposed that the addition of potassium salts to certain waste samples be considered to enhance technetium removal performance. Unexpected discovery of the potassium selectivity is an example of the potential impacts of careful and thorough analysis in scientific studies. The authors encourage utilization of the on-line ICP-ES monitor, which was developed as part of the RPP-WTP program, for future studies in support of the project.

(This Page Intentionally Left Blank)

6.0 References

Breuning, R. L., 2001. "Physical Property Optimization of SuperLig® 639", Report to BNFL on Task TWSC99-109 Task 7 performed by IBC Advanced Technologies, Inc., January.

Burgeson I. E, J. R. Deschane, D. L. Blanchard, Jr. 2002. "Small Column Testing of SuperLig® 639 for Removal of ^{99}Tc from Hanford Tank Waste Envelope A (241-AP-101)", Batelle Company document, PNWD-3222 (WTP-RPT-030), Rev. 0., December.

Duffey, C. E., L. L. Hamm, W. D. King, 2003. "Determination of Perrhenate (ReO_4^-) Absorption Kinetics from Hanford Waste Simulants Using SuperLig® 639 Resin", Westinghouse Savannah River Company document, WSRC-TR-2002-00548 (SRT-RPP-2002-00272), Rev. 0.

Duignan, M. R., 2000. "Final Report: Pilot-Scale Crossflow Ultrafiltration Test Using a Hanford Site Tank 241-AN-107 Waste Simulant – Envelope C + Entrained Solids + Strontium - Transuranic Precipitation", Westinghouse Savannah River Company document, BNF-003-98-0226, Rev. 0, March 20.

Eibling, R. E., C. A. Nash, 2001. "Hanford Waste Simulants Created to Support the Research and Development on the River Protection Project – Waste Treatment Plant", Westinghouse Savannah River Company document, WSRC-TR-2000-00338 (SRT-RPP-2000-00017), Rev. 0, February.

Hamm, L. L., F. G. Smith, D. J. McCabe, 2000. "Preliminary Ion Exchange Modeling for Removal of Technetium from Hanford Waste Using SuperLig® 639 Resin", Westinghouse Savannah River Company document, WSRC-TR-2000-00305 (SRT-RPP-2000-000305), Rev. 0, August.

Hamm, L. L., 2002. "Task Technical and Quality Assurance Plan for Ion Exchange Computer Model Upgrades", Westinghouse Savannah River Company document, WSRC-TR-2001-00041, Rev. 0 (SRT-RPP-2002-00014), July.

Hassan, N. M. and D. J. McCabe, 1997. "Hanford Envelope C Tank Waste Ion Exchange Column Study (U)", Westinghouse Savannah River Company document, SRTC-BNFL-018, Rev. 0, October 24.

Hassan, N. M., W. D. King, D. J. McCabe, M. L. Crowder, 2001. "Small-scale Ion Exchange Removal of Cesium and Technetium from Envelope B Hanford Tank 241-AZ-102", Westinghouse Savannah River Company document, WSRC-TR-2000-00419 (SRT-RPP-2000-000036), Rev. 0, January 17.

Hassan, N. M., C. A. Nash, 2002a. "Effects of Particle Size and Solution Temperature on SuperLig® 644 Resin Performance with AN-105 Simulant", Westinghouse Savannah River Company document, WSRC-TR-2001-00606 (SRT-RPP-2001-00223), Rev. 0, December.

Hassan, N. M., C. A. Nash, 2002b. "Evaluating Residence Time for SuperLig® 644 Columns with Simulated LAW Envelope B Simulant (U)", Westinghouse Savannah River Company document, WSRC-TR-2002-00163 (SRT-RPP-2002-00089), Rev. 0, December.

Hassan, N. M., C. A. Nash, 2002c. "Evaluating Residence Time for SuperLig® 644 Columns with Simulated LAW Envelope C (AN-107) Simulant (U)", Westinghouse Savannah River Company document, WSRC-TR-2002-00257 (SRT-RPP-2002-000133), Rev. 0, December.

IBC Advanced Technologies, Inc., 1996. "Simulant Test Results for Cs, Sr, Tc, and TRU SuperLigands", conducted for British Nuclear Fuels, Inc., October (report contains some proprietary information).

Johnson, M. E., 2001a. "Test Specification for Evaluating Effects of Resin Particle Size and Solution Temperature on SuperLig® 644 and SuperLig® 639 Resins Performance with LAW Envelope A Simulant", Washingtom Group International Company document, TSP-W375-01-00023, Rev. 0, February 20.

Johnson, M. E., 2001b. "Test Specification for Evaluating Residence Time for SuperLig® 639 and 644 Columns with Simulated LAW Envelope B Solution", Washington Group International Company document, TSP-W375-01-00021, Rev. 0, February 20.

Johnson, M. E., 2001c. "Test Specification for Evaluating Residence Time for SuperLig® 639 and 644 Columns with Simulated LAW Envelope C Solution", Washington Group International Company document, TSP-W375-01-00022, Rev. 0, February 20.

King, W. D., D. J. McCabe, N. M. Hassan, 2000. "Evaluation of SuperLig® 639 Ion Exchange Resin for the Removal of Rhenium from Hanford Envelope A Simulant", Westinghouse Savannah River Company document, BNF-003-98-0230, Rev. 0, April 13.

McCabe, D. J., 2001a. "Task Technical and Quality Assurance Plan for Evaluating Effects of Resin Particle Size and Solution Temperature on SuperLig® 644 and SuperLig® 639 Resins Performance with LAW Envelope A Simulant", Westinghouse Savannah River Company document, WSRC-TR-2001-00202, Rev. 0 (SRT-RPP-2001-00049), July 13.

McCabe, D. J., 2001b. "Task Technical and Quality Assurance Plan for Evaluating Residence Time for SuperLig® 639 and 644 Columns with Simulated LAW Envelope B Solution", Westinghouse Savannah River Company document, WSRC-TR-2001-00204, Rev. 0 (SRT-RPP-2001-00050), August 13.

Perry, J. H. (editor), 1973. Chemical Engineer's Handbook, 4th Edition, McGraw-Hill chemical engineering series, McGraw-Hill Book Company, Inc., New York. pp. 3-125 and 16-19.

Rard, J. A., 1991. "Chemical Thermodynamics of Technetium IV", Lawrence Livermore National Laboratory document, UCRL-JC-108178, September.

Reid, R. C., J. M. Prausnitz, and T. K. Sherwood, 1977. The Properties of Gases and Liquids, 3rd edition, McGraw-Hill chemical engineering series, McGraw-Hill Book Company, Inc., New York. pp. 590-592.

Saito, H. H. and C. A. Nash, 2002. "Task Technical and Quality Assurance Plan for Evaluating Residence Time for SuperLig® 639 and 644 Columns with Simulated LAW Envelope C Solution", Westinghouse Savannah River Company document, WSRC-TR-2001-00465, Rev. 0 (SRT-RPP-2000-00163), January 9.

Schroeder, N. C., S. Radzinski, J. Ball, K. Ashley, S. L. Cobb, B. Cutrell, J. M. Adams, C. Johnson, and G. D. Whitener, 1995. "Technetium Partitioning for the Hanford Tank Waste Remediation System: Anion Exchange Studies for Partitioning Technetium from Synthetic DSSF and DSS Simulants and Actual Hanford Wastes (101-SY and 103-SY) Using Reillex HPQ Resin, FY95 Final Report", Los Alamos National Laboratory document, LA-UR-95-4440.

Spencer, W. A., W. D. King, and F. M. Pennebaker, 2003. "Final Report: Technetium Monitor (U) Long Term Runs with ICP Spectrometer", Westinghouse Savannah River Company document, WSRC-TR-2002-00447 (SRT-RPP-2002-00219), Rev. 0, January 7.

Steimke, J. L., M. A. Norato, T. J. Steeper and D. J. McCabe, 2000. "Summary of Testing of SuperLig® 639 at the TFL Ion Exchange Facility," Westinghouse Savannah River Co. document, WSRC-TR-2000-00302 (SRT-RPP-2000-00008), Rev. 0, August.

(This Page Intentionally Left Blank)

Appendix A. Analysis Data for Hanford Waste Simulants

Summary

Replicate analysis results for individual samples of each simulant type are included. Analysis methods include: ICP-ES, IC Anion, Free OH^-, Total Base, TIC, TOC, density, and viscosity.

A.1 AN-105 Simulant Analysis (Experiments 1-4)

ICP-ES Analysis	Molar Concentrations				
ADS#	300174488	300174884	300174885	300175178	300175179
Al	0.515	0.571	0.571	0.545	0.537
B	2.17E-03	2.17E-03	2.20E-03	2.19E-03	2.22E-03
Ba	2.03E-06	1.60E-06	1.59E-06	1.47E-06	1.44E-06
Ca	2.41E-05	5.95E-04	5.95E-04	5.98E-04	5.98E-04
Cd	<9.27E-06	2.43E-05	2.43E-05	2.85E-05	2.84E-05
Cr	0.011	0.011	0.011	0.011	0.011
Fe	1.10E-05	3.53E-05	3.52E-05	3.97E-05	4.00E-05
Mg	<6.23E-06	<6.23E-06	<6.23E-06	<6.23E-06	<6.23E-06
Mo	3.84E-04	3.72E-04	3.84E-04	3.80E-04	3.89E-04
Na	4.915	4.915	4.959	5.002	5.002
Ni	3.35E-05	2.34E-05	2.44E-05	3.07E-05	3.17E-05
P	0.003	0.003	0.002	0.003	0.003
Pb	6.69E-04	8.42E-04	8.41E-04	8.69E-04	8.69E-04
Si	0.005	0.004	0.004	0.004	0.004
Sn	<1.93E-05	<1.93E-05	<1.93E-05	<1.93E-05	<1.93E-05
Sr	4.74E-07	4.46E-07	5.60E-07	4.30E-07	2.70E-07
Zn	1.63E-04	1.56E-04	1.56E-04	1.66E-04	1.66E-04
Zr	3.80E-06	5.56E-06	5.98E-06	5.23E-06	5.68E-06
K	0.092	0.096	0.096	0.097	0.093
S	0.006	0.006	0.006	0.005	0.005
IC Anion Analysis					
ADS#	300174488	300174884	300174885	300175178	300175179
Formate	0.031	0.033	NM	0.029	NM
Chloride	0.096	0.104	NM	0.091	NM
Nitrite	1.087	1.180	NM	1.039	NM
Nitrate	1.136	1.222	NM	1.073	NM
Phosphate	0.002	0.002	NM	0.002	NM
Sulfate	0.006	0.006	NM	0.005	NM
Oxalate	0.002	0.002	NM	0.001	NM
ADS#	300174488	300188452	300174885	300188454	300188457
Total C	NM	4330	NM	NM	5240
TIC	NM	2870	NM	NM	3620
TOC	NM	1460	NM	NM	1620
Total Base	NM	2.36	NM	2.39	NM
Free OH	NM	1.36	NM	1.46	NM

A.2 AN-105 Simulant Analysis (Experiments 5-7)

Molar Concentrations							
ICP-ES Analysis							
ADS#	**300182375**	**300182376**	**300188270**	**300183383**	**300183384**	**300184788**	**300184789**
Al	0.545	0.556	0.560	0.560	0.556	0.556	0.560
B	0.002	0.002	2.25E-03	0.002	0.002	0.002	0.002
Ba	1.75E-06	1.77E-06	1.87E-06	1.52E-06	1.59E-06	1.82E-06	1.89E-06
Ca	1.68E-05	1.611E-05	8.80E-06	1.68E-05	1.59E-05	1.55E-05	1.45E-05
Cd	2.03E-05	2.08E-05	1.59E-05	2.18E-05	2.21E-05	2.00E-05	2.04E-05
Cr	0.011	0.011	0.011	0.012	0.012	0.011	0.011
Cu	5.64E-06	5.35E-06	<9.27E-06	5.02E-06	5.43E-06	<9.27E-06	<9.27E-06
Fe	3.25E-05	3.28E-05	3.24E-05	3.24E-05	3.31E-05	3.13E-05	3.15E-05
Mg	<6.23E-06	<6.23E-06	<6.23E-06	<6.23E-06	<6.23E-06	<6.23E-06	<6.23E-06
Mo	3.80E-04	3.89E-04	3.92E-04	3.86E-04	3.88E-04	3.80E-04	3.84E-04
Na	4.741	4.785	4.915	4.915	4.959	4.915	4.828
Ni	<4.60E-06	<4.60E-06	1.06E-05	6.43E-06	4.95E-06	5.93E-06	4.82E-06
P	0.002	0.002	0.003	0.003	0.003	0.002	0.002
Pb	7.57E-04	7.87E-04	8.12E-04	8.65E-04	8.69E-04	7.82E-04	7.78E-04
Si	0.004	0.004	0.004	0.004	0.004	0.004	0.004
Sn	<1.93E-05	1.94E-05	<1.93E-05	<1.93E-05	<1.93E-05	2.595E-05	<1.93E-05
Sr	5.17E-07	4.45E-07	<5.71E-07	<5.71E-07	<5.71E-07	<5.71E-07	<5.71E-07
Zn	1.79E-04	1.82E-04	1.79E-04	1.87E-04	1.88E-04	1.78E-04	1.78E-04
K	0.085	0.088	0.103	0.094	0.093	0.095	0.097
Re	6.15E-05	6.33E-05	6.25E-05	6.42E-05	6.43E-05	6.12E-05	6.18E-05
S	0.006	0.006	0.006	0.006	0.006	0.006	0.006
IC Anion Analysis							
ADS#	**300182375**	**300182376**	**300188270**	**300183383**	**300188459**	**300188458**	**300184789**
Formate	0.031	NM	NM	NM	0.031	0.032	NM
Chloride	0.096	NM	NM	NM	0.098	0.101	NM
Nitrite	1.087	NM	NM	NM	1.104	1.143	NM
Nitrate	1.136	NM	NM	NM	1.030	1.117	NM
Phosphate	0.002	NM	NM	NM	0.002	0.002	NM
Sulfate	0.006	NM	NM	NM	0.005	0.005	NM
Oxalate	0.002	NM	NM	NM	0.002	0.002	NM
ADS#	**300182375**	**300182376**	**300188270**	**300183383**	**188463**	**188460**	NM
Total C	NM	NM	NM	NM	5410	5070	NM
TIC	NM	NM	NM	NM	3930	3710	NM
TOC	NM	NM	NM	NM	1480	1360	NM
Total Base	NM	NM	NM	NM	2.34	2.31	NM
Free OH	NM	NM	NM	NM	1.35	1.34	NM

A.3 AZ-102 Simulant Analysis (Experiment 8)

Molar Concentrations

ICP-ES Analysis

ADS#	300185465	300184106	300184107	300188464
Al	0.048	0.048	0.048	0.049
B	8.69E-04	8.76E-04	8.90E-04	1.02E-03
Ba	1.32E-06	1.89E-06	1.89E-06	2.71E-06
Ca	1.64E-03	1.78E-03	1.71E-03	1.69E-03
Cr	0.025	0.026	0.026	0.027
Fe	8.34E-06	8.59E-06	8.42E-06	8.72E-06
Mo	9.89E-04	1.04E-03	1.03E-03	1.14E-03
Na	4.872	4.480	4.437	4.872
P	8.86E-03	9.30E-03	9.23E-03	1.03E-02
Si	1.99E-04	2.78E-05	3.74E-05	2.72E-04
Sr	6.73E-06	7.08E-06	7.19E-06	6.54E-06
K	0.141	0.139	0.140	0.168
S	0.312	0.304	0.311	0.312

IC Anion Analysis

ADS#	300185465	300184106	300184107	300188464
Cl	<5.64E-04	<5.64E-04	<5.64E-04	NM
Formate	0.176	0.154	0.181	NM
Fluoride	0.056	0.066	0.077	NM
Nitrite	1.226	1.056	1.206	NM
Phosphate	0.024	0.011	0.012	NM
Oxalate	0.034	0.0124	0.0137	NM
Sulfate	0.649	0.258	0.302	NM
Nitrate	0.669	0.429	0.514	NM

ADS#	300185465	300184106	300184107	300188464
Total Base	1.223	1.210	1.220	NM
Free OH	0.269	0.180	0.187	NM

A.4 AN-107 Simulant Analysis (Experiment 9)

Molar Concentrations

ICP-ES Analysis

ADS#	300185508	300185509
Al	0.009	0.009
B	1.90E-03	1.94E-03
Ca	3.54E-03	3.57E-03
Cu	8.71E-05	8.64E-05
Fe	3.08E-04	3.13E-04
Mn	4.56E-05	4.45E-05
Mo	2.22E-04	2.19E-04
Na	5.655	5.829
Ni	0.011	0.011
P	9.72E-03	9.75E-03
Si	3.45E-04	3.41E-04
Sr	1.03E-03	1.04E-03
Zn	6.37E-04	6.20E-04
Zr	3.60E-05	3.19E-05
K	0.036	0.035
S	0.054	0.055

IC Anion Analysis

ADS#	300185508	300185509
Cl	0.028	0.027
Formate	0.146	0.139
Fluoride	0.093	0.095
Nitrite	0.865	0.828
Phosphate	0.0275	0.026
Oxalate	0.011	0.011
Sulfate	0.053	0.049
Nitrate	2.58	2.55

ADS#	300185508	300185509
Total Base	1.25	1.23
Free OH	0.56	0.545

Appendix B. Analysis Data for Experiment 1 (25 °C Loading with AN-105 Simulant and Resin Batch #990420DHC720067)

Summary

Analysis data and sample bed volume assignments are provided for samples collected during column loading, feed displacement, and elution.

B.1 Loading (ADS ICP-ES Data)

	Concentration (mg/L)											
Sample	FS-1	FS-2	FS-3	FS-4	FS-5	FS-6	FS-7	FS-8	FS-9	FS-10	FS-11	FS-12
ADS#	174489	174490	174491	174492	174493	174494	174495	174496	174497	174498	174499	174500
Al	13200	13700	13600	13800	13900	13800	13700	13800	13900	13800	14000	13800
B	22.5	23.9	24.5	24.1	24.1	24.0	24.0	24.1	24.1	24.4	24.0	24.0
Ba	0.32	0.29	0.28	0.29	0.28	0.29	0.28	0.29	0.28	0.28	0.29	0.27
Ca	1.31	1.01	0.93	0.95	0.91	0.97	1.00	0.91	0.93	0.97	0.90	0.88
Cd	<0.25	<0.25	0.21	0.21	0.20	0.18	0.19	0.19	0.18	0.18	0.21	0.17
Co	<0.088	<0.088	<0.088	<0.088	<0.088	<0.088	<0.088	<0.088	<0.088	<0.088	<0.088	<0.088
Cr	546	574	567	571	583	579	583	578	580	573	575	573
Cu	<0.1	<0.1	<0.1	<0.1	<0.1	<0.1	<0.1	<0.1	<0.1	<0.1	<0.1	<0.1
Fe	0.56	0.53	0.52	0.50	0.49	0.49	0.48	0.50	0.49	0.48	0.50	0.48
Li	<0.2	<0.2	<0.2	<0.2	<0.2	<0.2	<0.2	<0.2	<0.2	<0.2	<0.2	<0.2
Mg	<0.168	<0.168	<0.168	<0.168	<0.168	<0.168	<0.168	<0.168	<0.168	<0.168	<0.168	<0.168
Mn	<0.018	<0.018	<0.018	<0.018	<0.018	<0.018	<0.018	<0.018	<0.018	<0.018	<0.018	<0.018
Mo	35.8	37.0	38.0	36.9	37.0	36.8	36.7	37.3	36.9	37.2	37.57	37.0
Na	107000	111000	103000	108000	114000	112000	114000	115000	112000	111000	113000	111000
Ni	0.88	0.92	0.92	0.94	0.91	0.95	0.93	0.87	0.88	0.87	0.85	0.86
P	77.0	77.4	82.7	78.5	78.8	78.8	78.5	79.5	78.1	77.1	81.1	76.7
Pb	17.8	18.5	18.4	18.4	18.8	17.9	18.2	19.1	18.0	18.3	18.5	18.2
Si	129	133	137	135	136	130	134	134	136	133	136	134
Sn	<0.52	<0.52	<0.52	<0.52	<0.52	<0.52	<0.52	<0.52	<0.52	<0.52	<0.52	<0.52
Sr	0.055	0.048	0.038	0.048	0.039	0.051	0.056	0.042	0.037	0.05	0.04	0.03
Zn	4.31	4.43	4.53	4.40	4.52	4.40	4.40	4.47	4.45	4.46	4.54	4.45
Zr	<0.096	0.10	<0.096	0.10	0.10	0.13	<0.096	<0.096	0.10	0.10	<0.096	0.12
La	<1.4	<1.4	<1.4	<1.4	<1.4	<1.4	<1.4	<1.4	<1.4	<1.4	<1.4	<1.4
K	3270	3540	3800	3570	3580	3570	3550	3560	3570	3540	3610	3570
Re	0.21	0.25	0.40	0.62	1.22	1.57	1.96	2.18	2.49	2.95	3.18	3.58
S	196	208	209	206	206	204	203	204	216	205	209	205
Ag	<0.6	<0.6	<0.6	<0.6	<0.6	<0.6	<0.6	<0.6	<0.6	<0.6	<0.6	<0.6
Ce	<1.54	<1.54	<1.54	<1.54	<1.54	<1.54	<1.54	<1.54	<1.54	<1.54	<1.54	<1.54
Nd	<0.52	<0.52	<0.52	<0.52	<0.52	<0.52	<0.52	<0.52	<0.52	<0.52	<0.52	<0.52
BV	4.6	9.0	19.9	27.9	43.9	54.6	63.7	72.9	82.9	96.2	104.5	121.2
Re C/Co	0.039	0.046	0.073	0.112	0.222	0.286	0.356	0.396	0.454	0.537	0.580	0.652

B.2 Feed Displacement and Elution (Raw On-line ICP-ES Data for Na, K, Re)

BV	Re3460	K7698	Na3302
0.3	2.01162	2151.11	498.453
1.1	2.15614	971.219	289.548
1.9	2.02045	164.581	39.4736
2.7	2.32145	102.604	23.558
3.5	2.38791	93.1176	22.0286
4.3	2.34176	85.6335	21.0232
5.1	1.37164	6.2846	-0.18288
5.9	1.44915	6.22887	-0.27154
6.7	1.43512	6.29456	-0.19948
7.5	1.37988	6.42283	-0.266
8.3	1.33552	6.42268	-0.28816
9.1	1.46213	6.203	-0.24369
9.9	1.32733	6.06857	-0.30481
3.9	2.54557	108.437	28.6799
4.1	20.7725	220.02	21.268
4.4	24.689	212.381	21.1019
4.6	25.5776	204.398	20.6868
4.9	28.6552	207.454	21.2568
5.1	30.2516	197.471	21.0958
5.4	32.3825	167.858	18.9812
5.6	58.0574	60.6756	6.34462
5.9	12.0516	32.4606	2.92981
6.1	2.82542	24.1434	1.83375
6.4	1.7513	19.1313	1.28022
6.6	1.48796	16.9966	1.08618
6.9	1.52935	15.083	0.80346
7.1	1.45996	14.4944	0.72583
7.4	1.49375	13.7347	0.58752
7.6	1.51006	12.8729	0.54861
7.9	1.4698	12.0573	0.39305
8.1	1.39686	12.0396	0.33259
8.4	1.47375	11.3246	0.29364
8.6	1.39887	10.9527	0.25484
8.9	1.51842	10.7841	0.33804
9.1	1.43187	10.6628	0.21049
9.4	1.42665	8.53221	0
9.6	1.50685	10.5091	0.18282
9.9	1.47059	10.2415	0.21602
10.1	1.42712	9.63792	0.16072

B.3 Feed Displacement and Elution - Calibrated On-line ICP-ES Rhenium Data

BV	Re (M)	Re C/Co
0.3	7.77E-05	2.63
1.1	8.32E-05	2.82
1.9	7.80E-05	2.64
2.7	8.96E-05	3.04
3.5	9.22E-05	3.13
3.9	9.83E-05	3.33
4.1	8.02E-04	27.19
4.4	9.53E-04	32.31
4.6	9.88E-04	33.47
4.9	1.11E-03	37.50
5.1	1.17E-03	39.59
5.4	1.25E-03	42.38
5.6	2.24E-03	75.98
5.9	4.65E-04	15.77
6.1	1.09E-04	3.70
6.4	6.76E-05	2.29
6.6	5.74E-05	1.95
6.9	5.90E-05	2.00
7.1	5.64E-05	1.91
7.4	5.77E-05	1.95
7.6	5.83E-05	1.98
7.9	5.67E-05	1.92
8.1	5.39E-05	1.83
8.4	5.69E-05	1.93
8.6	5.40E-05	1.83
8.9	5.86E-05	1.99
9.1	5.53E-05	1.87
9.4	5.51E-05	1.87
9.6	5.82E-05	1.97
9.9	5.68E-05	1.92
10.1	5.51E-05	1.87
10.4	5.42E-05	1.84
10.6	5.67E-05	1.92
10.9	5.43E-05	1.84
11.1	5.77E-05	1.95
11.4	5.41E-05	1.83
11.6	5.61E-05	1.90
11.9	5.56E-05	1.89
12.1	5.68E-05	1.93
12.4	5.33E-05	1.81
12.6	5.25E-05	1.78

(This Page Intentionally Left Blank)

Appendix C. Analysis Data for Experiment 2 (45 °C Loading with AN-105 Simulant and Resin Batch #990420DHC720067)

Summary

Analysis data and sample bed volume assignments are provided for samples collected during column loading, feed displacement, and elution.

C.1 Loading (ADS ICP-ES Data)

Sample	FS-1	FS-2	FS-3	FS-4	FS-5	FS-6	FS-7	FS-8	FS-9	FS-10
ADS#	174886	174887	174888	174889	174890	174891	174892	174893	174894	174895
Al	14100	15200	15400	15300	14600	15800	15600	15400	15100	15500
B	22.5	23.9	24.1	24.4	23.1	24.5	24.1	24.3	23.8	25.4
Ba	0.34	0.25	0.22	0.22	0.20	0.23	0.23	0.22	0.22	0.22
Ca	1.10	0.65	0.54	0.51	0.58	0.56	0.57	0.59	0.53	0.54
Cd	0.60	0.64	0.66	0.65	0.59	0.65	0.65	0.65	0.67	0.72
Co	<0.088	<0.088	<0.088	<0.088	<0.088	<0.088	<0.088	<0.088	<0.088	<0.088
Cr	544	584	586	590	559	599	592	596	578	605
Cu	<0.1	<0.1	<0.1	<0.1	<0.1	<0.1	<0.1	<0.1	<0.1	<0.1
Fe	1.83	1.95	1.99	1.99	1.82	2.01	2.00	2.00	2.07	2.03
Li	<0.2	<0.2	<0.2	<0.2	<0.2	<0.2	<0.2	<0.2	<0.2	<0.2
Mg	<0.168	<0.168	<0.168	<0.168	<0.168	<0.168	<0.168	<0.168	<0.168	<0.168
Mn	<0.018	<0.018	<0.018	<0.018	<0.018	<0.018	<0.018	<0.018	<0.018	<0.018
Mo	34.3	38.5	38.5	37.6	34.8	38.6	39.0	38.0	37.8	38.2
Na	109000	117000	116000	117000	108000	119000	115000	119000	115000	120000
Ni	0.63	0.65	0.70	0.63	0.59	0.71	0.66	0.64	0.61	0.81
P	71.8	77.1	78.5	79.3	71.6	80.7	79.1	77.4	79.8	77.6
Pb	21.0	22.6	22.7	23.3	21.0	22.8	22.9	22.3	22.7	22.5
Si	118	125	128	127	118	128	125	126	120	126
Sn	<0.52	<0.52	<0.52	<0.52	<0.52	<0.52	<0.52	<0.52	<0.52	<0.52
Sr	0.089	0.054	0.036	0.034	0.039	0.035	0.034	0.032	0.032	0.039
Ti	<0.28	<0.28	<0.28	<0.28	<0.28	<0.28	<0.28	<0.28	<0.28	<0.28
V	<0.26	<0.26	<0.26	<0.26	<0.26	<0.26	<0.26	<0.26	<0.26	<0.26
Zn	3.94	4.17	4.25	4.27	3.89	4.29	4.21	4.20	4.27	4.46
Zr	0.16	0.14	0.15	0.17	0.15	0.15	0.16	0.16	0.16	0.16
La	<1.4	<1.4	<1.4	<1.4	<1.4	<1.4	<1.4	<1.4	<1.4	<1.4
K	3290	3700	3720	3750	3580	3900	3820	3750	3710	3690
Re	0.58	0.50	1.06	4.75	4.56	7.17	9.07	10.1	11.3	12.4
S	168	172	176	187	166	176	178	180	181	190
BV	4.1	7.3	15.7	35.5	35.7	43.9	53.2	62.5	71.8	81.6
Re C/Co	0.043	0.037	0.079	0.352	0.338	0.531	0.672	0.750	0.837	0.919

C.1 (cont.)

Sample	FS-11	FS-12	FS-13	FS-14	FS-15	FS-16	FS-17	FS-18	FS-19	FS-20
ADS#	174896	174898	174899	174900	174901	174902	174903	174904	174905	174906
Al	15600	15900	15800	16000	15700	15900	15600	15400	15600	15600
B	25.3	25.4	25.0	25.5	24.9	25.3	24.9	24.5	24.8	25.2
Ba	0.22	0.23	0.21	0.22	0.21	0.23	0.21	0.21	0.20	0.21
Ca	0.57	0.56	0.59	0.58	0.54	0.57	0.58	0.57	0.54	0.52
Cd	0.70	0.71	0.67	0.69	0.66	0.71	0.68	0.67	0.66	0.67
Co	<0.088	<0.088	<0.088	<0.088	<0.088	<0.088	<0.088	<0.088	<0.088	<0.088
Cr	609	612	602	616	599	601	603	584	597	604
Cu	<0.1	<0.1	<0.1	<0.1	<0.1	0.24	<0.1	<0.1	<0.1	<0.1
Fe	2.25	2.08	2.26	2.03	1.99	2.14	2.03	2.11	1.97	2.02
Li	<0.2	<0.2	<0.2	<0.2	<0.2	<0.2	<0.2	<0.2	<0.2	<0.2
Mg	<0.168	<0.168	<0.168	<0.168	<0.168	<0.168	<0.168	<0.168	<0.168	<0.168
Mn	<0.018	<0.018	<0.018	<0.018	<0.018	<0.018	<0.018	<0.018	<0.018	<0.018
Mo	38.8	39.4	38.6	38.1	37.3	38.3	38.2	38.2	38.2	39.3
Na	117000	121000	117000	124000	120000	117000	117000	114000	118000	120000
Ni	0.78	0.73	0.72	0.73	0.78	0.82	0.77	0.80	0.77	0.77
P	79.61	79.6	78.1	78.7	76.19	81.2	76.7	76.2	75.0	76.0
Pb	23.2	22.7	22.2	22.0	21.7	24.4	22.9	22.8	21.3	22.0
Si	127	124	123	125	120	120	116	113	113	115
Sn	<0.52	<0.52	<0.52	<0.52	<0.52	<0.52	<0.52	<0.52	<0.52	<0.52
Sr	0.035	0.026	0.024	0.024	0.022	0.032	0.024	0.023	0.026	0.025
Ti	<0.28	<0.28	<0.28	<0.28	<0.28	<0.28	<0.28	<0.28	<0.28	<0.28
V	<0.26	<0.26	<0.26	<0.26	<0.26	<0.26	<0.26	<0.26	<0.26	<0.26
Zn	4.51	4.52	4.41	4.43	4.36	5.20	4.45	4.41	4.34	4.42
Zr	0.16	0.16	0.13	0.15	0.13	0.12	0.15	0.14	0.15	0.14
La	<1.4	<1.4	<1.4	<1.4	<1.4	<1.4	<1.4	<1.4	<1.4	<1.4
K	3750	3790	3800	3830	3730	3750	3700	3670	3690	3740
Re	12.8	13.7	13.7	14.0	13.7	14.9	14.3	13.7	13.9	14.1
S	187	191	186	188	184	182	181	190	177	186
BV	85.1	94.4	113.0	122.3	131.6	140.6	149.9	159.2	168.5	177.8
Re C/Co	0.951	1.018	1.016	1.039	1.014	1.100	1.059	1.015	1.027	1.041

C.2 Feed Displacement and Elution (Raw On-line ICP-ES Data for Na, K, Re)

BV	K7698	Na3302	Re3460
0.6	8240.750	1188.210	2.451
1.3	7515.020	1112.880	3.119
2.1	396.307	76.079	26.384
2.9	221.082	42.522	42.481
3.4	246.860	47.934	37.244
3.6	326.432	52.839	55.897
3.9	377.279	53.522	77.253
4.1	426.331	50.529	91.695
4.4	359.353	42.338	106.310
4.6	183.852	20.904	145.417
4.9	140.457	15.737	87.923
5.1	107.721	11.702	20.844
5.4	89.852	9.366	2.527
5.6	81.222	8.204	0.670
5.9	76.204	7.512	0.365
6.1	69.161	6.659	0.044
6.4	62.886	6.012	0.116
6.6	58.291	5.381	-0.008
6.9	53.868	4.700	-0.044
7.1	50.216	4.418	-0.050
7.4	46.645	3.881	-0.014
7.6	43.989	3.532	0.044
7.9	41.513	3.443	0.033
8.1	40.779	3.216	-0.047
8.4	38.925	2.884	-0.003
8.6	36.243	2.796	0.025
8.9	34.873	2.524	0.125
9.1	33.170	2.386	0.161
9.4	32.932	2.380	0.216
9.6	31.397	2.214	0.144
9.9	30.392	1.998	0.125
10.1	28.411	1.777	0.194
10.4	27.790	1.755	0.307
10.6	26.527	1.594	0.316
10.9	27.059	1.556	0.293
11.1	26.056	1.511	0.313
11.4	25.875	1.478	0.354
11.6	24.849	1.395	0.379
11.9	24.932	1.301	0.412
12.1	24.014	1.124	0.468
12.4	24.052	1.096	0.426

C.3 Feed Displacement and Elution - Calibrated On-line ICP-ES Rhenium Data

BV	Re (M)	Re C/Co
0.6	4.55E-05	0.63
1.3	5.79E-05	0.80
2.1	4.90E-04	6.76
2.9	7.89E-04	10.88
3.4	6.92E-04	9.54
3.4	1.04E-03	14.32
3.6	1.43E-03	19.79
3.9	1.70E-03	23.49
4.1	1.97E-03	27.24
4.4	2.70E-03	37.26
4.6	1.63E-03	22.53
4.9	3.87E-04	5.34
5.1	4.69E-05	0.65
5.4	1.24E-05	0.17
5.6	6.79E-06	0.09
5.9	8.22E-07	0.01
6.1	2.16E-06	0.03
6.4	-1.54E-07	0.00
6.6	-8.23E-07	-0.01
6.9	-9.25E-07	-0.01
7.1	-2.57E-07	0.00
7.4	8.23E-07	0.01
7.6	6.17E-07	0.01
7.9	-8.74E-07	-0.01
8.1	-5.15E-08	0.00
8.4	4.63E-07	0.01
8.6	2.31E-06	0.03
8.9	2.98E-06	0.04
9.1	4.01E-06	0.06
9.4	2.67E-06	0.04
9.6	2.31E-06	0.03
9.9	3.60E-06	0.05
10.1	5.71E-06	0.08
10.4	5.86E-06	0.08
10.6	5.45E-06	0.08
10.9	5.81E-06	0.08
11.1	6.58E-06	0.09
11.4	7.04E-06	0.10
11.6	7.66E-06	0.11
11.9	8.69E-06	0.12
12.1	7.92E-06	0.11
12.4	1.11E-05	0.15

C.3 (cont.)

BV	Re (M)	Re C/Co
12.6	9.61E-06	0.13
12.9	1.11E-05	0.15
13.1	1.17E-05	0.16
13.4	1.28E-05	0.18
13.6	1.16E-05	0.16
13.9	1.24E-05	0.17
14.1	1.52E-05	0.21
14.4	1.50E-05	0.21
14.6	1.57E-05	0.22
14.9	1.59E-05	0.22
15.1	1.68E-05	0.23
15.4	1.70E-05	0.23
15.6	1.90E-05	0.26
15.9	1.69E-05	0.23
16.1	1.86E-05	0.26
16.4	1.82E-05	0.25
16.6	1.92E-05	0.26
16.9	2.62E-04	3.62
17.1	2.63E-04	3.63
17.4	2.61E-04	3.60
17.6	2.06E-04	2.85
17.9	2.29E-04	3.15
18.1	2.33E-04	3.22
18.4	2.28E-04	3.14
18.6	2.44E-04	3.36
18.9	2.70E-04	3.73
19.1	2.73E-04	3.76
19.4	3.09E-04	4.26
19.6	3.11E-04	4.29
19.9	1.98E-05	0.27
20.1	1.26E-04	1.74
20.4	1.22E-04	1.68
20.6	1.50E-04	2.07
20.9	1.13E-04	1.56

(This Page Intentionally Left Blank)

Appendix D. Analysis Data for Experiment 3 (35 °C Loading with AN-105 Simulant and Resin Batch #990420DHC720067)

Summary

Analysis data and sample bed volume assignments are provided for samples collected during column loading, feed displacement, and elution.

D.1 Loading (ADS ICP-ES Data)

Sample	FS-1	FS-2	FS-3	FS-4	FS-5	FS-6	FS-7	FS-8	FS-9	FS-10
ADS#	175180	175181	175182	175183	175184	175185	175186	175187	175188	175189
Al	13800	14400	14800	14900	14600	14700	14700	14800	15000	14900
B	22.7	23.8	24.4	24.5	24.1	24.2	24.2	24.1	24.6	25.0
Ba	0.28	0.28	0.22	0.20	0.20	0.19	0.21	0.21	0.20	0.19
Ca	0.89	0.85	0.51	0.49	0.52	0.59	0.49	0.49	0.49	0.47
Cd	0.69	0.73	0.73	0.75	0.74	0.73	0.73	0.73	0.75	0.71
Co	<0.088	<0.088	<0.088	<0.088	<0.088	<0.088	<0.088	<0.088	<0.088	<0.088
Cr	561	586	603	601	596	595	598	598	605	605
Cu	<0.1	<0.1	<0.1	<0.1	<0.1	<0.1	<0.1	<0.1	<0.1	<0.1
Fe	2.06	2.15	2.19	2.22	2.20	2.18	2.23	2.22	2.28	2.17
Li	<0.2	<0.2	<0.2	<0.2	<0.2	<0.2	<0.2	<0.2	<0.2	<0.2
Mg	<0.168	<0.168	<0.168	<0.168	<0.168	<0.168	<0.168	<0.168	<0.168	<0.168
Mn	<0.018	<0.018	<0.018	<0.018	<0.018	<0.018	<0.018	<0.018	<0.018	<0.018
Mo	34.7	35.2	36.6	37.3	36.5	36.5	37.6	37.1	37.8	36.4
Na	110000	113000	115000	116000	113000	115000	114000	115000	121000	117000
Ni	0.76	0.85	0.85	0.89	0.81	0.83	0.83	0.88	0.87	0.82
P	74.9	78.2	79.4	81.3	80.7	79.6	81.6	82.3	82.5	78.7
Pb	21.6	23.3	23.4	23.9	21.6	23.6	23.6	22.9	23.3	23.3
Si	114	117	120	119	121	121	121	121	122	123
Sn	<0.52	<0.52	<0.52	<0.52	<0.52	<0.52	<0.52	<0.52	<0.52	<0.52
Sr	0.060	0.056	0.034	0.031	0.023	0.028	0.023	0.023	0.029	0.03
Zn	4.16	4.35	4.39	4.45	4.40	4.36	4.54	4.46	4.53	4.35
Zr	0.15	0.17	0.15	0.16	0.16	0.12	0.14	0.16	0.16	0.15
La	<1.4	<1.4	<1.4	<1.4	<1.4	<1.4	<1.4	<1.4	<1.4	<1.4
K	3420	3660	3780	3780	3700	3720	3760	3770	3770	3790
Re	0.47	0.46	0.78	1.70	2.90	4.26	5.69	6.88	8.15	8.73
S	162	170	168	175	169	166	170	172	173	167
Ag	<0.6	<0.6	<0.6	<0.6	<0.6	<0.6	<0.6	<0.6	<0.6	<0.6
Ce	<1.54	<1.54	<1.54	<1.54	<1.54	<1.54	<1.54	<1.54	<1.54	<1.54
Nd	<0.52	<0.52	<0.52	<0.52	<0.52	<0.52	<0.52	<0.52	<0.52	<0.52
BV	5.0	9.0	18.0	27.0	36.0	45.0	54.0	63.0	72.0	81.0
Re C/Co	0.034	0.033	0.057	0.123	0.210	0.309	0.412	0.499	0.591	0.632

D.1 (cont.)

Sample	FS-11	FS-12	FS-13	FS-14	FS-15	FS-16	FS-17
ADS#	175190	175191	175192	175193	175194	175195	175196
Al	14800	14900	14900	14700	14800	14900	14800
B	24.6	24.8	24.5	24.4	24.5	24.5	24.5
Ba	0.19	0.20	0.18	0.20	0.20	0.21	0.18
Ca	0.52	0.48	0.46	0.46	0.49	0.48	0.46
Cd	0.75	0.76	0.73	0.71	0.73	0.74	0.73
Co	<0.088	<0.088	<0.088	<0.088	<0.088	<0.088	<0.088
Cr	601	603	600	599	601	603	606
Cu	<0.1	<0.1	<0.1	<0.1	<0.1	<0.1	<0.1
Fe	2.28	2.26	2.22	2.16	2.20	2.26	2.27
Li	<0.2	<0.2	<0.2	<0.2	<0.2	<0.2	<0.2
Mg	<0.168	<0.168	<0.168	<0.168	<0.168	<0.168	<0.168
Mn	<0.018	<0.018	<0.018	<0.018	<0.018	<0.018	<0.018
Mo	37.3	37.8	37.2	37.5	37.4	37.8	37.2
Na	117000	115000	115000	114000	116000	116000	118000
Ni	0.85	0.93	0.85	0.79	0.81	0.87	0.84
P	81.6	81.3	80.4	79.0	76.5	81.0	78.9
Pb	23.3	23.3	23.3	23.3	23.3	23.3	23.3
Si	122	121	119	119	122	121	124
Sn	<0.52	<0.52	<0.52	<0.52	<0.52	<0.52	<0.52
Sr	0.02	0.02	0.02	0.02	0.02	0.02	0.02
Zn	4.55	4.52	4.46	4.33	4.41	4.52	4.41
Zr	0.12	0.15	0.15	0.15	0.14	0.15	0.14
La	<1.4	<1.4	<1.4	<1.4	<1.4	<1.4	<1.4
K	3830	3820	3790	3790	3750	3840	3800
Re	9.92	10.5	11.0	11.2	11.8	12.4	12.3
S	175	173	171	171	167	171	170
Ag	<0.6	<0.6	<0.6	<0.6	<0.6	<0.6	<0.6
Ce	<1.54	<1.54	<1.54	<1.54	<1.54	<1.54	<1.54
Nd	<0.52	<0.52	<0.52	<0.52	<0.52	<0.52	<0.52
BV	90.0	99.0	108.0	117.0	126.0	135.0	144.0
Re C/Co	0.719	0.763	0.798	0.810	0.852	0.897	0.893

Appendix E. Analysis Data for Experiment 4 (25 °C Loading with AN-105 Simulant and Resin Batch #990420DHC720067 - Repeat)

Summary

Analysis data and sample bed volume assignments are provided for samples collected during column loading, feed displacement, and elution.

E.2 Feed Displacement and Elution (Raw On-line ICP-ES Data for Na, K, Re)

BV	Re3460	K7698	Na3302
0.4	0.45	367.63	180.18
1.2	0.42	295.53	161.19
1.9	0.25	289.71	132.85
2.6	0.43	174.96	71.81
3.3	0.85	76.41	21.11
4.1	1.31	61.65	14.46
4.8	1.41	61.68	14.62
5.0	3.81	70.02	13.61
5.3	18.02	92.69	12.64
5.5	23.51	101.09	12.75
5.8	40.80	84.27	9.24
6.0	77.54	62.49	5.83
6.3	108.36	49.86	3.77
6.5	87.35	44.18	2.63
6.8	23.16	38.36	1.71
7.0	4.57	34.53	1.12
7.3	1.06	33.82	1.03
7.5	0.21	31.80	0.82
7.8	-0.21	31.01	0.72
8.0	-0.19	31.07	0.60
8.3	-0.28	30.43	0.51
8.5	-0.29	29.26	0.48
8.8	-0.36	29.38	0.47
9.0	-0.38	29.34	0.36
9.3	-0.32	28.83	0.45
9.5	-0.36	29.68	0.36
9.8	-0.35	28.71	0.37
10.0	-0.36	28.28	0.28

(This Page Intentionally Left Blank)

Appendix F. Analysis Data for Experiment 5 (25 °C Loading with AN-105 Simulant and Resin Batch #IR20327022045)

Summary

Analysis data and sample bed volume assignments are provided for samples collected during column loading, feed displacement, and elution.

F.1 Loading (ADS ICP-ES Data)

Sample	FS-1	FS-2	FS-3	FS-4	FS-5	FS-6	FS-7	FS-8	FS-9	FS-10
ADS#	182377	182378	182379	182380	182381	182382	182383	182384	182385	182386
Al	9400	14500	14800	15000	14800	15100	14900	15000	14900	14800
B	15.6	23.3	23.9	24.0	23.7	23.8	23.6	23.8	24.1	24.1
Ba	0.24	0.26	0.25	0.24	0.23	0.24	0.22	0.24	0.24	0.24
Ca	2.10	0.81	0.72	0.66	0.69	0.67	0.64	0.67	0.69	0.67
Cd	0.30	0.53	0.55	0.57	0.54	0.55	0.55	0.56	0.56	0.56
Co	<0.088	<0.088	<0.088	<0.088	<0.088	<0.088	<0.088	<0.088	<0.088	<0.088
Cr	371	573	583	588	581	587	579	589	587	587
Cu	0.45	0.25	0.22	0.24	0.24	0.22	0.22	0.21	0.16	0.13
Fe	1.22	1.94	1.85	1.86	1.76	1.85	1.79	1.81	1.82	1.81
Li	<0.2	<0.2	<0.2	<0.2	<0.2	<0.2	<0.2	<0.2	<0.2	<0.2
Mg	<0.168	<0.168	<0.168	<0.168	<0.168	<0.168	<0.168	<0.168	<0.168	<0.168
Mn	<0.018	<0.018	<0.018	<0.018	<0.018	<0.018	<0.018	<0.018	<0.018	<0.018
Mo	23.0	36.0	36.3	37.3	35.8	37.3	36.3	36.9	36.4	36.6
Na	65700	109000	110000	114000	109000	112000	113000	112000	112000	111000
Ni	<0.124	<0.124	0.19	0.15	0.16	0.14	0.13	<0.124	<0.124	<0.124
P	45.3	70.3	71.4	73.3	70.4	73.3	71.1	72.8	72.1	72.4
Pb	12.4	20.0	20.8	21.3	19.8	20.7	20.3	20.9	20.7	20.8
Si	67.1	104	106	106	105	106	105	107	105	105
Sn	<0.52	<0.52	<0.52	<0.52	<0.52	<0.52	<0.52	<0.52	0.52	<0.52
Sr	0.05	0.04	0.04	0.03	0.03	0.04	0.03	0.04	0.04	0.05
Ti	<0.28	<0.28	<0.28	<0.28	<0.28	<0.28	<0.28	<0.28	<0.28	<0.28
V	<0.26	<0.26	<0.26	<0.26	<0.26	<0.26	<0.26	<0.26	<0.26	<0.26
Zn	3.07	4.79	4.81	4.90	4.70	4.91	4.76	4.89	4.83	4.86
Zr	<0.096	<0.096	0.11	<0.096	0.15	<0.096	<0.096	<0.096	<0.096	<0.096
La	<1.4	<1.4	<1.4	<1.4	<1.4	<1.4	<1.4	<1.4	<1.4	<1.4
K	828	3350	3390	3570	3520	3460	3450	3510	3440	3400
Re	<0.1	0.18	0.13	0.22	0.20	0.27	0.30	0.40	0.48	0.53
S	118	189	190	199	194	190	192	192	196	191
BV	1.3	5.5	8.9	17.9	26.8	35.6	44.5	47.7	53.5	62.4
Re C/Co	NM	0.02	0.01	0.02	0.02	0.02	0.03	0.03	0.04	0.05

F.1 (cont.)

Sample	FS-11	FS-12	FS-13	FS-14	FS-15	FS-16	FS-17	FS-18	FS-19	FS-20
ADS#	182387	182388	182389	182360	182361	182362	182363	182364	182365	182366
Al	14900	14700	15200	15100	15200	15000	14900	15100	15000	14800
B	24.2	23.8	24.2	24.6	24.5	24.1	24.2	24.1	24.0	23.8
Ba	0.24	0.23	0.24	0.26	0.26	0.25	0.25	0.25	0.24	0.24
Ca	0.70	0.64	0.67	0.65	0.64	0.65	0.67	0.63	0.65	0.65
Cd	0.56	0.54	0.55	0.59	0.58	0.56	0.56	0.57	0.55	0.55
Co	<0.088	<0.088	<0.088	<0.088	<0.088	<0.088	<0.088	<0.088	<0.088	<0.088
Cr	587	578	587	607	600	603	606	600	602	598
Cu	0.16	0.17	0.16	<0.1	0.11	0.12	0.12	0.12	0.12	0.13
Fe	1.80	1.74	1.78	1.84	1.85	1.83	1.82	1.82	1.78	1.76
Li	<0.2	<0.2	<0.2	<0.2	<0.2	<0.2	0.22	<0.2	<0.2	<0.2
Mg	<0.168	<0.168	<0.168	<0.168	<0.168	<0.168	<0.168	<0.168	<0.168	<0.168
Mn	<0.018	<0.018	<0.018	<0.018	<0.018	<0.018	<0.018	<0.018	<0.018	<0.018
Mo	36.6	35.9	36.3	36.5	36.8	36.2	36.0	36.3	35.6	35.5
Na	114000	110000	117000	111000	109000	111000	109000	109000	110000	109000
Ni	<0.124	0.15	<0.124	<0.124	<0.124	<0.124	<0.124	<0.124	<0.124	<0.124
P	71.5	70.6	71.7	72.3	72.6	71.5	71.3	71.9	70.3	70.3
Pb	20.5	20.5	19.7	21.6	22.6	22.3	22.2	22.0	21.9	21.9
Si	105	103	105	107	106	106	106	105	105	105
Sn	<0.52	<0.52	<0.52	<0.70	<0.70	<0.70	<0.70	<0.70	<0.70	<0.70
Sr	0.03	0.03	0.03	0.04	0.04	0.04	0.04	0.04	0.04	0.04
Ti	<0.28	<0.28	<0.28	0.30	<0.28	<0.28	<0.28	<0.28	<0.28	<0.28
V	<0.26	<0.26	<0.26	<0.26	<0.26	<0.26	<0.26	<0.26	<0.26	<0.26
Zn	4.81	4.71	4.78	4.91	4.93	4.82	4.80	4.85	4.73	4.73
Zr	<0.096	<0.096	<0.096	<0.096	0.15	<0.096	<0.096	<0.096	0.17	<0.096
La	<1.4	<1.4	<1.4	<1.4	<1.4	<1.4	<1.4	<1.4	<1.4	<1.4
K	3510	3530	3410	3350	3290	3290	3510	3460	3390	3370
Re	0.69	0.84	0.94	1.25	1.46	1.66	1.98	2.17	2.16	2.51
S	196	185	196	192	191	190	190	191	186	186
BV	63.5	71.3	73.9	80.3	89.2	98.1	107.1	116.0	122.1	124.9
Re C/Co	0.06	0.07	0.08	0.11	0.13	0.14	0.17	0.19	0.19	0.22

F.1 (cont.)

Sample	FS-21	FS-22	FS-23	FS-24	FS-25	FS-26	FS-27	FS-28
ADS#	182367	182368	182369	182370	182371	188267	188268	188269
Al	15000	15000	14700	15700	14700	14900	15100	15300
B	23.8	23.9	23.6	24.8	23.1	23.7	24.1	24.7
Ba	0.25	0.25	0.23	0.25	0.24	0.27	0.29	0.25
Ca	0.65	0.64	0.67	0.74	0.65	0.33	0.34	0.35
Cd	0.57	0.57	0.54	0.57	0.55	0.44	0.43	0.45
Co	<0.088	<0.088	<0.088	<0.088	<0.088	<0.088	<0.088	<0.088
Cr	599	603	572	601	579	586	588	598
Cu	0.12	0.12	0.16	0.16	0.13	<0.25	<0.25	<0.25
Fe	1.83	1.81	1.73	1.93	1.81	1.84	1.91	1.82
Li	<0.2	<0.2	<0.2	<0.2	<0.2	<0.25	<0.25	<0.25
Mg	<0.168	<0.168	<0.168	<0.168	<0.168	<0.168	<0.168	<0.168
Mn	<0.018	<0.018	<0.018	<0.018	<0.018	<0.018	<0.018	<0.018
Mo	36.2	36.1	35.6	39.8	35.8	37.6	38.2	37.6
Na	110000	110000	108000	110000	109600	115000	115000	116000
Ni	<0.124	<0.124	<0.124	<0.124	<0.124	0.26	0.36	0.29
P	71.6	71.2	70.3	80.7	75.7	78.2	80.2	78.0
Pb	21.9	23.0	19.7	22.1	22.5	22.2	22.8	22.2
Si	105	105	104	118	104	104	105	106
Sn	<0.70	<0.70	<0.52	<0.52	<0.52	<0.70	<0.70	<0.70
Sr	0.04	0.04	0.03	0.04	0.04	<0.05	0.068	<0.05
Ti	<0.28	<0.28	<0.28	<0.28	<0.28	<0.28	<0.28	<0.28
V	<0.26	<0.26	<0.26	<0.26	<0.26	<0.26	<0.26	<0.26
Zn	4.82	4.80	4.69	5.14	4.79	4.9	5.0	4.8
Zr	0.11	<0.096	<0.096	<0.096	0.12	0.1	<0.096	0.2
La	<1.4	<1.4	<1.4	<1.4	<1.4	<1.4	<1.4	<1.4
K	3320	3360	3470	3340	3440	3820	3990	4070
Re	2.88	2.84	3.04	3.42	3.64	4.2	4.6	4.7
S	190	189	180	218	186	196	200	198
BV	133.8	142.8	142.8	151.7	160.6	169.6	178.5	187.4
Re C/Co	0.25	0.24	0.26	0.29	0.31	0.36	0.39	0.40

(This Page Intentionally Left Blank)

Appendix G. Analysis Data for Experiment 6 (35 °C Loading with AN-105 Simulant and Resin Batch #IR20327022045)

Summary

Analysis data and sample bed volume assignments are provided for samples collected during column loading, feed displacement, and elution.

G.1 Loading (ADS ICP-ES Data)

Sample	FS-1	FS-2	FS-3	FS-4	FS-5	FS-6	FS-7	FS-8	FS-9	FS-10	FS-11
ADS#	183352	183353	183354	183355	183356	183357	183358	183359	183360	183361	183362
Al	9040	12800	15000	15200	15200	14900	15200	15200	15200	15300	15000
B	13.5	19.1	22.1	22.2	22.3	22.4	22.5	22.6	22.7	22.4	22.1
Ba	0.19	0.23	0.23	0.23	0.23	0.23	0.24	0.24	0.25	0.24	0.23
Ca	1.45	1.14	0.66	0.64	0.63	0.69	0.64	0.63	0.69	0.64	0.64
Cd	0.30	0.43	0.50	0.49	0.50	0.49	0.51	0.51	0.52	0.51	0.47
Co	<0.088	<0.088	<0.088	<0.088	<0.088	<0.088	<0.088	<0.088	<0.088	<0.088	<0.088
Cr	355	498	577	573	578	566	576	574	577	577	566
Cu	0.13	0.13	0.10	0.10	<0.1	0.10	0.12	0.12	0.11	0.11	0.12
Fe	1.03	1.44	1.66	1.64	1.64	1.61	1.68	1.66	1.68	1.68	1.66
Li	<0.2	<0.2	<0.2	<0.2	<0.2	<0.2	<0.2	<0.2	<0.2	<0.2	<0.2
Mg	<0.168	<0.168	<0.168	<0.168	<0.168	<0.168	<0.168	<0.168	<0.168	<0.168	<0.168
Mn	<0.018	<0.018	<0.018	<0.018	<0.018	<0.018	<0.018	<0.018	<0.018	<0.018	<0.018
Mo	20.4	28.7	33.4	33.0	33.1	32.6	33.2	33.3	33.2	34.0	32.7
Na	68100	95900	112300	115100	115100	111600	112900	115700	114400	116000	114000
Ni	<0.20	<0.20	<0.20	<0.20	<0.20	<0.20	<0.20	<0.20	<0.20	<0.20	<0.20
P	45.8	62.7	73.2	71.9	71.8	70.1	72.0	70.5	72.7	73.9	70.9
Pb	12.1	16.7	20.0	20.1	19.5	19.4	19.9	19.4	19.5	20.2	19.3
Si	61.4	85.7	99.1	98.6	99.5	97.6	98.9	98.2	99.4	98.5	97.7
Sn	<0.52	<0.52	<0.52	<0.52	<0.52	<0.52	<0.52	<0.52	<0.52	0.6	<0.52
Sr	<0.070	<0.070	<0.070	<0.070	<0.070	<0.070	<0.070	<0.070	<0.070	<0.070	<0.070
Ti	<0.35	<0.35	<0.35	<0.35	<0.35	<0.35	<0.35	<0.35	<0.35	<0.35	<0.35
V	<0.26	<0.26	<0.26	<0.26	<0.26	<0.26	<0.26	<0.26	<0.26	<0.26	<0.26
Zn	2.7	3.8	4.4	4.3	4.3	4.3	4.3	4.4	4.4	4.4	4.3
Zr	<0.096	0.14	0.18	<0.096	0.12	0.12	0.16	0.18	0.12	0.12	<0.096
La	<1.4	<1.4	<1.4	<1.4	<1.4	<1.4	<1.4	<1.4	<1.4	<1.4	<1.4
K	1100	2550	3460	3600	3650	3570	3420	3430	3450	3560	3500
Re	<0.1	<0.1	<0.1	<0.1	<0.1	0.17	0.27	0.44	0.64	0.94	1.24
S	106	147	170	168	168	165	170	170	170	174	169
BV	1.5	2.8	11.9	20.9	30.0	39.1	48.1	57.2	66.2	75.3	84.4
Re C/Co	<0.01	<0.01	<0.01	<0.01	<0.01	0.01	0.02	0.04	0.05	0.08	0.10

G.1 (cont.)

Sample	FS-12	FS-13	FS-14	FS-15	FS-16	FS-17	FS-18	FS-19	FS-20	FS-21	FS-22	FS-23
ADS#	183363	183364	183365	183366	183367	183368	183369	183370	183371	183372	183373	183374
Al	15200	15000	14900	14800	14900	15200	15200	15300	15000	15100	15000	15100
B	22.2	21.8	21.8	21.8	21.8	23.6	24.1	24.4	24.5	24.6	24.8	25.0
Ba	0.24	0.23	0.22	0.23	0.22	0.20	0.20	0.21	0.20	0.20	0.21	0.22
Ca	0.64	0.68	0.62	0.72	0.62	0.71	0.71	0.72	0.68	0.72	0.69	0.69
Cd	0.52	0.49	0.49	0.49	0.49	0.55	0.57	0.58	0.56	0.57	0.58	0.59
Co	<0.088	<0.088	<0.088	<0.088	<0.088	<0.088	<0.088	<0.088	<0.088	<0.088	<0.088	<0.088
Cr	553	545	544	543	547	577	591	602	586	599	601	606
Cu	0.10	0.11	<0.1	0.10	0.11	0.15	0.15	0.13	0.14	0.12	0.13	0.13
Fe	1.66	1.63	1.62	1.62	1.61	1.74	1.79	1.78	1.74	1.77	1.79	1.82
Li	<0.2	<0.2	<0.2	<0.2	<0.2	0.31	<0.2	<0.2	<0.2	<0.2	<0.2	<0.2
Mg	<0.168	<0.168	<0.168	<0.168	<0.168	<0.168	<0.168	<0.168	<0.168	<0.168	<0.168	<0.168
Mn	<0.018	<0.018	<0.018	<0.018	<0.018	<0.018	<0.018	<0.018	<0.018	<0.018	<0.018	<0.018
Mo	34.0	33.1	33.0	33.4	33.4	34.7	35.9	36.0	35.5	36.0	36.2	37.2
Na	116000	116000	115000	113000	115000	114000	114000	113000	115000	113000	114000	113000
Ni	0.15	0.14	<0.124	0.14	0.15	0.18	0.20	0.18	0.19	0.20	0.16	0.20
P	74.2	72.1	71.9	73.1	73.7	77.8	80.1	80.5	79.3	80.0	80.4	83.3
Pb	20.1	20.0	19.3	19.6	19.8	21.9	22.3	22.6	22.0	22.2	22.5	23.9
Si	97.6	97.1	96.9	97.2	96.6	98.8	99.4	101	99.5	99.3	100	101
Sn	<0.80	<0.80	<0.80	<0.80	<0.80	<0.80	<0.80	<0.80	<0.80	<0.80	<0.80	<0.80
Sr	<0.070	<0.070	<0.070	<0.070	<0.070	<0.070	<0.070	<0.070	<0.070	<0.070	<0.070	<0.070
Ti	<0.28	<0.28	<0.28	<0.28	<0.28	<0.28	<0.28	<0.28	<0.28	<0.28	<0.28	<0.28
V	<0.26	<0.26	<0.26	<0.26	<0.26	<0.26	<0.26	<0.26	<0.26	<0.26	<0.26	<0.26
Zn	4.42	4.31	4.29	4.33	4.31	4.70	4.86	4.87	4.81	4.88	4.92	5.02
Zr	0.12	0.11	<0.096	0.11	0.10	0.16	0.15	0.14	0.15	0.14	0.17	0.15
La	<1.4	<1.4	<1.4	<1.4	<1.4	<1.4	<1.4	<1.4	<1.4	<1.4	<1.4	<1.4
K	3550	3520	3650	3540	3530	3620	3610	3700	3580	3650	3650	3640
Re	1.69	2.00	2.40	2.95	3.38	4.15	4.75	5.24	5.69	6.22	6.70	7.29
S	175	172	172	174	175	185	190	190	187	190	190	194
BV	93.4	102.5	111.5	120.6	129.7	138.7	147.8	156.9	165.9	175.0	184.0	193.1
Re C/Co	0.14	0.17	0.20	0.25	0.28	0.35	0.40	0.44	0.48	0.52	0.56	0.61

Appendix H. Analysis Data for Experiment 7 (45 °C Loading with AN-105 Simulant and Resin Batch #IR20327022045)

Summary

Analysis data and sample bed volume assignments are provided for samples collected during column loading, feed displacement, and elution.

H.1 Loading (ADS ICP-ES Data)

Sample	FS-1	FS-2	FS-3	FS-4	FS-5	FS-6	FS-7	FS-8	FS-9	FS-10
ADS#	184723	184724	184725	184726	184727	184728	184729	184730	184731	184732
Al	14100	15110	15300	14980	14840	14780	14690	15010	14800	14890
B	23.0	24.2	24.3	24.2	24.1	23.9	23.8	24.5	23.8	24.0
Ba	0.24	0.22	0.21	0.22	0.22	0.23	0.21	0.23	0.22	0.23
Ca	1.13	0.62	0.67	0.61	0.58	0.56	0.60	0.63	0.57	0.57
Cd	0.53	0.53	0.53	0.52	0.53	0.53	0.52	0.54	0.54	0.53
Co	<0.088	<0.088	<0.088	<0.088	<0.088	<0.088	<0.088	<0.088	<0.088	<0.088
Cr	551	583	587	577	574	578	570	587	579	582
Cu	0.22	0.19	0.18	0.18	0.16	0.16	0.15	0.17	0.16	0.15
Fe	1.7	1.8	1.8	1.7	1.8	1.8	1.7	1.8	1.8	1.8
Li	<0.2	0.2	<0.2	<0.2	<0.2	<0.2	<0.2	<0.2	<0.2	<0.2
Mg	<0.168	<0.168	<0.168	<0.168	<0.168	<0.168	<0.168	<0.168	<0.168	<0.168
Mn	<0.018	<0.018	<0.018	<0.018	<0.018	<0.018	<0.018	<0.018	<0.018	<0.018
Mo	34.0	36.2	36.0	35.5	35.7	36.7	35.0	36.8	36.4	36.7
Na	99000	111000	109600	111600	110000	106000	108000	110000	109000	110000
Ni	0.35	0.16	0.87	0.17	0.16	0.18	0.15	<0.124	0.14	0.17
P	69.0	72.0	71.9	71.0	71.3	73.3	70.1	73.5	73.0	73.8
Pb	18.6	19.7	19.5	19.2	19.3	19.7	19.2	19.9	19.6	20.0
Si	103	107	108	108	106	106	105	107	106	106
Sn	<0.70	<0.70	<0.70	<0.70	<0.70	<0.70	<0.70	<0.70	<0.70	<0.70
Sr	0.079	<0.050	<0.050	<0.050	<0.050	<0.050	<0.050	<0.050	<0.050	<0.050
Ti	<0.28	<0.28	<0.28	<0.28	<0.28	<0.28	<0.28	<0.28	<0.28	<0.28
V	<0.26	<0.26	<0.26	<0.26	<0.26	<0.26	<0.26	<0.26	<0.26	<0.26
Zn	4.6	4.7	4.7	4.6	4.6	4.8	4.5	4.7	4.7	4.7
Zr	0.22	0.26	0.24	0.24	0.20	0.15	0.23	0.16	0.18	0.18
La	<1.4	<1.4	<1.4	<1.4	<1.4	<1.4	<1.4	<1.4	<1.4	<1.4
K	3470	4050	4150	3950	3950	3970	3930	4040	4010	4040
Re	<0.1	<0.1	<0.1	<0.1	0.23	0.54	0.94	1.7	1.6	2.4
S	184	186	191	190	176	192	184	187	182	188
BV	4.2	13.0	21.9	30.7	39.6	48.4	57.3	65.6	66.1	75.0
Re C/Co	<0.008	<0.008	<0.008	<0.008	0.02	0.05	0.08	0.14	0.14	0.21

H.1 (cont.)

Sample	FS-11	FS-12	FS-13	FS-14	FS-15	FS-16	FS-17	FS-18	FS-19	FS-20
ADS#	184733	184734	184735	184736	184737	184738	184739	184740	184741	184742
Al	15040	15210	15350	15370	15370	15160	14990	14740	14750	14790
B	24.1	24.3	24.7	24.7	24.4	24.8	24.0	23.8	23.7	24.1
Ba	0.22	0.23	0.23	0.23	0.23	0.27	0.26	0.25	0.24	0.28
Ca	0.56	0.58	0.59	0.58	0.56	0.92	0.64	0.63	0.61	0.68
Cd	0.56	0.53	0.57	0.56	0.54	0.54	0.53	0.52	0.52	0.53
Co	<0.088	<0.088	<0.088	<0.088	<0.088	<0.088	<0.088	<0.088	<0.088	<0.088
Cr	588	591	603	593	598	581	575	565	569	570
Cu	0.17	0.34	0.16	0.18	0.18	<0.25	<0.25	<0.25	<0.25	<0.25
Fe	1.8	1.9	1.9	1.8	1.8	1.82	1.84	1.91	1.80	2.08
Li	<0.2	<0.2	<0.2	<0.2	<0.2	<0.2	<0.2	<0.2	<0.2	<0.2
Mg	<0.168	<0.168	<0.168	<0.168	<0.168	<0.168	<0.168	<0.168	<0.168	<0.168
Mn	<0.018	<0.018	<0.018	<0.018	<0.018	<0.018	<0.018	<0.018	<0.018	<0.018
Mo	36.6	36.7	38.1	37.4	37.3	36.3	35.5	35.31	35.61	36.3
Na	112000	111000	112000	114000	111000	111000	110000	108400	110500	110000
Ni	0.13	0.16	<0.124	0.15	0.17	0.17	0.15	0.16	0.17	0.16
P	73.3	73.6	76.1	74.8	74.4	72.4	70.4	69.8	70.4	71.9
Pb	20.4	20.1	20.6	20.3	20.3	20.6	20.6	19.9	20.7	20.8
Si	107	108	110	108	108	108	106	105	106	122
Sn	<0.70	<0.70	<0.70	<0.70	<0.70	<1.0	<1.0	<1.0	<1.0	<1.0
Sr	<0.050	<0.050	<0.050	<0.050	<0.050	0.071	0.055	<0.050	<0.050	<0.050
Ti	<0.28	<0.28	<0.28	<0.28	<0.28	<0.28	<0.28	<0.28	<0.28	0.3
V	<0.26	<0.26	<0.26	<0.26	<0.26	<0.26	<0.26	<0.26	<0.26	<0.26
Zn	4.7	4.8	4.9	4.8	4.8	4.8	4.6	4.6	4.6	4.8
Zr	0.27	0.25	0.22	0.22	0.24	0.2	0.1	0.2	0.1	<0.096
La	<1.4	<1.4	<1.4	<1.4	<1.4	<1.4	<1.4	<1.4	<1.4	<1.4
K	4070	4120	4170	4120	4160	3800	3780	3770	3750	3750
Re	3.1	3.2	4.3	5.1	6.0	6.7	7.3	7.9	8.3	8.7
S	189	194	186	198	195	187	183	181	182	187
BV	83.8	84.8	92.7	101.5	110.4	119.3	128.1	137.0	137.3	145.8
Re C/Co	0.27	0.28	0.37	0.45	0.53	0.59	0.64	0.69	0.73	0.77

H.1 (cont.)

Sample	FS-21	FS-22	FS-23	FS-24	FS-25	FS-26	FS-27	FS-28
ADS#	184743	184744	184745	184746	184747	184748	184749	184750
Al	14560	14740	14650	14730	15180	14860	15100	14970
B	23.9	24.1	23.8	24.0	24.4	24.4	24.4	24.3
Ba	0.24	0.25	0.25	0.26	0.26	0.25	0.25	0.26
Ca	0.61	0.65	0.61	0.64	0.62	0.62	0.64	0.61
Cd	0.54	0.53	0.53	0.53	0.54	0.54	0.53	0.54
Co	<0.088	<0.088	<0.088	<0.088	<0.088	<0.088	<0.088	<0.088
Cr	567	577	569	572	585	584	587	586
Cu	<0.25	<0.25	<0.25	<0.25	<0.25	<0.25	<0.25	<0.25
Fe	1.88	1.80	1.78	1.76	1.79	1.81	1.81	1.79
Li	<0.2	<0.2	<0.2	<0.2	<0.2	<0.2	<0.2	<0.2
Mg	<0.168	<0.168	<0.168	<0.168	<0.168	<0.168	<0.168	<0.168
Mn	<0.018	<0.018	<0.018	<0.018	<0.018	<0.018	<0.018	<0.018
Mo	36.5	36.0	35.9	36.0	36.6	36.6	36.2	36.9
Na	110000	109000	112000	110000	113000	108000	111000	113000
Ni	<0.124	0.13	<0.124	<0.124	<0.124	0.13	0.14	0.12
P	72.8	71.1	71.2	71.3	72.7	72.6	71.9	73.1
Pb	21.6	20.4	20.4	21.0	20.9	20.3	20.3	21.0
Si	105	107	106	107	109	108	107	108
Sn	<1.0	<1.0	<1.0	<1.0	<1.0	<1.0	<1.0	<1.0
Sr	<0.050	<0.050	<0.050	<0.050	<0.050	<0.050	<0.050	<0.050
Ti	<0.28	<0.28	<0.28	<0.28	<0.28	<0.28	<0.28	<0.28
V	<0.26	<0.26	<0.26	<0.26	<0.26	<0.26	<0.26	<0.26
Zn	4.8	4.7	4.7	4.7	4.8	4.8	4.7	4.8
Zr	0.1	0.1	<0.096	<0.096	<0.096	<0.096	<0.096	<0.096
La	<1.4	<1.4	<1.4	<1.4	<1.4	<1.4	<1.4	<1.4
K	3690	3700	3730	3700	3910	3740	3830	3780
Re	9.3	9.0	9.4	9.8	10.3	10.5	10.6	10.8
S	187	184	184	185	188	188	185	188
BV	154.7	155.6	163.5	172.4	181.2	190.1	198.9	207.8
Re C/Co	0.81	0.79	0.83	0.86	0.90	0.92	0.93	0.95

(This Page Intentionally Left Blank)

Appendix I. Analysis Data for Experiment 8 (25 °C Loading with AZ-102 Simulant and Resin Batch #IR20327022045)

Summary

Analysis data and sample bed volume assignments are provided for samples collected during column loading, feed displacement, and elution.

I.1 Loading (ADS ICP-ES Data)

Sample	FS-1	FS-5	FS-10	FS-12	FS-15	FS-17	FS-20	FS-22	FS-25	FS-26
ADS#	185459	185460	185461	188465	185462	188466	185463	188467	185464	188468
Al	1240	1310	1370	1330	1290	1330	1240	1300	1290	1370
B	10.3	9.5	10.2	10.3	9.3	10.2	8.5	9.7	8.3	9.8
Ba	0.20	0.23	0.25	0.33	0.16	0.35	0.18	0.34	0.18	0.46
Ca	60.4	65.2	82.1	66.9	64.6	70.3	63.0	63.0	65.4	77.2
Cd	<0.028	<0.028	<0.028	<0.028	<0.028	<0.028	<0.028	<0.028	<0.028	<0.028
Co	<0.088	<0.088	<0.088	<0.088	<0.088	<0.088	<0.088	<0.088	<0.088	<0.088
Cr	1280	1350	1410	1380	1320	1380	1270	1370	1330	1360
Cu	<0.25	<0.25	<0.25	<0.1	<0.25	<0.1	<0.25	<0.1	<0.25	<0.1
Fe	0.52	0.54	0.60	0.41	0.49	0.44	0.49	0.56	0.48	0.52
Li	<0.2	<0.2	<0.2	<0.2	<0.2	<0.2	<0.2	<0.2	<0.2	0.2
Mg	<0.168	<0.168	<0.168	<0.168	<0.168	<0.168	<0.168	<0.168	<0.168	<0.168
Mn	<0.040	<0.040	<0.040	0.0	<0.040	0.0	<0.040	0.0	<0.040	0.1
Mo	97.7	98.6	116	99.2	96.0	106	96.1	104	94.8	128
Na	106000	113000	112000	113000	112000	112000	106000	113000	112000	111000
Ni	<0.124	<0.124	<0.124	0.15	<0.124	0.17	<0.124	0.14	<0.124	0.28
P	282	288	339	293	278	309	277	302	277	375
Pb	<1.38	<1.38	<1.38	<1.38	<1.38	<1.38	<1.38	<1.38	<1.38	<1.38
Si	6.9	6.8	8.1	7.77	6.7	8.49	6.0	8.16	5.9	12.0
Sn	<1.0	<1.0	<1.0	0.6	<1.0	1.0	<1.0	0.7	<1.0	1.4
Sr	0.60	0.61	0.61	0.57	0.59	0.57	0.57	0.56	0.58	0.58
Ti	<0.30	<0.30	<0.30	<0.28	<0.30	<0.28	<0.30	<0.28	<0.30	<0.28
V	<0.26	<0.26	<0.26	<0.26	<0.26	<0.26	<0.26	<0.26	<0.26	<0.26
Zn	<0.74	<0.74	<0.74	<0.74	<0.74	<0.74	<0.74	<0.74	<0.74	<0.74
Zr	<0.096	<0.096	<0.096	<0.096	0.2	<0.096	<0.096	<0.096	0.1	<0.096
La	<1.4	<1.4	<1.4	<1.4	<1.4	<1.4	<1.4	<1.4	<1.4	<1.4
K	5340	5590	5560	6500	5710	6890	5260	6010	5550	7570
Re	<0.1	<0.1	0.37	1.0	1.86	3.4	4.86	6.9	8.76	12.1
S	9860	10300	10200	9960	10000	9880	9670	9860	10100	9940
BV	3.7	34.2	71.3	89.0	115.5	133.2	159.8	177.5	204.0	212.9
Re C/Co	NM	NM	0.010	0.024	0.051	0.083	0.134	0.171	0.241	0.297

(This Page Intentionally Left Blank)

Appendix J. Analysis Data for Experiment 9 (25 °C Loading with AN-107 Simulant and Resin Batch #IR20327022045)

Summary

Analysis data and sample bed volume assignments are provided for samples collected during column loading, feed displacement, and elution.

J.1 Loading (ADS ICP-ES Data)

Sample	FS-1	FS-2	FS-3	FS-4	FS-5	FS-6	FS-7	FS-8	FS-9	FS-10
ADS#	186735	186736	186737	186738	186739	186740	186741	186742	186743	186744
Al	240	240	241	241	239	241	242	241	240	240
B	21.7	21.9	22.5	22.4	22.7	22.8	23.0	23.0	22.5	22.6
Ba	<0.024	<0.024	<0.024	<0.024	<0.024	<0.024	<0.024	<0.024	<0.024	<0.024
Ca	141	139	143	140	136	138	142	144	140	138
Cd	<0.028	<0.028	<0.028	<0.028	<0.028	<0.028	<0.028	<0.028	<0.028	<0.028
Co	<0.15	<0.15	<0.15	<0.15	<0.10	<0.10	<0.10	<0.10	<0.10	<0.10
Cr	0.3	0.6	0.4	0.3	0.35	0.30	0.37	0.33	0.31	0.33
Cu	2.3	2.3	2.6	2.4	<0.25	<0.25	<0.25	<0.25	<0.25	<0.25
Fe	17.4	16.8	17.3	17.1	17.2	17.1	17.7	17.7	17.5	17.5
Li	<0.2	0.20	0.21	<0.2	<0.2	<0.2	<0.2	<0.2	0.21	<0.2
Mg	<0.168	<0.168	<0.168	<0.168	<0.168	<0.168	<0.168	<0.168	<0.168	<0.168
Mn	0.57	0.54	0.54	0.53	0.55	0.54	0.57	0.56	0.54	0.54
Mo	22.8	21.4	21.7	21.3	22.1	21.6	22.3	22.4	21.5	21.7
Na	131000	129000	130000	131000	127000	131000	135000	130000	132000	127000
Ni	306	301	304	305	304	305	311	308	305	306
P	323	303	311	305	312	306	317	315	302	307
Pb	<1.38	<1.38	<1.38	<1.38	<1.38	<1.38	<1.38	<1.38	<1.38	<1.38
Si	11.3	11.5	13.8	12.6	12.5	11.3	11.8	12.2	11.0	11.1
Sn	0.55	0.54	<0.52	0.70	<0.52	0.6	<0.52	<0.52	<0.52	<0.52
Sr	87.4	86.0	88.7	86.7	84.3	85.6	88.0	88.7	86.9	85.9
Ti	<0.28	<0.28	<0.28	<0.28	<0.28	<0.28	<0.28	<0.28	<0.28	<0.28
V	<0.26	<0.26	<0.26	<0.26	<0.26	<0.26	<0.26	<0.26	<0.26	<0.26
Zn	19.7	19.2	19.4	19.5	19.5	19.6	19.8	19.8	19.5	19.6
Zr	0.82	0.80	0.93	0.91	0.86	0.95	0.97	0.93	0.92	0.90
La	<1.4	<1.4	<1.4	<1.4	<1.4	<1.4	<1.4	<1.4	<1.4	<1.4
K	1560	1580	1600	1590	1470	1560	1590	1590	1590	1600
Re	<0.1	<0.1	0.42	0.71	1.5	1.4	1.9	2.2	2.4	2.8
S	1710	1680	1700	1720	1720	1710	1730	1720	1730	1720
BV	6.4	7.7	16.7	25.8	34.9	43.9	53.0	62.0	71.1	80.2
Re C/Co	<0.018	<0.018	0.07	0.12	0.26	0.25	0.33	0.39	0.42	0.49

J.1 (cont.)

Sample	FS-11	FS-12	FS-13	FS-14	FS-15	FS-16	FS-17	FS-18	FS-19	FS-20
ADS#	186745	186746	186747	186748	186749	186750	186751	186752	186753	186754
Al	240	240	241	241	240	240	241	240	239	236
B	22.6	22.6	22.7	22.5	22.3	22.2	22.9	22.5	22.4	22.4
Ba	<0.024	<0.024	<0.024	<0.024	<0.024	<0.024	<0.024	<0.024	<0.024	<0.024
Ca	140	140	142	139	137	138	141	138	138	138
Cd	<0.028	<0.028	<0.028	<0.028	<0.028	<0.028	<0.028	<0.028	<0.028	<0.028
Co	<0.10	<0.10	<0.10	<0.10	<0.10	<0.10	<0.10	<0.10	<0.10	<0.10
Cr	0.29	0.30	0.30	0.28	0.28	0.27	0.23	0.27	0.24	0.25
Cu	<0.25	<0.25	<0.25	<0.25	<0.25	2.61	2.60	2.56	2.58	2.27
Fe	17.2	17.1	17.5	17.2	17.2	17.2	17.3	17.1	17.1	16.9
Li	<0.2	<0.2	<0.2	<0.2	<0.2	<0.2	<0.2	<0.2	<0.2	<0.2
Mg	<0.168	<0.168	<0.168	<0.168	<0.168	<0.168	<0.168	<0.168	<0.168	<0.168
Mn	0.54	0.54	0.56	0.54	0.54	0.54	0.54	0.54	0.53	0.54
Mo	21.5	21.4	22.3	21.4	21.8	21.6	21.6	21.5	21.3	21.8
Na	135000	129000	128000	128000	131000	127000	132000	134000	132000	128000
Ni	306	306	307	308	305	307	307	306	304	300
P	303	298	315	300	307	308	308	304	298	304
Pb	<1.38	<1.38	<1.38	<1.38	<1.38	<1.38	<1.38	<1.38	<1.38	<1.38
Si	14.8	12.3	11.7	10.8	11.0	13.7	14.1	13.0	11.9	13.9
Sn	0.5	<0.52	0.6	<0.52	<0.52	0.55	<0.52	<0.52	<0.52	0.84
Sr	86.5	86.8	87.8	86.0	84.8	85.2	87.7	85.7	85.5	85.4
Ti	<0.28	<0.28	<0.28	<0.28	<0.28	<0.28	<0.28	<0.28	<0.28	<0.28
V	<0.26	<0.26	<0.26	<0.26	<0.26	<0.26	<0.26	<0.26	<0.26	<0.26
Zn	19.5	19.6	19.6	19.7	19.5	19.7	19.5	19.4	19.5	19.2
Zr	0.98	0.93	0.91	0.93	0.85	0.90	0.86	0.91	0.86	0.80
La	<1.4	<1.4	<1.4	<1.4	<1.4	<1.4	<1.4	<1.4	<1.4	<1.4
K	1600	1600	1610	1620	1610	1510	1580	1600	1610	1590
Re	2.9	3.2	3.5	3.6	3.8	4.0	4.3	4.4	4.6	4.9
S	1730	1710	1730	1700	1680	1730	1720	1700	1690	1660
BV	89.2	98.3	107.3	116.4	125.5	134.5	152.6	170.8	188.9	207.0
Re C/Co	0.51	0.56	0.62	0.63	0.68	0.70	0.75	0.77	0.81	0.85

J.1 (cont.)

Sample	FS-21	FS-22	FS-23	FS-24	FS-25	FS-26	FS-27	FS-28	FS-29
ADS#	186755	186756	186757	186758	186759	186760	186761	186762	186763
Al	234	234	243	243	243	241	240	241	239
B	22.0	22.0	22.9	22.6	23.0	22.7	22.5	22.6	22.3
Ba	<0.024	<0.024	<0.024	<0.024	<0.024	<0.024	<0.024	<0.024	<0.024
Ca	135	137	140	141	141	140	140	137	138
Cd	<0.028	<0.028	<0.028	<0.028	<0.028	<0.028	<0.028	<0.028	<0.028
Co	<0.10	<0.10	<0.10	<0.10	<0.10	<0.10	<0.10	<0.10	<0.10
Cr	0.25	0.25	0.25	0.27	0.23	0.23	0.21	0.23	0.23
Cu	2.30	2.23	2.33	2.37	2.40	2.40	2.40	2.34	2.32
Fe	16.6	16.5	17.0	17.3	17.0	17.1	17.0	17.0	17.0
Li	0.2	<0.2	<0.2	<0.2	<0.2	<0.2	<0.2	<0.2	<0.2
Mg	<0.168	<0.168	<0.168	<0.168	<0.168	<0.168	<0.168	<0.168	<0.168
Mn	0.53	0.53	0.54	0.56	0.54	0.54	0.54	0.53	0.54
Mo	21.2	21.0	21.5	22.2	21.6	21.7	21.6	21.5	21.8
Na	127000	130000	132000	128000	132000	134000	132000	132000	131000
Ni	298	298	308	308	308	307	306	307	307
P	300	298	303	314	305	305	305	305	303
Pb	<1.38	<1.38	<1.38	<1.38	<1.38	<1.38	<1.38	<1.38	<1.38
Si	13.1	12.5	14.8	16.1	15.1	13.6	13.0	12.8	12.6
Sn	0.58	0.54	0.63	<0.52	0.59	0.58	0.61	0.77	0.53
Sr	83.1	84.8	86.6	87.3	87.7	86.7	87.0	85.2	85.4
Ti	<0.28	<0.28	<0.28	<0.28	<0.28	<0.28	<0.28	<0.28	<0.28
V	<0.26	<0.26	<0.26	<0.26	<0.26	<0.26	<0.26	<0.26	<0.26
Zn	19.1	19.1	19.7	19.6	19.7	19.5	19.6	19.6	19.6
Zr	0.83	0.85	0.80	0.81	0.85	0.90	0.77	0.88	0.83
La	<1.4	<1.4	<1.4	<1.4	<1.4	<1.4	<1.4	<1.4	<1.4
K	1580	1580	1640	1650	1660	1660	1650	1650	1640
Re	4.8	4.8	5.1	5.3	5.2	5.3	5.4	5.4	5.5
S	1660	1670	1700	1720	1730	1710	1710	1710	1700
BV	216.1	225.1	243.2	261.4	279.5	297.6	315.7	333.8	352.0
Re C/Co	0.84	0.84	0.89	0.94	0.92	0.94	0.94	0.94	0.96

(This Page Intentionally Left Blank)

Appendix K. Additional On-line Data for Experiment 2 (45 °C Loading Experiment with AN-107 Simulant and Resin Batch #IR20327022045)

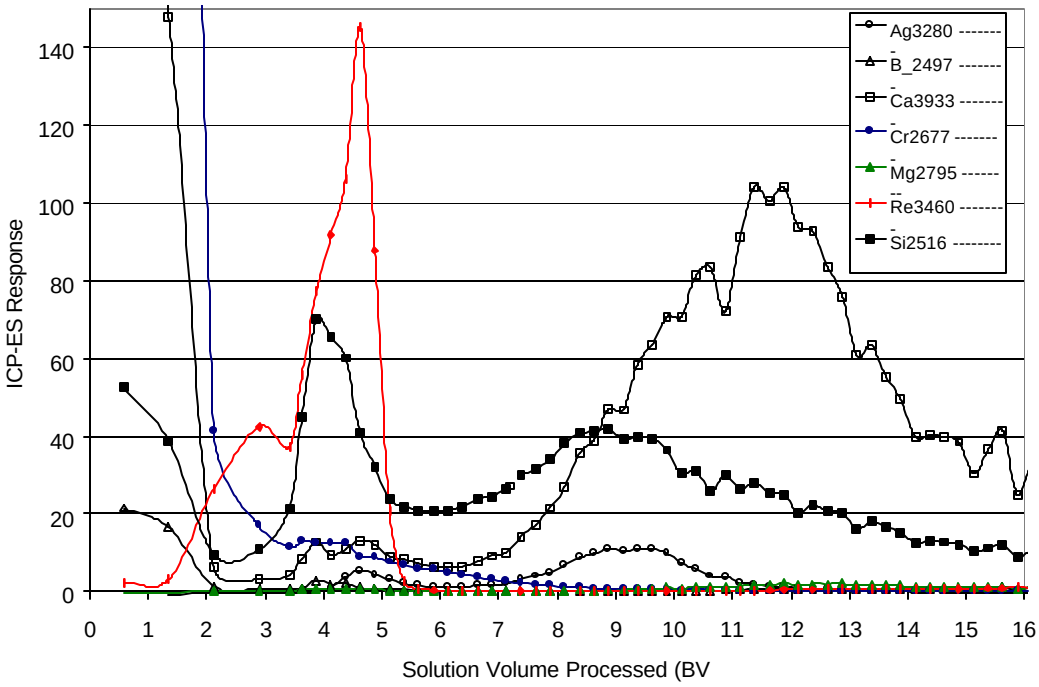

(This Page Intentionally Left Blank)

Appendix L. Elements Monitored with the On-line ICP-ES Instrument

Al
Ar
B
C
Ca
Cr
Cu
Fe
K
Mg
Mn
Mo
Na
Ni
Pb
Re
Si
Sr
Y

(This Page Intentionally Left Blank)

Appendix M. Additional On-line Data for Experiment 5 (25 °C Loading with AN-105 Simulant and Resin Batch #IR20327022045)

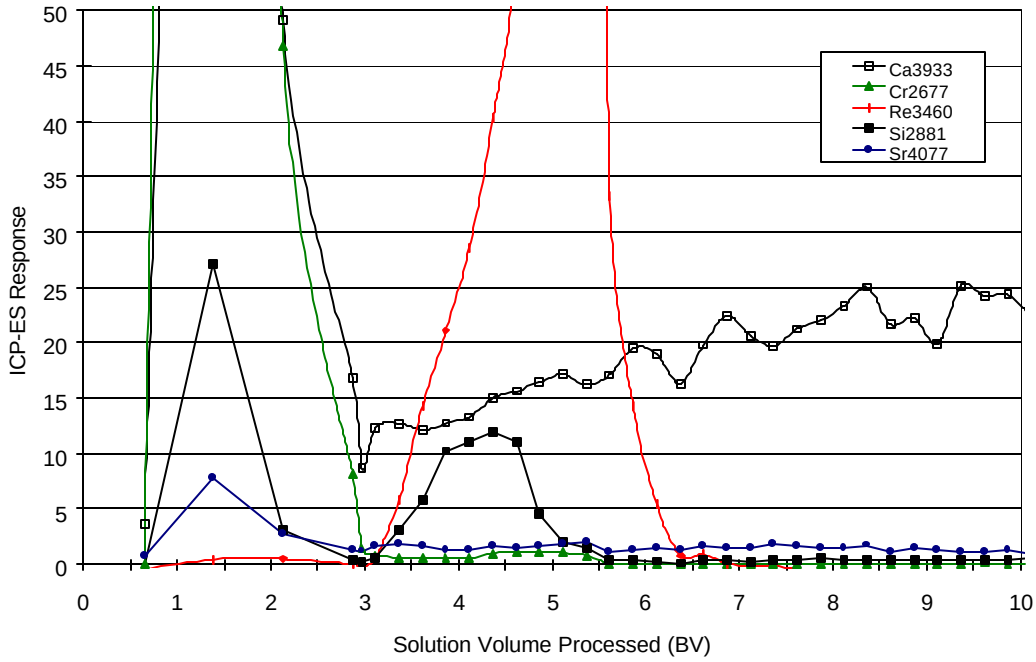

(This Page Intentionally Left Blank)

Appendix N. Additional On-line Data for Experiment 8 (25 °C Loading with AZ-102 Simulant and Resin Batch #IR20327022045).

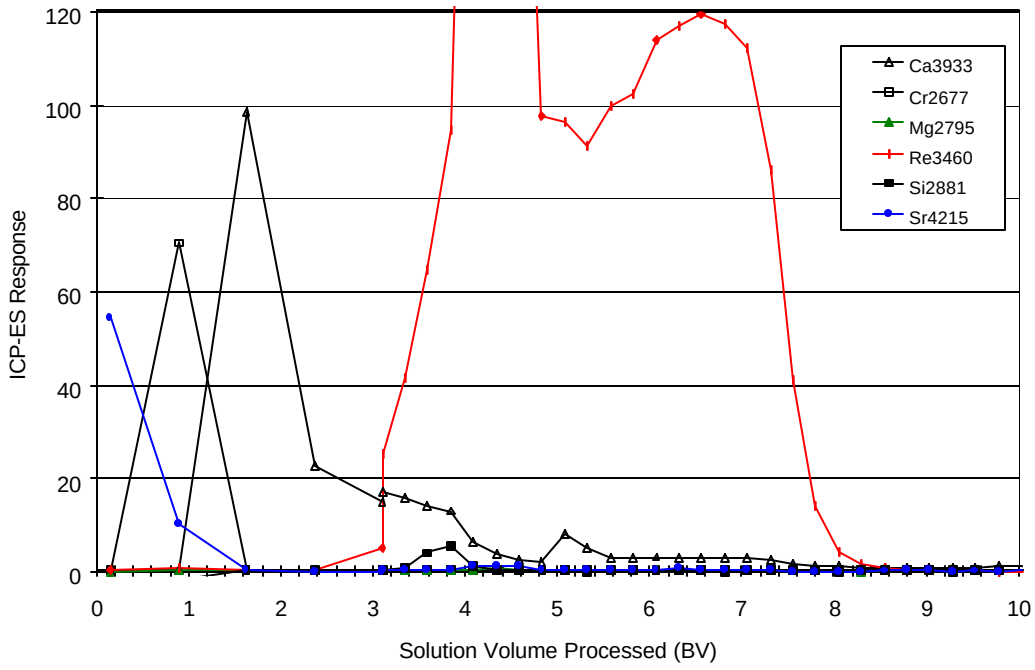

(This Page Intentionally Left Blank)

Appendix O. Additional On-line Data for Experiment 9 (25 °C Loading with AN-107 Simulant and Resin Batch #IR20327022045)

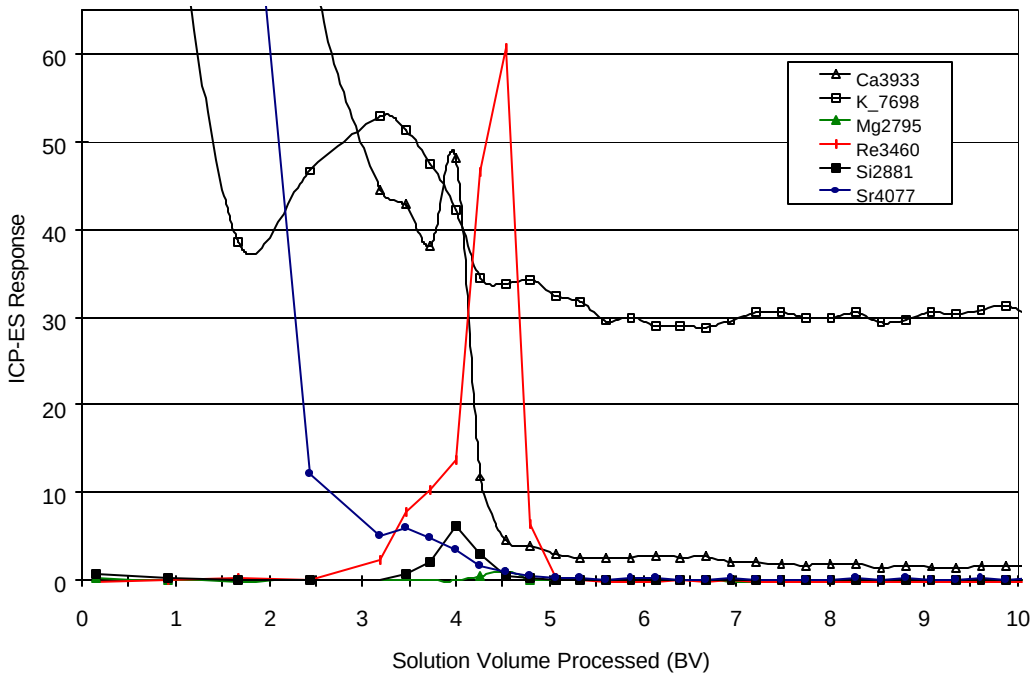

(This Page Intentionally Left Blank)

Appendix P. Data Recorded During Thermal Shock Testing With SuperLigÒ 639 Resin Batch #IR20327022045 (Experiment 10).

Summary

Data is provided that was obtained from thermal shock tests. Temperature data was collected at 0, 5, and 30 minute intervals during each contact period. Number counts were obtained by manually counting the numbers of cracked and total particles in photographs obtained by optical microscopy for various resin samples. Two photographs were obtained for each sample. Duplicate samples were collected at each sampling time. Microtrac and Lasentec FBRM particle analysis data is also summarized.

P.1 Temperature Data

Cycle #	Contact Time[1] (min.)	Temp.[2] (°C)	Activity
0	0	23.8	sample placed in beaker #1
0	30	24.3	AR[3] and AR-D samples collected
1	0	54.3	sample transferred to beaker #2
1	30	64.8	no activity
1	0	30.3	sample transferred to beaker #1
1	5	27.1	no activity
1	30	24.6	collected 1 and 1-D samples
2	0	57.3	sample transferred to beaker #2
2	5	62.4	no activity
2	30	64.7	no activity
2	0	30.5	sample transferred to beaker #1
2	5	26.9	no activity
2	30	24.5	collected 2 and 2-D samples
3	0	61.8	sample transferred to beaker #2
3	5	64.8	no activity
3	30	64.7	no activity
3	0	31.6	sample transferred to beaker #1
3	5	26.1	no activity
3	30	24.5	collected 3 and 3-D samples
4	0	55.5	sample transferred to beaker #2
4	5	60.8	no activity
4	30	64.6	no activity
4	0	29.7	sample transferred to beaker #1
4	5	27.0	no activity
4	30	24.4	collected 4 and 4-D samples

Appendix P.1 (cont.)

Cycle #	Contact Time[1] (min.)	Temp.[2] (°C)	Activity
5	0	56.9	sample transferred to beaker #2
5	5	61.6	no activity
5	30	64.5	no activity
5	0	30.1	sample transferred to beaker #1
5	5	26.9	no activity
5	30	24.5	collected 5 and 5-D samples
6	0	57.4	sample transferred to beaker #2
6	5	61.6	no activity
6	30	64.7	no activity
6	0	29.6	sample transferred to beaker #1
6	5	26.5	no activity
6	30	24.3	collected 6 and 6-D samples
7	0	58.2	sample transferred to beaker #2
7	5	61.3	no activity
7	30	64.7	no activity
7	0	30.3	sample transferred to beaker #1
7	5	26.6	no activity
7	30	24.3	collected 7 and 7-D samples
8	0	57.8	sample transferred to beaker #2
8	5	61.6	no activity
8	30	64.7	no activity
8	0	28.9	sample transferred to beaker #1
8	5	25.7	no activity
8	30	24.4	collected 8 and 8-D samples
9	0	58.2	sample transferred to beaker #2
9	5	61.8	no activity
9	30	64.7	no activity
9	0	28.3	sample transferred to beaker #1
9	5	25.7	no activity
9	30	24.4	collected 9 and 9-D samples
10	0	58.9	sample transferred to beaker #2
10	5	61.2	no activity
10	30	64.6	no activity
10	0	27.8	sample transferred to beaker #1
10	5	26.1	no activity
10	30	24.6	collected 10 and 10-D samples

[1] contact time at each temperature in a given cycle
[2] measured temperature of the water/resin slurry at the times indicated
[3] AR = as-received

P.2 Particle Counting Data from Micrographs

Sample	Photograph #	Total Particles	Fissured Particles	% of Fissured Particles
AR	1	125	2	1.6
AR	2	158	3	1.9
AR-D	1	110	3	2.7
AR-D	2	125	3	2.4
1	1	84	5	6.0
1	2	94	4	4.3
1-D	1	258	6	2.3
1-D	2	353	4	1.1
5	1	128	3	2.3
5	2	67	2	3.0
5-D	1	100	2	2.0
5-D	2	53	3	5.7
10	1	216	6	2.8
10	2	197	3	1.5
10-D	1	129	3	2.3
10-D	2	161	3	1.9

[1] AR = as-received

P.3 Microtrac Particle Size Analysis Data

Sample	Volume-Weighted Mean Diameter (mm)	Number-Weighted Mean Diameter (mm)
AR	312	419
AR-D	316	427
1	316	425
1-D	312	422
5	327	436
5-D	323	429
10	327	436
10-D	323	429

P.4 Lasentec Chord Length Analysis Data

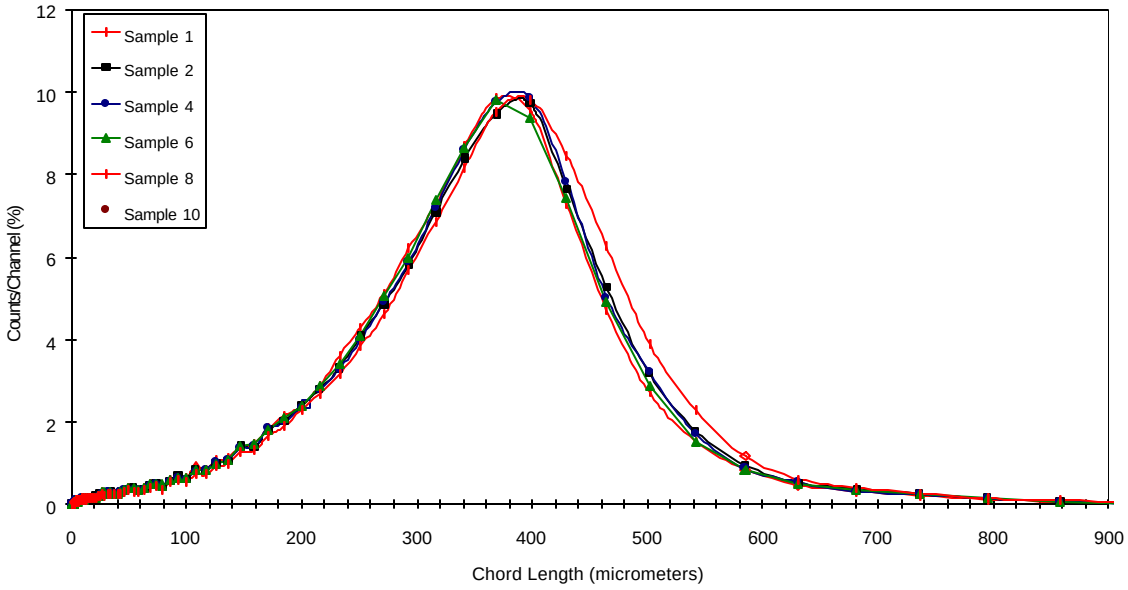

Sample	Mean Chord Length (mm)	Square-weighted Mean Chord Length (mm)	% of Chords <100 mm	% of Chords <10 mm
1	312	419	10.2	1.7
2	316	427	10.7	1.9
4	316	425	10.5	1.8
6	312	422	10.8	1.8
8	327	436	9.7	1.8
10	323	429	9.7	1.7